MODELLING
SIMULTANEOUS HEAT AND MASS TRANSFER IN WOOD

by

Ming Shao

Thesis submitted to the Faculty of the

Virginia Polytechnic Institute and State University

in partial fulfillment of the requirements for the degree of

MASTER OF SCIENCE

in

Wood Science and Forest Products

APPROVED:

F.A. Kamke, Chairman

L. T. Watson

C. E. Frazier

May, 1994

Blacksburg, Virginia

MODELLING SIMULTANEOUS HEAT AND MASS TRANSFER IN WOOD

by

Ming Shao

Committee Chairman: Frederick A. Kamke
Wood Science and Forest Products

(ABSTRACT)

The fundamental and quantitative study of heat and mass transfer processes in wood plays an important role for understanding many important production processes, such as wood drying and hot-pressing. It will help us improve the existing products and production techniques and develop new manufacturing technology. The most difficult aspect of the study is the complicated interactions of heat and mass transfer mechanisms. Extensive characterization of these physical processes using a strictly experimental approach is extremely difficult because of the excessively large number of variables that must be considered. However, mathematical modeling and numerical techniques serve as a powerful tool to help us understand the complicated physical processes.

The goal of this research is to model the simultaneous heat and mass transfer in wood. The specific objectives of this research are:

1) develop a computer simulation program, implementing an existing one-dimensional mathematical drying model, using a finite difference approach, to numerically evaluate the mathematical model.

2) study sensitivity of the heat and mass transfer model to determine the effects of wood physical properties and environmental conditions on the drying processes.

ACKNOWLEDGEMENTS

I would like to express my sincere gratitude and appreciation to Dr. Frederick A. Kamke and Dr. Layne T. Watson for their valuable guidance, encouragement, advice and help.

I also want to thank Dr. Charles E. Frazier for his kindly help and continuous encouragement.

Finally, I want to thank my parents for all their love and understanding. And most importantly, I would like to thank my husband for his encouragement and support during my study.

TABLE OF CONTENTS

LIST OF TABLES

LIST OF FIGURES

NOMENCLATURE

Chapter II

A	area perpendicular to the direction of heat flow through,	m^2
D	bound water diffusion coefficient of wood,	m^2/s
D_a	coefficient of interdiffusion of water vapor in bulk air,	cm^2/s
D_v	water vapor diffusion coefficient of air in the lumens of wood,	cm^2/s
G	specific gravity of the solid wood	
G_m	specific gravity of moist cell wall substance	
H	humidity,	%
J	mass flux,	$kg/m^2/s$
K	permeability,	$m^2.m.s/kg$
K'	specific permeability,	m^2
K_g	gas permeability,	$m^2.m.s/kg$
L	length of specimen in the flow direction,	m
M	moisture content (oven-dry base)	%
P	pressure,	Pa
Q	volumetric flow rate,	m^3/s
R	universal gas constant,	cal/mol/K
T	temperature,	K
c	specific heat,	J/kg/K
h	relative vapor pressure	
k_h	convection heat trnsfer coefficient,	$W/m^2.K$
p_o	saturated vapor pressure,	cm Hg
q	rate of heat flux,	J/s
q''	convective heat flux,	W/m^2
t	time,	s
w_m	weight of moist wood,	kg
w_o	weight of dry wood,	kg
z	distance,	m
κ	thermal conductivity,	J/s/m/K
α	thermal diffusivity,	m^2/s
ρ	material density,	kg/m^3
ϱ_w'	density of water,	g/cm^3
μ	chemical potential,	cal/mol
μ^o_1	chemical potential of liquid water at 1 atm,	cal/mol
τ_{zy}	momentum flux,	N/m^2
η	viscosity,	kg/m/s

Chapter III

D_b	boundary water diffusivity,	kg.s/m^3
D^{eff}	effective gas diffusivity,	m^2/s
K_f	permeability of free water,	m^2
K_g	relative gas permeability,	m^2
M_a	molecular weight of air,	kg/mol
M_v	molecular weight of water vapor,	kg/mol
P_c	capillarity pressure,	Pa
R	gas constant,	J/mol/K
S_v	water vapor entropy,	J/mol/K
T	temperature,	K
h_a	enthalpy of air,	J/kg
h_v	enthalpy of water vapor,	J/kg
h_b	enthalpy of boundary water,	J/kg
h_f	enthalpy of free water,	J/kg
h_d	enthalpy of solid wood,	J/kg
n_a	air flux,	kg/m^2/s
n_b	bound water flux,	kg/m^2/s
n_f	free water flux,	kg/m^2/s
n_v	water vapor flux,	kg/m^2/s
p_a	air pressure,	Pa
p_v	partial water pressure,	Pa
t	time,	s
z	space variable,	m
κ	thermal conductivity of moist wood,	W/s/K
ρ_a	air density	kg/m^3
ρ_b	bound water density,	kg/m^3
ρ_f	free water density,	kg/m^3
ρ_m	water content,	kg/m^3
ρ_v	water vapor density,	kg/m^3
ρ_w	liquid water density,	kg/m^3
ϵ	effective void fraction.	
ϵ_d	dry wood void fraction.	
η_g	gas viscosity,	kg/m/s
η_w	liquid viscosity,	kg/m/s
μ_b	chemical potential,	J/kg

Chapter IV

D_b	bound water diffusivity,	$kg.s/m^3$
K_g	relative gas permeability of wet wood,	m^2
K_g^d	gas permeability of dry wood,	m^2
K_f	effective liquid water permeability,	m^2
K_f^s	saturate water permeability,	m^2
S_{ir}	irreducible saturation, fraction.	
T	temperature,	K.
k_h	convective heat transfer coefficient,	$W/m^2/K$
k_m	convective mass transfer coefficient,	$mol/m^2/s$
p_a	air pressure,	Pa
p_v	water vapor pressure,	Pa
ρ_{cell}	density of cell wall substance,	kg/m^3
ρ_d	density of dry wood,	kg/m^3
ρ_f	density of free water,	kg/m^3
ρ_m	density of water per unit volume of wood,	kg/m^3
ρ_w	density of liquid water,	kg/m^3.
α	attenuation factor	
ϵ	effective porosity	
ϵ_d	dry wood void fraction,	%

CHAPTER I

INTRODUCTION

Heat and mass transfer is a very important research subject in the areas of wood science and forest products. The fundamental and quantitative study of heat and mass transfer processes will give us a better understanding of many important production processes, such as wood drying and hot-pressing, help us improve the existing products and production techniques and develop new manufacturing technology.

The hot pressing operation has been identified as one of the most important and expensive operations in the manufacture of wood based composites. Wood-based composites are produced in highly automated processes where the wood and adhesive components are flat pressed using extreme heat and pressure. The wood-adhesive system must deform sufficiently to produce an intimate wood-adhesive-wood contact. Three major interactive physical processes are involved during hot pressing, which include heat and moisture transfer, adhesion, and viscoelastic behavior of the wood component. During composite manufacture, heat energy is transferred from hot platens to the composite by conduction and then by conduction and convection as moisture is changed to water vapor and driven to the core of the mat. At high temperature and in the presence of moisture, wood materials become soft and are easily compacted by pressing pressure to form high density board. In the meantime, the thermosetting adhesive is cured. A quantitative understanding of the heat and mass

transfer process is important if we are to improve the performance of existingproducts, to reduce pressing times, and to design processes for the manufacture of new products with specific properties. Heat transfer affects hot pressing time, heat energy consumption and hence production efficiency. Heat and moisture affect the viscoelastic behavior of wood composite materials and hence affect the mechanical properties of the composite. Therefore, heat and moisture transfer during hot pressing affects the rate and extent of adhesive cure and adhesive flow, and hence affects the bond strength of the composite.

Wood drying is another area which involves heat and mass transfer. Drying is a key processing step in the use of wood products. For many end-users, wood must be formally dried to overcome consequential shrinking and swelling, and to eliminate warping, splitting, cracking, and other harmful effects of uncontrolled drying. A large amount of energy is required to evaporate water in wood from the green state to end-use condition. Water may occur in wood in three forms: liquid (or free) water in the cell cavities, water vapor in the cell cavities, and bound (or hygroscopic) water in the cell walls. Moisture movement may occur by mass flow of liquid water and vapor through the cell capillary structure, diffusion of bound water occurs through the network of cell walls, and convective mass transfer from the surface.

The drying of moist wood is a complicated process involving simultaneous heat and mass transfer phenomena. Drying behavior can be influenced by a rather large variety of independent factors, including ambient conditions of temperature, air velocity, and relative humidity, and wood properties such as density, permeability,

and hygroscopicity. Studying the process of heat and mass transfer during wood drying may help to improve existing drying methods and to develop new drying technology.

Because of these important applications mentioned above, there has been a long progression of research relating to heat and mass transfer in wood. The transport mechanisms in wood are fairly well known. The most difficult aspect is the complicated interactions of heat and mass transfer mechanisms. Extensive characterization of those physical processes using a strictly experimental approach is extremely difficult because of the excessively large number of variables that must be considered. However, mathematical modeling and numerical techniques serve as a powerful tool to help us understand the complicated physical processes. Numerical modeling can be used to simulate many heat and mass transfer process, such as hot pressing and wood drying, for a variety of physical conditions and material properties. In addition, sensitivity studies can be performed to determine the effects of different physical properties and different material properties on those manufacturing processes.

The specific objectives of this research are:

1) develop a computer simulation program, implementing an existing one-dimensional mathematical drying model, using a finite difference approach, to numerically evaluate the mathematical model.

2) study sensitivity of the heat and mass transfer model to determine the

effects of wood physical properties and environmental conditions on the drying processes.

Chapter II will recall the fundamental principles of heat and mass transfer, and review the research development on mathematical and numerical modeling of drying and hot pressing. Chapter III will briefly introduce Stanish's drying model and describe the numerical approach to solve the model. Chapter IV will discuss the simulation results, and justify the numerical model. Chapter V will include the conclusions and some suggestions of future work.

CHAPTER II

FUNDAMENTALS: HEAT AND MASS TRANSFER

Heat and mass transfer are two important physical processes, which are commonly involved in wood drying and wood composite manufacture. In order to model the two processes, the fundamentals of heat and mass transfer and their interactions must be understood.

2.1 HEAT TRANSFER

2.1.1 Heat Transfer Mechanisms

There are three distinct mechanisms of heat transfer: conduction, which is the transfer of heat through rigid materials; convection, which results in the transfer of heat between relatively hot and cold portions of a fluid by mixing; and radiation, which involves the transfer of electromagnetic energy in the absence of a conveying medium (Frank, 1990).

Wood is a porous and hygroscopic material consisting of a combination of solid substance (cell wall) and air pockets (voids). Therefore, heat may flow in wood by all of the above mechanisms acting simultaneously. Heat transfer through a solid is by conduction. Heat transfer through the voids of moist wood is essentially by vapor convection, especially at relatively high temperatures. Radiation may only play a significant role when heat is transferred through the voids of dry materials under

extreme conditions. Wood and wood based materials, then, offer resistance to heat flow because of the small air pockets in them, as well as the resistance of the wood substance itself to heat transfer.

2.1.2 Conductive Heat Transfer

2.1.2.1 Fourier's Law

Conduction is a process by which heat flows from a region of higher temperature to a region of lower temperature within a medium (solid, liquid, or gas) or between different mediums in direct physical contact. In conductive heat flow, the energy is transmitted by direct molecular communication without appreciable permanent displacement of the molecules.

In the solution of heat conduction problems, it is necessary to determine whether a process is of the steady- or unsteady-state type. When the rate of heat flow in a system does not vary with time, the temperature at any point does not change and steady-state conditions prevail. Under steady-state conditions, the rate of heat input at any point of the system must be exactly equal to the rate of heat loss, and no change in internal energy can take place. It often takes a long time for a system to attain such a steady-state condition. When the temperatures at various points in a system change with time, the heat flow is transient, or unsteady. Such heat flow problems are encountered during warm-up or cool-down periods.

The basic law of heat conduction was established by Fourier. The steady-state

heat conduction transfer through the wood may be described by Fourier's first law:

$$q = - \kappa A \frac{dT}{dz} , \qquad (2.1)$$

where q - rate of heat flux, J/s
κ - thermal conductivity, J/s/m/K
A - area perpendicular to the direction of heat flow through, m^2
dT/dz - temperature gradient at the section, K/m

The thermal conductivity (κ) is the energy per unit time (q) which flows through a thickness (z) of a substance with a surface area (A) under a steady-state temperature difference between faces of T_1 and T_2. Equation (2.1) provides a definition of thermal conductivity.

The unsteady-state heat transfer may be described by Fourier's second law:

$$\frac{\partial T}{\partial t} = \alpha \frac{\partial^2 T}{\partial z^2} , \qquad (2.2)$$

where T - temperature, K
t - time, s
z - distance, m
α - thermal diffusivity, ($\alpha = k/\rho c$), m^2/s
κ - thermal conductivity, J/s/m/K
c - specific heat, J/kg/K
ρ - material density, kg/m^3

2.1.2.2 Effects of Thermal Conductivity

So far, the thermal conductivity of wood has been recognized to vary with: density, moisture content, temperature, direction of heat flow with respect to grain, heartwood or sapwood, type and quantity of extractive and the presence of defects

(Ward, 1960; Kollmann, 1975). A selection of these factors will be considered.

1) Density and Moisture Effect

The thermal conductivity of wood has been found to be linearly correlated with density (Rowley, 1933; MacLean, 1941; Kollmann, 1956, 1975). MacLean (1941) derived an equation for oven-dry wood based on English units, which was:

$$\kappa = 1.39G + 0.165 \qquad (2.3)$$

where G - specific gravity of the solid wood
κ - thermal conductivity, Btu. in./ft^2.hr.°F

This relationship appears to be accurate for all species tested ranging in specific gravity from 0.11 to 0.76 (Kollmann, 1975). Wangaard (1969) maintained that the density appears to be the only variable which significantly affects thermal conductivity.

MacLean (1941) modified equation (2.3) to account for the effect of wood moisture at an average temperature of 25°C.

$$\text{for } M < 40\% \qquad \kappa = G(1.39 + 0.026M) + 0.165$$
$$\text{for } M > 40\% \qquad \kappa = G(1.39 + 0.036M) + 0.165 \qquad (2.4)$$

where G - specific gravity based on oven dry weight and volume at moisture content
M - moisture content (oven-dry base)
κ - thermal conductivity in Btu.in./hr.ft^2.°F

Rowley (1933) first found thermal conductivity increased linearly with moisture content. However, Kollmann (1956) found there was no linear relationship existing above a wood density of 800 kg/m^3. Kollmann (1975) also found that at the same density, thermal conductivity increases in proportion to the moisture content.

2) Temperature Effects

Studies of the variation of thermal conductivity with temperature are few. In a review of thermal conductivity literature, Gammon (1987) provided a group of data for oven-dry wood based on the work of MacLean (1941), Maku (1954) and others. For wood with temperatures below 100°C, there was general agreement that thermal conductivity of wood linearly increased with rising temperature.

3) Grain Direction Effects

The thermal conductivity of wood in the radial direction has been found to be about 5 to 10 % greater than in the tangential direction (Wangaard, 1969). Conductivity in the longitudinal direction has been found to be about 2.25 to 2.75 times the conductivity across the grain (Kollmann, 1975) when moisture content was 6% to 10%.

Kollmann and Malmquist (1956) developed a model to describe the effect of fiber orientation on thermal conductivity. Wood and wood-based composite materials were defined as composing of layers of fiber material and air. Parallel arrangement of the fibers in the direction of heat flow created maximum "heat bridge" effect, and parallel arrangement of the fibers perpendicular to the direction of the heat flow created minimum "heat bridge" effect. The minimum and maximum thermal conductivity could be calculated from layer thicknesses and the conductivity of air and wood cell wall substance. For a body with a mixed arrangement of layers, a weighted average conductivity was obtained by means of the "bridge factor" concept. Therefore, the thermal conductivity of solid wood, particleboard and fiberboard was

separated by simply varying the "bridge factor".

2.1.3 Composite Materials

Kollmann and Malmquist (1956) summarized thermal conductivity data from many sources. This showed the dependence of the thermal conductivity of wood, particleboard and fiberboard upon specific gravity. Solid wood had the highest conductivity value, and fiberboard the lowest, with plywood being intermediate. Lewis (1967) tested fiberboard and particleboard and obtained the same results. The thermal conductivity of particleboard varied with temperature (Gilbo, 1951; Kollmann, 1951, 1975; Lewis, 1967; Ward and Skaar 1963). The same is true for waferboard (Nanassy, 1978). There is general agreement that there is a small positive linear effect of temperature on the conductivity value (Humphrey, 1982, 1989).

The thermal conductivity of wood-based composites is also affected by moisture content. Since it is difficult to prevent moisture movement in the current test methods, few experimental results have been published. Nanassy (1978) reported that, as would be expected, the thermal conductivity of waferboard increases with an increase in moisture content.

Kamke (1989a,b) measured the thermal conductivity for several types of commercially produced wood-based panels. For a given specific gravity, the descending order of thermal conductivity values for wood-based composites tested are: solid wood, plywood, particleboard, and fiberboard. The tests also reveal that increasing the moisture content or the specific gravity will increase thermal

conductivity. The relationship between thermal conductivity and either moisture content or specific gravity appears to be linear.

2.1.4 Convection Heat Transfer

Convection heat transfer occurs between a surface and a moving fluid when they are at different temperatures (Frank, 1990). The convection heat transfer inside solid wood is not significant, because only low fluid flow velocity can be achieved. However, convection is often significant at the wood surface, where the heat transfers between a fluid (such as air) in motion and a bounding surface when the two are at different temperatures. The convection heat transfer occurs due to the combined effects of conduction and bulk fluid motion.

Newton's law of cooling for convection is expressed as:

$$q'' = k_h \, (T_s - T_\infty) \ , \qquad (2.5)$$

where q", the convective heat flux(W/m^2), is proportional to the difference between the surface and fluid temperatures, T_s and T_∞, respectively. The convection heat transfer coefficient, k_h ($W/m^2.K$), encompasses all the parameters, such as surface geometry and the nature of the fluid motion, that influence convective heat transfer in the boundary layer.

For wood-based composites, such as particleboard, while there is still sufficient moisture present locally within the mattress to allow vapor generation in thepresence of heat, convective heat transfer will be seen in addition to conduction.

Convection occurs because heat transferred into the mattress causes vaporization of the furnish moisture, thus increasing the water vapor pressure. This creates a vapor pressure gradient across the board thickness, and this in turn causes flow, and transfers the heat content of the vapor. Convection heat transfer often happens at the solid surface due to the surface fluid flow.

2.1.5 Radiation

The radiative heat transfer is likely to be insignificant compared to conduction at temperatures below 200°C. Therefore, radiation heat transfer will not be considered here.

2.2 MOISTURE TRANSFER

2.2.1 Wood Moisture Relations

Wood is a hygroscopic porous solid. The dry basis moisture content of wood is defined as:

$$MC = 100\ \frac{(w_m - w_o)}{w_o} \qquad (2.6)$$

where w_m - weight of moist wood, kg
w_o - weight of dry wood, kg

Wood generally contains water in three forms: liquid water partially or completely filling the cell cavities, water vapor in the cell cavity spaces, and water

bound in the cell wall.

When wood is at equilibrium with its environment, the moisture content of wood is defined as equilibrium moisture content (EMC). The moisture content at which a given cell has lost all of its cavity water and contains only water vapor in the cavities, and the cell wall is fully saturated, is defined as the fiber saturation point (FSP). The moisture content at FSP ranges from 20% to 40% of the dry weight of wood depending on temperature and wood species. The well known sorption isothermal relationship between the relative humidity and the equilibrium moisture content is plotted in Figure 2.1.

2.2.2 Water Transfer Mechanisms

There have been numerous research publications relating to heat and mass transfer in wood. Siau (1984) and Skaar (1988) have written about the fundamentals of heat and mass transfer in wood. Their work has also covered a great deal of research literature on those subjects. The transport of fluids through wood may be subdivided into two main classifications (Siau, 1984). The first is the bulk flow of fluids through the interconnected voids of the wood structure under the influence of a static or capillary pressure gradient. This is sometimes designated as momentum transfer because it can be attributed to a momentum-concentration gradient. The second is diffusion consisting of two types: intergas diffusion, which includes the transfer of water vapor through the air in the lumens of the cells, and bound-water diffusion, which takes place within the cell walls of wood.

2.2.3 Bulk flow

Viscous (laminar) flow is the important mechanism involved in flow of liquid and vapor through a porous medium. The flow of fluids through wood and other porous solids is described by Darcy's law.

2.2.3.1 Darcy's Law

Darcy's law for liquids:

$$K = \frac{Flux}{Gradient} = \frac{Q/A}{\Delta P/L} , \qquad (2.7)$$

where K - permeability, $m^2.m.s/kg$
Q - volumetric flow rate, m^3/s
L - length of specimen in the flow direction, m
A - cross section area, m^2
P - pressure, Pa

Darcy's law for gas:

$$K_g = -\frac{Q}{A\frac{dP}{dz}} , \qquad (2.8)$$

where K_g - gas permeability, $m^2.m.s/kg$
dP/dz - pressure gradient, Pa/m

The magnitude of the bulk flow of a fluid through wood is determined by its permeability. Permeability is a measure of the ease with which fluids are transported through a porous solid under the influence of a pressure gradient. Permeability can also be calculated from the specific permeability.

Specific permeability is equal to the product of permeability and viscosity. Its

value is not affected by the measuring fluid and it is only a function of the porous structure of the medium.

$$K' = K \eta \ , \qquad (2.9)$$

where K - permeability, m^2 m s/kg
K'- specific permeability, m^2
η - viscosity, kg/m/s

Viscosity is internal fluid friction which requires the application of a force to cause one layer of a fluid to flow smoothly past an adjacent layer or to cause one surface to move relative to another when there is a fluid between them. Both gases and liquids possess viscosity. This physical situation is defined by Newton's law of viscosity.

$$\tau_{yz} = - \eta \frac{dv_y}{dz} \ , \qquad (2.10)$$

where τ_{yz} is the momentum flux (N/m^2), dv_y/dz is the velocity gradient (m/s/m), and η is the viscosity (kg/m/s).

2.2.3.2 Effects of Permeability

1) Moisture Effects

Wood above the fiber saturation point (FSP) would be expected to have a very low permeability because high capillary pressures must be overcome to force air bubbles through the minute pit openings. When the moisture content is below the

fiber saturation point, generally the permeability of softwoods increases as moisture content decreases (Comstock, 1968).

2) Species Variation Effects

Permeability is an extremely variable property of wood. It is clear that a solid must be porous to be permeable, but it does not necessarily follow that all porous bodies are permeable. Permeability can only exist if the void spaces are interconnected by openings. Many measurements have been done (Smith and Lee, 1958; Comstock, 1970, Kininmonth, 1971) to determine both the longitudinal and transverse permeability for a variety of wood species. Siau (1984) has summarized (Table 2.1) approximate values for a few common classifications of wood.

3) Composite Effects

For wood-based composites, the coefficient of permeability decreases as the panel is compressed. The transverse permeability of particleboard is usually much higher than the longitudinal permeability, and very much higher than the transverse permeability of the wood from which the board is made (Humphrey, 1982). Permeability decreases as particleboard density increases (Lehmann, 1972, Bolton and Humphrey, 1994).

2.2.4 Diffusion

The second classification of moisture movement in wood is diffusion consisting of two types: intergas diffusion, which includes the transfer of water vapor through

the air in the lumens of the cells, and bound-water diffusion, which takes place within the cell walls of wood.

2.2.4.1 Isothermal Moisture Diffusion

Diffusion is molecular mass flow under the influence of a concentration gradient (Siau, 1984). Therefore a static pressure difference is not necessary for diffusion to occur. Fick's first law, which is analogous to Darcy's and Fourier's laws, represents the relationship between the flux and the concentration gradient under steady-state conditions. When applied to water-vapor transport through wood it may be written as:

$$J = - D \frac{dc}{dz} , \qquad (2.11)$$

where D - bound water diffusion coefficient of wood, m^2/s
J - mass flux, $kg/m^2/s$
dc/dz - moisture concentration gradient, $kg/m^3/m$

There are several alternative ways of expressing the potential which drives moisture through wood. For example, bound water diffusion can also be shown to be proportional to gradients in water vapor pressure and chemical potential. Under isothermal conditions, these driving forces will yield equivalent results using Fick's law.

2.2.4.2 Nonisothermal Moisture Diffusion

In most wood-drying processes temperature gradients are present and there is,

therefore, some coupling of heat and moisture transport. One such coupling phenomenon is known as thermal diffusion. This is the process by which moisture diffuses through wood under the influence of a temperature gradient. In other words, when wood is subjected to a temperature gradient it will not remain at an uniform moisture content but will approach a nonuniform moisture distribution.

Nonisothermal experiments were discussed by Siau (1980). They were performed with relatively steep thermal gradients of approximately 10°C/cm and the specimens were encapsulated to prevent net moisture movement to the outside and to ensure a net flux of zero within the specimens at equilibrium. After equilibrium had been established, the specimens were sliced to determine the moisture content and partial-vapor-pressure profiles between two parallel surfaces across which a temperature gradient was applied. In all cases the results indicated the highest moisture content on the cool side and the highest partial vapor pressure in the warm side. The application of Fick's law would predict a net flux from the cool to the warm side using a gradient of moisture content and a flux in the reverse direction based upon a gradient of partial vapor pressure.

Nonisothermal moisture movement can be analyzed as due to a gradient of chemical potential (Skaar, 1988; Siau, 1984). Chemical potential is the partial molar Gibbs free energy, which determines whether equilibrium has been attained in a system. The chemical potential of a natural hygroscopic porous solid material, wood, is defined by Siau (1984):

$$\mu = \mu_1^0 + R\,T \ln h\,, \qquad (2.12)$$

where μ - chemical potential, cal/mol
R - universal gas constant, cal/mol/K
h - relative vapor pressure, Pa
T - temperature, K
μ^o_1 - chemical potential of liquid water at 1 atm, cal/mol

Chemical substances move from higher to lower chemical potential by diffusional transport and by chemical reaction. Thus in a system at constant T and P, diffusive flow of a component from higher to lower μ lowers the Gibbs free energy.

Stanish (1986) developed an equation based on a gradient of chemical potential to describe moisture transport through wood. His equation included both bound-water and water-vapor diffusion. For isothermal diffusion, the chemical potential gradient was expressed in terms of vapor pressure gradients. Stanish's equation included both vapor and bound water transport through wood under nonisothermal conditions. Furthermore, it was expressed in terms of the vapor pressure and temperature in the wood rather than in terms of moisture content and temperature gradients. In order to use the equations on experiments in which moisture contents rather than vapor pressure gradients are measured, it is necessary to know the sorption isotherms. On the other hand, for analyzing data based on vapor pressure measurements Stanish's equations are most suitable.

2.2.4.3 Effects of Diffusion Coefficient

1) Water-Vapor Diffusion Coefficient

The coefficient for the transport of water vapor through the lumens can be calculated from the coefficient of interdiffusion of water vapor in air (Siau, 1984). A semi-empirical equation for this coefficient was derived by Dushman (1962), which is based upon a moisture concentration gradient on air:

$$D_a = 0.220\left(\frac{76}{P}\right)\left(\frac{T}{273}\right)^{1.75}, \qquad (2.13)$$

where D_a - coefficient of interdiffusion of water vapor in bulk air, cm^2/s
P - total pressure, cm Hg
T - temperature, K

By applying the ideal gas law, D_a can be converted to D_v, which is based upon the concentration of moisture in the cell-wall substance in equilibrium with the air.

$$D_v = \frac{18 D_a p_o}{G_M \rho_w' RT}\frac{dH}{dM}, \qquad (2.14)$$

where D_v - water vapor diffusion coefficient of air in the lumens of wood, cm^2/s
G_m - specific gravity of moist cell wall substance.
ϱ_w'- density of water, g/cm^3
H - humidity, %
p_o - saturated vapor pressure, cm Hg
M - moisture content, %

From the Equation 2.14 , D_v is a function of temperature and moisture content.

2) Bound Water Diffusion Coefficient

Stamm (1959) measured the longitudinal bound-water diffusion coefficient of the cell-wall substance of the wood by filling the lumens with a low-melting

metal alloy. The longitudinal bound water diffusion coefficient D_{BL} has been found to increase exponentially as moisture content increases from 0 to 30% , and ranges from 0 to $14x10^{-7}$ cm^2/s (Stamm, 1959). This may be explained by the lower bonding energy between the sorption sites and the bound-water molecules at higher moisture content.

Stamm (1964) also found that the longitudinal bound-water diffusion coefficient D_{BL} of cell-wall substance was approximately three times that in the tangential and two times that in the radial directions. Assuming an average, $D_{BL} = 2.5\ D_{BT}$, where D_{BT} is transverse bound-water diffusion coefficient of cell-wall substance.

Stamm (1964) and Choong (1963) found that the transverse diffusion coefficient increases rapidly with temperature in accordance with the Arrhenius equation. Siau (1984) has included both Stamm's and Choong's work and calculated the values of D_{BT} and D_v at various temperatures and moisture contents, which show the strong dependence of D_{BT} on both temperature and moisture content.

Siau (1984) has derived both transverse moisture diffusion and longitudinal moisture diffusion models. The models combine the flow paths of bound water and water vapor, and calculate the transverse diffusion coefficient D_T and longitudinal diffusion coefficients D_L based on the values of cell wall diffusion coefficient D_{BT} and water vapor diffusion coefficient D_v.

2.3 MODELLING HEAT AND MOISTURE TRANSFER

2.3.1 Wood Drying

There has been a long progression of research relating to the mechanisms of heat and mass transfer in wood. The most intriguing aspect of these mechanisms is their interaction, which is best typified by a drying process (Kamke and Watson, 1990). Mathematical drying models differ in the literature by the emphasis on which mechanism controls drying at what stage of drying. The models are divided into three general types: diffusion models; empirical models; and models based on heat, mass, and momentum transport properties (Rosen, 1982). The diffusion type models (Siau, 1984) are based on Fick's Second Law of Diffusion. The driving force of diffusion could be moisture concentration, vapor pressure or chemical potential. This type of model has a simple mathematical analysis, but generally a poor fit to drying data because of some questionable theoretical assumptions. Many practical empirical models (Kollman, 1951; Wang and Beall, 1975; Bramhall, 1976; Rosen, 1980, 1982) have been presented in the wood drying literature. This type of model has a good fit to drying data, and is completely flexible in approach, but has no reliability when extrapolating outside of the data range, because they are not based on principles of drying theory. Much general theory has been developed for the drying of porous materials (Berger and Pei, 1973; Luikov, 1966, 1975), which leads to the development of drying models from transport properties of wood. This type of model, with complex analyses based on wood structure and multiphase flow, is always described in a system of partial differential equations (Lowery, 1972; Thomas et al, 1980; Spolek and Plumb, 1980; Bramhall, 1979; Stanish, 1986). The third type of

drying model is the closest to theoretical principles of wood drying and has the best appreciation for interrelationships among variables affecting drying. These complex models depend on many physical parameters whose values may not be known in advance, and the solutions require sophisticated computer programs.

2.3.2 Hot Pressing

The wood component in a flakeboard mat during hot-pressing is subjected to rapidly changing gas pressure, temperature, and humidity (Kamke and Casey, 1988a,b). Temperature and moisture gradients are developed within the mat, which influence mechanisms involved in the panel formation. Mathematical models have been developed to predict internal temperature and moisture content in particleboard during hot-pressing (Bowen, 1970; Kayihan, 1983; Harless et al. 1987; Humphrey, 1982, 1989). These models treat the mat as a continuum with a characteristic void volume. Local thermodynamic equilibrium is assumed, therefore any resistance to heat and mass transfer between the gas phase and the adjacent wood component is neglected. The internal temperature and gas pressure of wood-based composites during processing can be measured experimentally (Kamke and Casey, 1988a,b). The data can be used as a method to determine the composition of the gas phase surrounding the wood component. With a knowledge of the internal gas phase, the exchange of heat and mass across the boundary of the flake surface can be determined using a fundamental heat and mass transfer model (Kamke and Wolcott, 1991).

Table 2.1. Permeability for some common classifications of wood (based on Siau, 1984).

Permeability darcys			
			Longitudinal
100	10^2	-	Red Oak
50			
10	10^1	-	Basswood
5			
1	10^0	-	Maple, Pine sapwood, Douglas-fir sapwood
0.5			
0.1	10^{-1}	-	Spruces
0.05			Cedars
0.01	10^{-2}	-	Douglas-fir heartwood
0.005			White Oak heartwood
0.001	10^{-3}	-	Cedar heartwood
0.0005			Douglas-fir heartwood (intermountain)
			Transverse
0.0001	10^{-4}	-	(The species are in approximately
0.00005			the same order as those for longitudinal
0.00001	10^{-5}	-	permeabilities)
0.000005			
0.000001	10^{-6}	-	

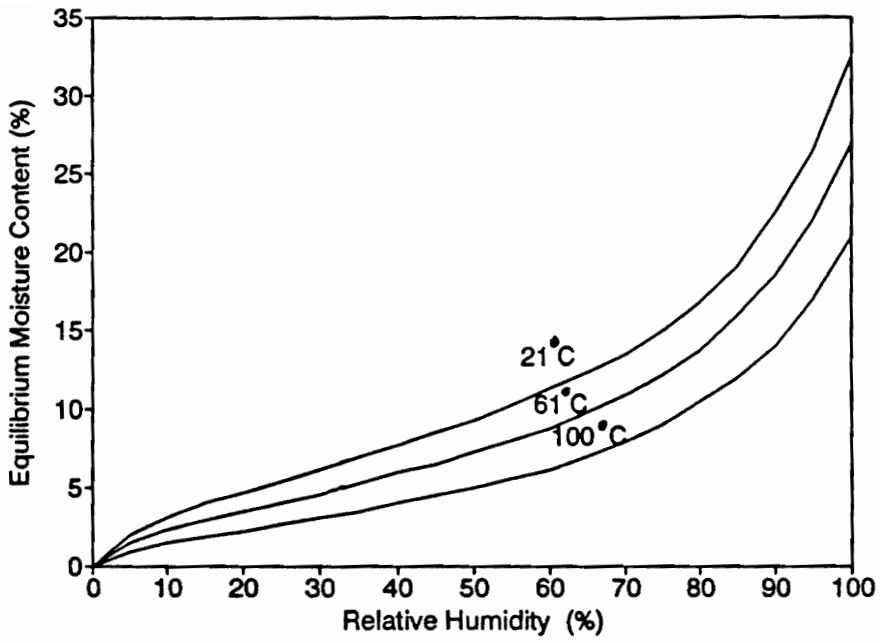

Figure 2.1. Sorption isotherms of wood at three temperatures (based on Siau 1984).

CHAPTER III

MODELLING SIMULTANEOUS HEAT AND MASS TRANSFER IN WOOD

3.1 Introduction

In the forest products industry there are important production processes which directly involve simultaneous heat and mass transfer, such as wood drying and hot pressing. The greatest difficulty of studying these processes is the complicated interactions of heat and mass transfer mechanisms. Extensive characterization of those physical processes using a strictly experimental approach is extremely difficult because of the excessively large number of variables that must be considered. However, mathematical modeling and numerical techniques will serve as a powerful tool to help us understand and optimize the complicated physical process.

A mathematical model of wood drying developed by Stanish et al. (1986) has been applied in this research to study heat and mass transfer. In this model, mathematical formulations for the transport rates are incorporated into one-dimensional partial differential material and energy balance equations which are coupled with algebraic relations for local phase equilibria. The details of the model development can be fund in several literature sources (Schajer et al. 1984, Stanish et al. 1985, 1986).

In this chapter, the principle of this mathematical model will be briefly reviewed, and the numerical technique we applied to solve the model will be discussed.

3.2 Mathematical Model of Heat and Mass Transfer

3.2.1 Assumptions

There are several basic assumptions applied to this model:

1. Mass and energy transfer are one-dimensional.

2. Moisture of wood can exist in three different phases: vapor, bound water, and free water.

3. Local thermal and phase equilibria are always obeyed.

4. Migration of the bound water occurs by molecular diffusion process derived by the chemical potential of the bond molecules.

5. Bulk flows of liquid and gases follow Darcy' law.

3.2.2 Heat and Mass Transfer Mechanisms

Water inside solid wood can exist in three phases: liquid (free water in void), gas (water vapor) and bound (sorbed water in cell wall). In the model, the mass of each water component is expressed as mass per unit volume of wood.

1) For the liquid phase, the migration rate of the free liquid phase is assumed to follow Darcy's law for flow through porous media. Therefore, the flux is proportional to the gradient in pressure within the liquid. The total pressure within the liquid phase is equal to the total local gas pressure less the capillary pressure associated with the gas-liquid interface. Bulk flows of liquid and gases follow Darcy's Law:

$$n_f = - \rho_w \frac{K_f}{\eta_w} \frac{\partial}{\partial z} (p_a + p_v - P_c) \quad , \qquad (3.1)$$

where n_f - free water flux, $kg/m^2/s$
ρ_w - liquid water density, kg/m^3
K_f - permeability of free water, m^2
η_w - liquid viscosity, kg/m/s
p_a - air pressure, Pa
p_v - partial water vapor pressure, Pa
P_c - capillarity pressure, Pa
z - space variable, m

The total gas pressure within the liquid phase is equal to total local gas pressure ($p_a + p_v$) less the capillary pressure, P_c. The gas pressure is defined as:

$$p_v = \frac{R\ T\ \rho_v}{\epsilon\ M_v} \quad ,$$

$$p_a = \frac{R\ T\ \rho_a}{\epsilon\ M_a} \quad , \qquad (3.2)$$

where R - gas constant, J/mol/K
M_a - molecular weight of air, kg/mol
M_v - molecular weight of water vapor, kg/mol
ρ_a - air density, kg/m^3
ρ_v - water vapor density, kg/m^3
T - temperature, K
ϵ - effective void fraction

$$\epsilon = \epsilon_d - \frac{\rho_f}{\rho_w} \quad , \qquad (3.3)$$

where ϵ_d - dry wood void fraction
ρ_f - free water density, kg/m^3
ρ_w - liquid water density, kg/m^3

The capillary pressure, P_c (Pa) is defined as:

$$P_c = 10000\left(\frac{\rho_f}{\epsilon_d\,\rho_w}\right)^{-0.61} \quad . \qquad (3.4)$$

2) For the gas phase, the mass transport for the flux of water vapor, n_v, in a binary gas mixture (air and water vapor) is described with the convective or bulk-flow term expressed in the form of Darcy's law for flow through porous media and the molecular diffusion. The flux of air, n_a, is given by a completely analogous form.

$$n_v = -\frac{\rho_v}{\epsilon}\frac{K_g}{\eta_g}\frac{\partial}{\partial z}(p_a+p_v) - \frac{M_v}{\epsilon}\left(\frac{\rho_a}{M_a}+\frac{\rho_v}{M_v}\right)D^{eff}\frac{\partial}{\partial z}\left(\frac{p_v}{p_a+p_v}\right) \qquad (3.5)$$

$$n_a = -\frac{\rho_a}{\epsilon}\frac{K_g}{\eta_g}\frac{\partial}{\partial z}(p_a+p_v) - \frac{M_a}{\epsilon}\left(\frac{\rho_a}{M_a}+\frac{\rho_v}{M_v}\right)D^{eff}\frac{\partial}{\partial z}\left(\frac{p_a}{p_a+p_v}\right) \qquad (3.6)$$

where n_v - water vapor flux, $kg/m^2/s$
n_a - air flux, $kg/m^2/s$
K_g - relative gas permeability, m^2
η_g - gas viscosity, kg/m/s
D^{eff} - effective gas diffusivity, m^2/s

3) For the bound phase, the flux of bound water, n_b, is assumed to be proportional to the gradient in the chemical potential of the bound molecules and to the volume fraction of space occupied by the cell wall matrix. Since thermodynamic equilibrium is assumed at every location, the chemical potential of the bound molecules is by definition equal to the chemical potential of the water vapor. This is an important premise developed in Stanish's model (Stanish, 1986). Bound water migration is a molecular diffusion process whose flux is proportional to the gradient in the chemical potential of the sorbed molecules. No assumptions regarding

temperature-driven diffusion are necessary because a contribution from the temperature gradient arises from the chemical potential expression.

$$n_b = -D_b(1-\epsilon_d)\,\partial\frac{\mu_b}{\partial z}$$

$$= -D_b(1-\epsilon_d)\left[-\left(\frac{S_v}{M_v}\right)\frac{\partial T}{\partial z}+\left(\frac{\epsilon}{\rho_v}\right)\frac{\partial p_v}{\partial z}\right], \qquad (3.7)$$

where n_b - bound water flux, $kg/m^2/s$
D_b - boundary water diffusivity, $kg.s/m^3$
S_v - water vapor entropy, J/mol/K
μ_b - chemical potential, J/kg

3.2.3 Governing Equations

The mathematical description of this model is a comprehensive set of fundamental heat and mass equations coupled with thermodynamic phase equilibrium expressions. Since the physical properties vary in both space and time, transport properties which are functions of physical properties therefore also vary in space and time.

There are five governing equations included in this mathematical model:

1. mass balance for air;

2. mass balance for water;

3. energy balance of air and water;

4. phase equilibrium condition describing vapor-liquid saturation relations derived from steam table;

5. phase equilibrium condition describing the bound water sorption relation derived by Simpson (1971).

The five equations are:

$$\frac{\partial}{\partial t}(\rho_a) = -\frac{\partial}{\partial z}(n_a) \quad , \tag{3.8}$$

$$\frac{\partial}{\partial t}(\rho_v+\rho_b+\rho_f) = -\frac{\partial}{\partial z}(n_v+n_b+n_f) \quad , \tag{3.9}$$

$$\frac{\partial}{\partial t}(\rho_a h_a+\rho_v h_v+\rho_b h_b+\rho_f h_f+\rho_d h_d) = -\frac{\partial}{\partial z}(n_a h_a+n_v h_v+n_b h_b+n_f h_f-\kappa\frac{\partial T}{\partial z}) \quad , \tag{3.10}$$

$$\rho_v^{sat} = \epsilon \exp[-46.49 + 0.26179T - 5.014*10^{-4}T^2 + 3.4712*10^{-7}T^3] \quad , \tag{3.11}$$

$$\rho_v = \rho_v^{sat}\{a_4(T) + [a_4^2(T) + \frac{1}{a_1(T)\ a_2^2(T)}]^{0.5}\} \quad , \tag{3.12}$$

where t - time, s
z - space variable, m
h_a - enthalpy of air, J/kg
h_v - enthalpy of water vapor, J/kg
h_b - enthalpy of boundary water, J/kg
h_f - enthalpy of free water, J/kg
h_d - enthalpy of solid wood, J/kg
κ - thermal conductivity of moist wood, W/s/K

a_1 to a_4 are bound water equilibrium coefficients which are given empirically by the following definitions:

$$a_1 = -45.7 + 0.3216(T) - 5.012x10^{-4}(T)^2 \quad ,$$
$$a_2 = -0.1722 + 4.732x10^{-3}(T) - 5.553x10^{-6}(T)^2 \quad ,$$
$$a_3 = 1417 - 9.43(T) + 1.853x10^{-2}(T)^2 \quad ,$$
$$a_4 = \frac{[1-(\frac{18\rho_d}{a_3\rho_b})]}{2a_2} - \frac{[1+(\frac{18\rho_d}{a_3\rho_b})]}{2a_1a_2} \quad .$$

The model contains five equations including five dependent variables: the density of air (ρ_a), density of water vapor (ρ_v), density of bound water (ρ_b), density of free water (ρ_f) and temperature (T). The density here can also be referred to as the content of air, water vapor, bound water and free water respectively. The five parameters vary with the two independent variables: space (z) and time (t). They are actually a set of coupled differential-algebraic equations.

3.2.4 Initial Conditions and Boundary Conditions

The three partial differential balance equations [(3.8), (3.9), (3.10)] require initial profiles of temperature, air content and water content. They also require satisfaction of three boundary conditions at the surfaces of the solid wood. First, the total gas pressure at each surface must equal the ambient pressure. Second, the total flux of moisture within the solid at each surface must equal the flux of water vapor through the external boundary layer. Third, the total energy flux within the solid at each surface must equal the total energy flux through the external boundary layer. Conditions at each boundary are independent of each other, may vary with time, and are characterized by convective heat and moisture transfer coefficients.

3.3 Numerical Solutions

The analytical solution for such a complicated set of partial differential equations is not known. To solve this mathematical model, numerical methods are needed. In this research, the numerical technique applied is the finite difference method.

3.3.1 Transformation of Mathematical Model

The mathematical model described by the equations, (3.8) - (3.12), is represented as a set of coupled differential-algebraic equations. A more computationally efficient approach (Stanish et al, 1985, 1986) can be applied to reduce the number of dependent variables from five to three.

It is assumed in this model that local thermal and phase equilibria are always obeyed inside solid wood. Therefore, if the local free water density is non-zero, the gas phase at that point is assumed saturated at the local temperature. In the absence of free water, the gas phase is assumed to be in equilibrium with respect to the local bound water content and temperature. Based on those assumptions, the two equilibrium equations (3.11) and (3.12) are incorporated into the three balance equations (3.8), (3.9) and (3.10). As a result, ρ_m replaces the three separate variables, i.e. $\rho_m = \rho_v + \rho_b + \rho_f$. By applying the phase equilibrium conditions, the set of differential-algebraic equations is transformed to a set of three second order partial differential equations (PDE's). Figure 3.1 illustrates the logic of the variable separation procedure.

3.3.2 Finite Difference Approximation

The mass flux n_f in equation (3.1) can be expressed as:

$$n_f = -f_{f1}\frac{\partial f_{f2}}{\partial z} \quad , \qquad (3.13)$$

where

$$f_{f1} = f_{f1}(\rho_m, T) = \frac{\rho_w K_f}{\eta_w} \quad ,$$
$$f_{f2} = f_{f2}(\rho_a, \rho_m, T) = p_a + p_v - P_c \quad .$$

Similarly, the mass flux expressions in equation (3.5), (3.6), and (3.7) can be expressed as:

$$n_v = -f_{v1}\frac{\partial f_{v2}}{\partial z} - f_{v3}\frac{\partial f_{v4}}{\partial z} \quad , \qquad (3.14)$$

where

$$f_{v1} = f_{v1}(\rho_a, \rho_m, T) = \frac{\rho_v K_g}{\epsilon \eta_g} \quad ,$$
$$f_{v2} = f_{v2}(\rho_a, \rho_m, T) = p_a + p_v \quad ,$$
$$f_{v3} = f_{v3}(\rho_a, \rho_m, T) = \frac{M_v}{\epsilon}\left(\frac{\rho_a}{M_a} + \frac{\rho_v}{M_v}\right) D^{eff} \quad ,$$
$$f_{v4} = f_{v4}(\rho_a, \rho_m, T) = \frac{p_v}{p_a + p_v} \quad .$$

$$n_a = -f_{a1}\frac{\partial f_{a2}}{\partial z} - f_{a3}\frac{\partial f_{a4}}{\partial z} \quad , \qquad (3.15)$$

where

$$f_{a1} = f_{a1}(\rho_a, \rho_m, T) = \frac{\rho_a K_g}{\epsilon \eta_g} \quad ,$$
$$f_{a2} = f_{a2}(\rho_a, \rho_m, T) = p_a + p_v \quad ,$$
$$f_{a3} = f_{a3}(\rho_a, \rho_m, T) = \frac{M_a}{\epsilon}\left(\frac{\rho_a}{M_a} + \frac{\rho_v}{M_v}\right) D^{eff} \quad ,$$
$$f_{a4} = f_{a4}(\rho_a, \rho_m, T) = \frac{p_a}{p_a + p_v} \quad .$$

$$n_b = -f_{b1}\frac{\partial f_{b2}}{\partial z} - f_{b3}\frac{\partial f_{b4}}{\partial z} \quad , \qquad (3.16)$$

where

$$f_{b1} = f_{b1}(\rho_m, T) = D_b(1-\epsilon_d)\frac{S_v}{M_v} \quad ,$$
$$f_{b2} = f_{b2}(T) = T \quad ,$$
$$f_{f3} = f_{b3}(\rho_m, T) = D_b(1-\epsilon_d)\frac{1}{\rho_v} \quad ,$$
$$f_{b4} = f_{b4}(\rho_m, T) = p_v \quad .$$

Bring the equations (3.13), (3.14), (3.15), and (3.16) to the mass balance and energy balance equations, (3.8) - (3.10), the mathematical model, with the simplification, can be described as:

$$\frac{\partial \rho_a}{\partial t} = \frac{\partial f_{a1}}{\partial z}\frac{\partial f_{a2}}{\partial z} + f_{a1}\frac{\partial^2 f_{a2}}{\partial z^2} + \frac{\partial f_{a3}}{\partial z}\frac{\partial f_{a4}}{\partial z} + f_{a3}\frac{\partial^2 f_{a4}}{\partial z^2} \quad , (3.17)$$

$$\frac{\partial \rho_m}{\partial t} = \frac{\partial f_{v1}}{\partial z}\frac{\partial f_{v2}}{\partial z} + f_{v1}\frac{\partial^2 f_{v2}}{\partial z^2} + \frac{\partial f_{v3}}{\partial z}\frac{\partial f_{v4}}{\partial z} + f_{v3}\frac{\partial^2 f_{v4}}{\partial z^2} \quad , \qquad (3.18)$$
$$+ \frac{\partial f_{b1}}{\partial z}\frac{\partial f_{b2}}{\partial z} + f_{b1}\frac{\partial^2 f_{b2}}{\partial z^2} + \frac{\partial f_{b3}}{\partial z}\frac{\partial f_{b4}}{\partial z} + f_{b3}\frac{\partial^2 f_{b4}}{\partial z^2}$$
$$+ \frac{\partial f_{f1}}{\partial z}\frac{\partial f_{f2}}{\partial z} + f_{f1}\frac{\partial^2 f_{f2}}{\partial z^2}$$

$$\frac{\partial T}{\partial t} = \frac{\partial f_{e1}}{\partial z}\frac{\partial f_{e2}}{\partial z} + f_{e1}\frac{\partial^2 f_{e2}}{\partial z^2} + f_{e3}\frac{\partial f_{e1}}{\partial z} \quad . \qquad (3.19)$$

where f_{e1}, f_{e2}, and f_{e3} are the function of ρ_a, ρ_m, and T.

The first and second derivatives of each function expression appearing at the right hand side of the equations, (3.17) - (3.19), are approximated at each mesh point in finite difference froms. Equally spaced mesh points are chosen as $z_o < z_1 < z_2$ ..... $< z_n < z_{n+1}$. The derivatives are replaced by centered difference approximations:

$$f_i' = \frac{f_{i+1} - f_{i-1}}{2h} \quad , \qquad (3.20)$$

$$f_i'' = \frac{f_{i+1} - 2f_i + f_{i-1}}{h^2} \quad , \qquad (3.21)$$

where

$$h = \frac{z_{n+1} - z_o}{n+1} \quad .$$

Alllying the finite difference approximations, the group of coupled second order partial differential equations (PDE's) becomes a group of coupled ordinary differential equations (ODE's) with the spatial form:

$$\frac{d}{dt}\begin{bmatrix} \rho_{a1} \\ \rho_{m1} \\ T_1 \\ \rho_{a2} \\ \rho_{m2} \\ T_2 \\ . \\ . \\ . \\ . \\ . \\ \rho_{an} \\ \rho_{mn} \\ T_n \end{bmatrix} = \begin{bmatrix} f_1(\rho_{a1},\rho_{m1},T_1,\rho_{a2},\rho_{m2},T_2) \\ f_2(\rho_{a1},\rho_{m1},T_1,\rho_{a2},\rho_{m2},T_2) \\ f_3(\rho_{a1},\rho_{m1},T_1,\rho_{a2},\rho_{m2},T_2) \\ f_4(\rho_{a1},\rho_{m1},T_1,\rho_{a2},\rho_{m2},T_2,\rho_{a3},\rho_{m3},T_3) \\ f_5(\rho_{a1},\rho_{m1},T_1,\rho_{a2},\rho_{m2},T_2,\rho_{a3},\rho_{m3},T_3) \\ f_6(\rho_{a1},\rho_{m1},T_1,\rho_{a2},\rho_{m2},T_2,\rho_{a3},\rho_{m3},T_3) \\ . \\ . \\ . \\ . \\ . \\ f_{3n-2}(\rho_{a(n-1)},\rho_{m(n-1)},T_{n-1},\rho_{an},\rho_{mn},T_n) \\ f_{3n-1}(\rho_{a(n-1)},\rho_{m(n-1)},T_{n-1},\rho_{an},\rho_{mn},T_n) \\ f_{3n}(\rho_{a(n-1)},\rho_{m(n-1)},T_{n-1},\rho_{an},\rho_{mn},T_n) \end{bmatrix} \qquad (3\text{-}22)$$

3.3.3 Numerical Procedure (LSODE)

The coupled ODE's are numerically integrated using a specialized solver, LSODE, developed by Hindmash (1980). LSODE is an initial value ordinary differential equation solver, which solves ODE systems given explicitly as $dy/dt = f(t,y)$. This particular solver has the option of using a knowledge of the sparsity structure of the Jacobian matrix to avoid redundant computation of zero-valued entries, and handles the stiff equations encountered here reliably and effectively.

To apply the numerical solver, first we need to write a main program, which calls subroutine LSODE once for each point at which solutions for ρ_m and T are desired. Second we should write a user-supplied subroutine, which provides LSODE with the values at the right hand side of equation (3.22).

3.3.4 Structure of Computer Program

Figure 3.2 shows the structure of the computer program for solving the mathematical model of heat and mass transfer. The computations included in the user-supplied subroutine FEX are:

1) Variable Separation

We have shown how the equilibrium relationships are used to allow the solver to work with the three dependent variables ρ_a, ρ_m, and T. At the start of each evaluation at the right-hand side of equation (3.22), the subroutine extracts the individual phases (ρ_f,ρ_v,ρ_b) from the total moisture ρ_m using the vapor and bound water equilibrium relations.

2) Boundary Conditions

The conditions at the two boundaries are independent of each other, may vary with time, and are characterized by convective transfer coefficients. At each time step of numerical integration, the boundary values (ρ_{ao}, $\rho_{a(n+1)}$, ρ_{mo}, $\rho_{m(n+1)}$, T_o, $T_{o(n+1)}$) at the surfaces are unknown. To satisfy the boundary condition requirements described in section 3.2.3, the boundary values are determined explicitly by applying the numerical routine HYBRD1 to solve a nonlinear system of equations.

3) Finite Difference Approximation

The subroutine then uses all five dependent variables (ρ_a,ρ_f,ρ_v,ρ_b,T) at all mesh points to approximate the heat and mass flow quantities as well as the mass and energy balances at the right hand side of equation (3.22), using finite differences.

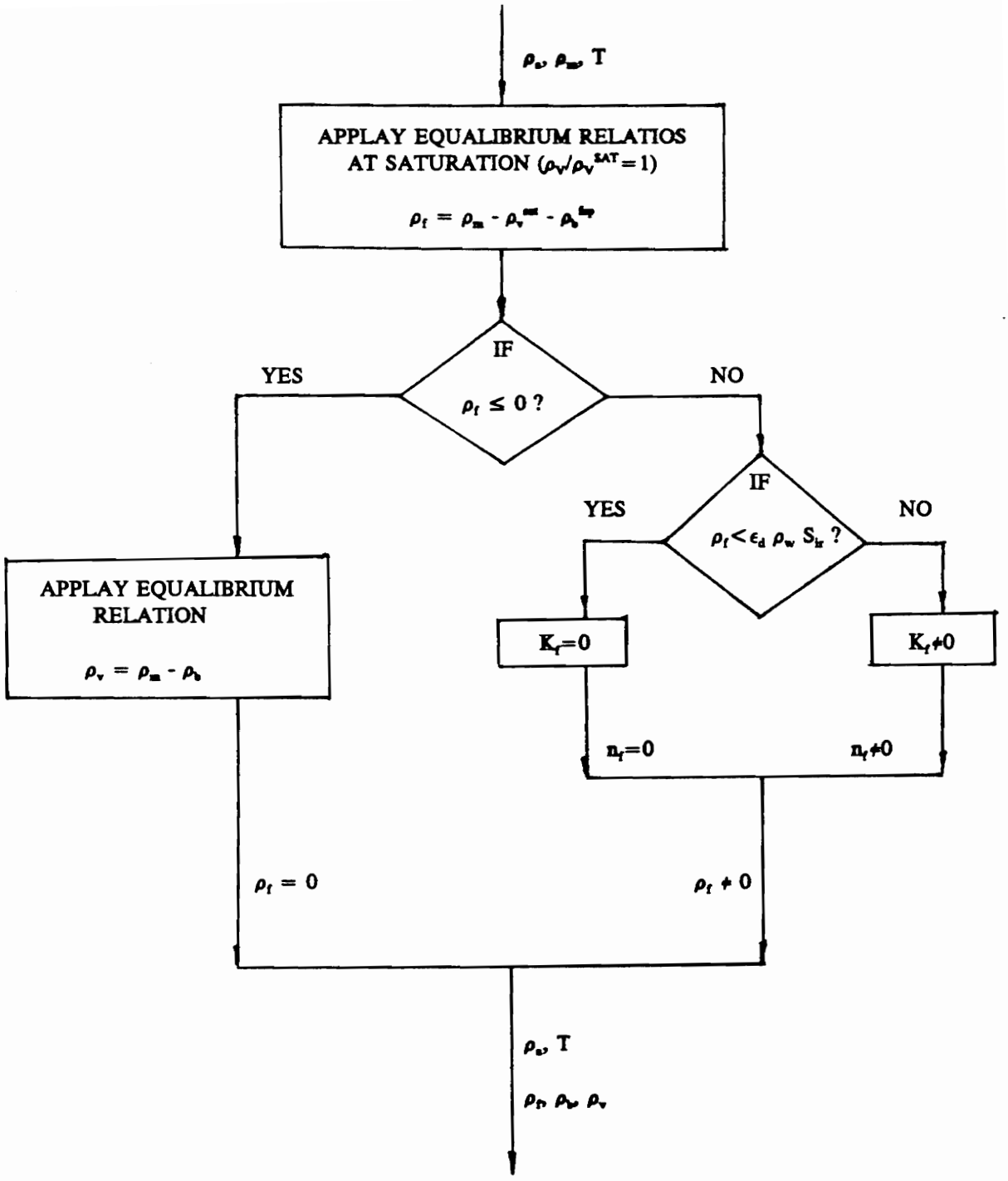

Figure 3.1 Scheme of variable separation.

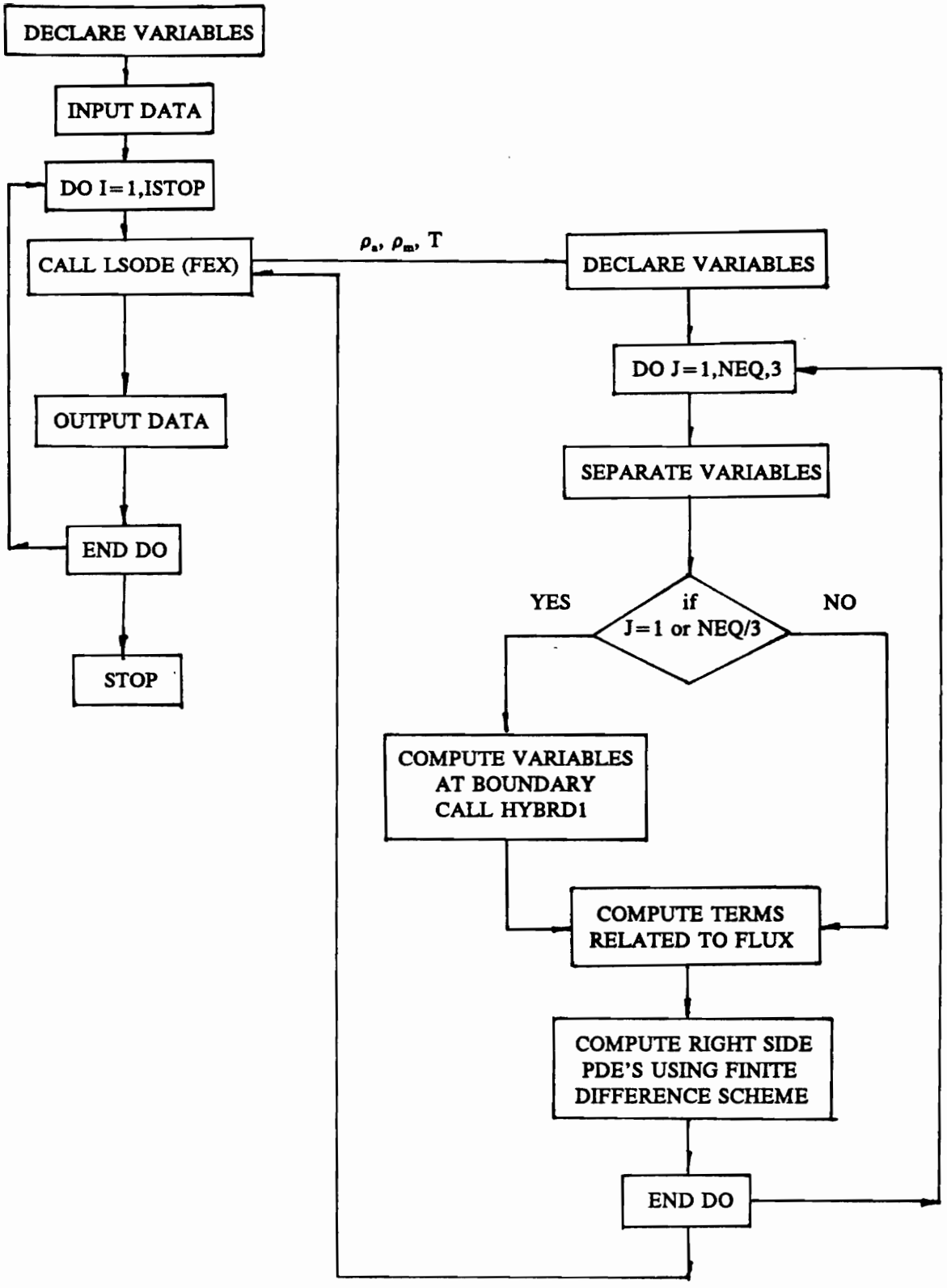

Figure 3.2 Structure of computer program.

CHAPTER IV

RESULTS AND DISCUSSION

4.1 Introduction

The following subjects are discussed in this chapter:

1) The modeling results from the finite difference method;

2) The sensitivity study of the drying parameters on the heat and mass transfer using the finite difference method.

4.2 Numerical Results of Finite Difference Method

The computer model has been developed to solve the one dimensional heat and mass transfer problem. Three coupled partial differential equations are discretized at their right hand sides with finite-difference approximations, which results in a system of ordinary differential equations (ODE's). The ODE's are solved by the specific initial value ODE solver LSODE.

To test the model's computational performance, the one dimensional wood drying process is simulated. Symmetric boundary conditions are assumed. The species is assumed to be a softwood, and is 50.8 mm (2 inch) in thickness.

The input for the numerical model is listed in Table 4.1. To select the basic drying parameters, we refer to the simulation results by Stanish et.al (1986). The simulation is performed for a 50.8 mm (2 in) thick of southern pine lumber specimen, which was dried symmetrically in one dimension. The dry temperature was 75 °C

with air velocity of 13 m/s, and dew point of 10 °C. Fitting the simulation results to the experimental data yielded the following set of model parameters:

$K_g^d = 5.0 \times 10^{-15}$ m^2

$K_f^s = 5.0 \times 10^{-16}$ m^2

$\alpha = 0.05$

$D_b = 3.0 \times 10^{-13}$ $kg.s/m^3$

$S_{ir} = 0.1$

$k_h = 87$ $W/m^2/K$

4.2.1 Central Temperature and Average Moisture Content

The center temperature and average moisture content were chosen to represent the trend of the heat and mass transfer processes. Figure 4.1 shows the modeling results by applying the finite difference method. In this graph, one line represents the temperature increase as the time increases at the center of the specimen. The other line represents the change of the average moisture content of the specimen as time progresses. By observation, the center temperature quickly reaches steady state. The average moisture content of the wood continuously reduces as drying time increases. Therefore, the process of heat transfer is much faster than that of mass transfer. Figure 4.2. shows the moisture drying rate. The moisture drying rate in the early stage is high, because the free water inside the specimen has a higher energy level than bound water, and is easily transported inside the cell wall lumen. The drying rate reduces as the time increases, because the bound water is more difficult to remove.

4.2.2 Temperature Profile

Figure 4.3 shows the temperature profile as it changes with time. It is noticed from the figure that the temperature near the surfaces increases very fast. The temperature close to the center of the specimen increases more slowly. Eventually the temperature becomes uniformly distributed throughout the whole thickness of the specimen. Figure 4.3 also shows that in the early drying stage the difference between the surface and the center is great. As the time proceeds, the temperature difference disappears.

4.2.3 Moisture Profile

Figure 4.4. shows the moisture profile of the simulation results. The model simulation indicates that at 80°C, the external wood surface dries very rapidly with an accompanying rise of the internal temperature. A wet-line drying front appears, with the wood outside below the fiber saturation point and that inside still retaining some liquid water. The liquid water is conveyed from the interior to the drying front, but at a rate slower than the transport of moisture from the front to the wood surface, The front therefore travels inward through the wood as drying proceeds. These observations suggest that at this drying temperature, both external heat transfer and internal moisture transport play important roles in determining the drying rate, however, internal moisture transport predominates.

4.2.4 Comments on Numerical Solution

The modeling results have been compared to the results reported by Stanish et al (1986). A close agreement was found. We have evaluated the number of intervals necessary for consistent and accurate modeling results, and found that 167 intervals are adequate. The following sensitivity study uses 167 intervals in all simulations.

4.3 Sensitivity Study

The wood drying process is an extremely complicated physical process, which includes simultaneous heat and mass transfer. There are numerous factors and parameters involved in the wood drying process, which makes it difficult and inefficient to study the interactions of heat and mass transfer during wood drying by only an experimental approach.

The primary advantages of the mathematical modelling approach are: (1) to predict the drying process based on the existing drying parameters; (2) to study the sensitivity of each drying parameters during the wood drying process. The sensitivity study will give us better understanding of the interaction of heat and mass transfer, and help us to optimize the drying operation.

There are different ways to carry out the sensitivity studies. A simple and direct approach was chosen to test the sensitivity of the model. One set of drying conditions including all the necessary drying parameters, was selected as the control or base drying case. To discuss the sensitivity of each drying parameter, the parameter discussed is varied at different values while the remainder of the drying parameters remain unchanged. The differences in the center temperature and average

moisture content caused by variation of the parameter was observed. The purpose of the sensitivity study is to determine the effects of each individual drying parameter on the drying process, and to give a reasonable physical explanation to those effects. In addition, the sensitivity study provides information to asses the reliability of the modelling approach.

The drying parameters are divided into two groups: the first group represents the material properties. The second group includes the initial and boundary conditions. In order to make an easy comparison, all the results of the sensitivity study are based on drying parameters described in Table 4.1.

4.3.1 Material Physical Properties

4.3.1.1 Dry Wood Gas Permeability K_g^d

The mass transport of water vapor in the air and water vapor mixture consists of two types of flux. One results from Darcy's law for flow through the porous media. The other results from the molecular diffusion of water vapor in air. The convective or bulk flow rate depends on the relative permeability K_g.

The relative permeability K_g of wet wood is directly related to the dry wood gas permeability K_g^d. The effective gas permeability of wood is defined as:

$$K_g = K_g^d \left(1 - \frac{\rho_f}{\epsilon_d \rho_w}\right) \qquad (4.1)$$

where K_g - relative gas permeability of wet wood, m^2.

K_g^d - gas permeability of dry wood, m^2.
ρ_f - density of free water, kg/m^3.
ρ_w - density of liquid water, kg/m^3.
ϵ_d - dry wood void fraction, %.

Based on equation (4.1), the higher the dry wood gas permeability, the higher becomes the wood effective gas permeability. During the wood drying process, the free water continuously decreases, causing the effective gas permeability of wood to increase.

The dry wood gas permeability values are varied at $\pm 50\%$ of $5x10^{-15}$ m^2. There is no change observed in either the average moisture content or the center temperature. Then the gas permeability values are varied at $5x10^{-15}$, $5x10^{-16}$ and $5x10^{-17}$ m^2. These values are comparable to the transverse gase permeability listed in Table 2.1. Permeability is an extremely variable property of wood. It would by expected to vary in several orders among the softwood species.

Figure 4.5 shows the effects of the dry wood gas permeability on moisture transfer. The results indicate that the moisture drying rate decreases as dry wood gas permeability decreases. High gas permeability of dry wood means low resistance to the bulk flow of water vapor, which results in faster moisture movement. This is consistent with Darcy's law for flow through porous media, where the bulk flow rate is proportional to the effective permeability. We also notice that as the dry wood gas permeability increases, the effects on moisture transfer becomes less significant. It may suggest that at the conditions simulated, the build up of air and water vapor pressure is limited to some extent, where increasing gas permeability has less effects on the gas phase moisture transfer.

Figure 4.6 shows some effects of gas permeability on the temperature increase. For the conditions simulated, the permeability increase has no effect on the rate of the center temperature rise, due to the increase in bulk flow of water vapor.

4.3.1.2 Attenuation Factor α

We have mentioned that the mass transport of water vapor in the air and water vapor mixture consists of two types of flux. One results from Darcy's law for flow through porous media. The second results from the molecular diffusion of water vapor in the air. The molecular diffusion rate depends on the effective diffusivity D^{eff}. For the binary air-gas mixture of air and water vapor, considering the porous solid and the nature of wood cellulose components and wood structure, Stanish (1986) defined the effective diffusivity as:

$$D^{eff} = \alpha\ \epsilon^2\ D_{AB}$$
$$= \alpha\ \epsilon^2\ 2.20x0^{-5} \left(\frac{101325}{p_a + p_v}\right) \left(\frac{T}{273.15}\right)^{1.75} \qquad (4.2)$$

where ϵ - effective porosity.
T - temperature, K
p_a - air pressure, Pa
p_v - water vapor pressure, Pa
α - attenuation factor

The attenuation factor accounts for the hindrance of diffusion due to wood structure and porosity. Based on the equation (4.2), changing the attenuation factor will change the effective diffusivity of wood. Therefore, the study of the effects of attenuation factor on moisture transfer is directly related to the study of the effective

diffusivity on moisture transfer.

The attenuation factor values were varied within the range $\pm$ 50% of 0.05 (0.025, 0.0375, 0.05, 0.0625 and 0.075). Figure 4.7 shows the effects of attenuation factor on the moisture drying rate. The results indicate that as the attenuation factor increases, the moisture transfer rate increases. Because the increase in attenuation factor causes the increase in the effective gas diffusivity, the mass transfer rate increases.

Figure 4.8 shows the effects of the attenuation factor on the heat transfer process. As the attenuation factor increases, the heat transfer rate slightly increases due to the increase in mass flow.

4.3.1.3 Bound Water Diffusivity D_b

As reviewed in the previous chapter, the flow of bound water is assumed to obey Fick's law of diffusion. The flow rate of bound water depends on the bound water diffusivity, and the gradient in chemical potential. The bound water diffusivity is varied at $\pm$50% of 3.0×10^{-13} kg.s/m^3. There is no change observed in either the average moisture content or the center temperature. The sensitivity of bound water diffusion coefficient is then tested at the diffusivity values of 3.0×10^{-11}, 3.0×10^{-12}, and 3.0×10^{-13} kg.s/m^3. These values are comparable to the transverse bound water diffision coefficients of wood cell wall described in literature (Skaar, 1988; Siau, 1984). Bound water D_b is assumed a constant in this model.

Figure 4.9 shows the effects of the bound water diffusivity on the moisture

drying process. The results illustrate that as the bound water diffusivity increases, the moisture drying rate increases. This result is consistent with Fick's diffusion law. The graph also shows that when diffusivity is reduced to certain values, the effects on the moisture drying process are limited. This may suggest that at the high diffusivity values, the diffusion flow of bound water is the most significant mechanism of moisture transfer.

Figure 4.10 shows the effects of bound water diffusivity on the center temperature rise. The results show that the increase of bound water diffusivity slightly reduces the rate of the temperature increase. This phenomena could be explained by the chemical potential which is the driving force of bound water diffusion. As described before, the chemical potential of the bound water is determined by the chemical potential of water vapor. Chemical potential of water vapor is affected by both the temperature and water vapor pressure. High vapor pressure and low temperature will lead to a high value of water vapor chemical potential. Therefore, the higher bound water flux results from higher water vapor gradient and lower temperature gradient.

4.3.1.4 Saturated Water Permeability K_f^s

The relative permeability of the solid to liquid flow is dependent on the relative saturation and on the permeability of the solid when the voids are completely filled by liquid. Below a certain critical relative saturation, or irreducible saturation, the relative permeability falls to zero and liquid migration ceases due to a loss of

continuity in the liquid phase. Above the irreducible saturation, the relative permeability increases with increasing relative saturation. For wood the effective permeability is expressed by (Stanish, 1986):

$$K_f \begin{cases} = 0 & \rho_f < \epsilon_d \rho_w S_{ir} \\ = K_f^s \left[1-\cos\left(\frac{\pi}{2}\frac{(\rho_f/\epsilon_d\rho_w)-S_{ir}}{1-S_{ir}}\right)\right] & \rho_f \geq \epsilon_d \rho_w S_{ir} \end{cases} \qquad (4.3)$$

where S_{ir} -- irreducible saturation, fraction.

Based on the equation (4.3), effective liquid water permeability K_f (m^2) is dependent on the saturate water permeability K_f^s (m^2). Increasing the saturated water permeability will increase the effective liquid water permeability.

The saturated water permeability values were varied at $\pm$ 50% of 5.0×10^{-16} m^2. There is no change observed in either the average moisture content or the center temperature. The sensitivity of the saturated water permeability is then tested at the values of 5×10^{-15}, 5×10^{-16}, and 5×10^{-17}. Permeability of liquid water is expected to vary in several order because of the microstructure variation of wood. The results indicate that at 40% initial moisture content, the saturated water permeability does not affect the heat and mass transfer process significantly. Increasing the saturated water permeability does not affect the rate of moisture drying and temperature rise. A similar observation was also made at 60% initial moisture content. The possible explanation could be that at this moisture level at relatively high temperature 80°C, the Darcy's flow of the free water phase is not significant due to the small amount of free water in the cell lumen. Figure 4.11 and 4.12 shows the modelling results.

4.3.1.5 Density ρ_d

The density of the dry wood affects the porosity, which is defined as:

$$\epsilon_d = 1 - \frac{\rho_d}{\rho_{cell}} \qquad (4.4)$$

where ρ_d - density of dry wood, kg/m^3
ρ_{cell} - density of cell wall substance, kg/m^3

The porosity determines the fractional volume not occupied by cell wall substance inside the wood specimen. Because both free water and water vapor will travel through cell lumens, the porosity will definitely affect the drying process. We have discussed in Chapter II, that the porous structure of wood does not necessarily mean that it is highly permeable. But if the wood is permeable, the increase of porosity will increase the permeability of the wood. Also, as the porosity increases, cell wall substance takes up less space. Therefore, more free water may exist in the lumens above the fiber saturation point. Because bound water has a lower energy level than free water and water vapor, the water in the cell lumen is easier to remove than bound water inside the cell wall.

The density of the dry wood also affects the thermal conductivity, which is defined in this model (Stanish, 1986) as:

$$\kappa = \frac{\rho_d}{1000}\left[0.40 + 0.50\frac{\rho_m}{\rho_d}\right] + 0.24 \qquad (4.5)$$

where ρ_d - density of dry wood, kg/m^3.
ρ_m - density of water per unit volume of wood, kg/m^3.

From equation (4.5), the conductivity also is affected by the moisture content. In chapter II, we have discussed that increasing moisture content of wood will increase its thermal conductivity. At high moisture content, the term related to moisture content in equation (4.5) is significant, and can not be neglected.

Figure 4.13 shows the combined effects of porosity and thermal conductivity on the drying process. The dry wood density was examined over the range of $\pm 50\%$ of 480 kg/m_3, which are 240, 360, 480, 600 and 720 kg/m^3. From equation (4.4) and (4.5) the porosity values of dry wood are calculated as 0.84, 0.76, 0.68, 0.60, and 0.52, and the thermal conductivity values of wood at 40% moisture content are calculated as 0.356, 0.404, 0.452, 0.500 and 0.548 W/s/K. The results indicate that the porosity has more significant effects on moisture transfer. As the porosity decreases, the moisture movement slows down.

Figure 4.14 shows the combined effects of porosity and thermal conductivity on the heat transfer process. The graph shows that although the thermal conductivity increases as the wood density increases, the highest rate of temperature increase during the initial stage happens at the lowest wood density. This is because at lower wood density there is less water to evaporate for the same amount of energy transferred to the specimen. Because the higher density wood requires more energy for the latent heat of vaporization, there is less energy available to supply the specific heat necessary to increase temperature. This effect is most evident when the moisture content is greater than the FSP.

4.3.2 Initial Conditions and Boundary Conditions

4.3.2.1 Initial Moisture Content

To determine the effects of the wood moisture content on the heat and moisture transfer processes, the initial moisture content of the wood specimen was varied within the range of $\pm 50\%$ of 40 %, which was 20%, 30%, 40%, 50% and 60%. The other drying parameters remain unchanged. Figure 4.15 shows how the average moisture content changes as the drying time increases. In the time period observed, the drying rate increases as the initial moisture content increases. This is because when the moisture content is above the FSP, there is more existing free water at higher moisture content than at lower moisture content. Since the water vapor and free water in the cell wall lumen have a higher energy level than the bound water inside the cell wall, the water vapor and free water require less energy to be removed than the bound water does. When the moisture content is below the FSP, the water vapor pressure decreases as the moisture content decreases. For the same reason, more energy is required to remove the water at lower moisture content than at higher moisture content.

Figure 4.16 shows the effects of initial moisture content on the heat transfer. As the initial moisture content decreases, the center temperature increases much more quickly. This is because that at lower initial moisture content, there is less water to evaporate for the same amount of energy transferred to the specimen, which causes the temperature to increase more quickly.

4.3.2.2 Drying Temperature

To investigate the sensitivity of the drying temperature on the heat and mass transfer process, the simulation was conducted at drying temperatures of 60°C, 70°C, 80°C and 90°C. Figure 4.17 shows the effects of drying temperature on the moisture drying process. The results indicate that as the drying temperature increases, the moisture transfer rate increases. These results demonstrate the interactions of heat transfer and moisture transfer. The increase of temperature increases the water vapor pressure, therefore increasing the rate of moisture movement. The results show the drying rate is mainly controlled by the temperature.

Figure 4.18 shows the effects of the drying temperature on the heat transfer. The results indicate that it takes longer time to reach steady-state heat transfer for a higher drying temperature.

4.3.2.3 Relative Humidity (RH)

The effects of the relative humidity at the boundary on the mass transfer is shown in Figure 4.19. At the boundary, the total gas pressure remains at atmospheric pressure (1 atm), and the relative humidity is varied at 2%, 10%, 20% and 30%, while the other drying parameters remain unchanged. The results show that convective mass transfer at the surface is reduced and surface moisture content decreases at a slower rate. Consequently, the potential for moisture transfer inside the wood is reduced.

Figure 4.20 shows the effects of relative humidity on the heat transfer. The

results indicate that the relative humidity does not significantly influence the process of heat transfer. Because the process of heat transfer is much faster than that of mass transfer, the temperature at the boundary will quickly reach the drying temperature.

4.3.2.4 Heat Transfer Coefficient k_h

Figure 4.21 shows the effects of heat transfer coefficient on the process of mass transfer. The results indicate that the heat transfer coefficient does not affect the mass transfer process significantly. This means the drying rate for this simulated wood specimen is controlled by mass transfer mechanisms, as would be expected for thick wood.

Figure 4.22 shows the effects of heat transfer coefficient on the heat transfer process. The heat transfer coefficient was varied within the range of $\pm 0\%$ of 50 $J/s/m^2/K$, which was 25, 37.5, 50, 62.5 and 75 $J/s/m^2/K$. The results indicate that the heat transfer coefficient at the drying boundary affects the heat transfer process. As the heat transfer coefficient increases, the heat transfer rate increases and it takes less time to reach the steady-state heat transfer.

4.3.2.5 Mass Transfer Coefficient k_m

Mass transfer coefficient affects the moisture drying rate. The mass transfer coefficient is determined from the drying conditions, such as the air speed, and the type of flow, such as turbulent flow or laminate flow. Figure 4.23 shows the effects of mass transfer coefficient on the mass transfer process. The mass transfer

coefficient values were varied within the range of $\pm 50\%$ of 0.03 mol/m^2/s, which were 0.015, 0.0225, 0.03, 0.0375 and 0.045 mol/m^2/s. The results indicate that the mass transfer coefficient at the drying boundary affects the mass transfer process. As the mass transfer coefficient increases, the moisture transfer rate increases.

Figure 4.24 shows the effect of mass transfer coefficient on the process of heat transfer. The results indicate that the mass transfer coefficient does not effect the heat transfer process significantly.

4.3.3 Summary of Sensitivity Study

Extensive characterization of those physical processes using a strictly experimental approach is extremely difficult because of the excessively large number of variables that must be considered. However, using the numerical model we can perform the sensitivity studies to determine the effects of the wood properties and environmental conditions on the heat and mass transfer process. Based on the drying conditions and simulated wood specimen chosen, some comments could be made.

a) The heat transfer process happens much faster than the mass transfer process during wood drying. Therefore, the interactions of heat and mass transfer is more significant before the heat transfer reaches the steady-state. Then the temperature becomes a constant factor.

b) Temperature and initial moisture content are the most sensitive and determining parameters for the process of heat and mass transfer in wood.

c) The coefficients of effective gas permeability, effective gas diffusivity and

bound water diffusivity have significant effects on transport processes, especially the mass transport process. These parameters are greatly affected by the wood structure, temperature, and moisture content.

d) The drying boundary condition, especially the convective heat and mass transfer coefficients and the humidity, can affect the rate of wood drying. However, the thick specimen that was used in the simulation was more influenced by internal mechanisms of mass transfer.

4.4 Justification of the Numerical Approaches

The important advantage of the finite difference method is that it is easily implemented to solve the problems of heat and mass transfer, which usually involve solving the partial differential equations. What we need to do is to discretize the spatial derivatives of the partial differential equation, and apply the numerical ODE solver LSODE to integrate in time. It has been proved that the finite difference method works reasonably well for solving the one dimensional mathematical model of heat and mass transfer.

One of the disadvantages of the finite difference method is that unequally spaced mesh points are difficult to implement. For the one dimensional heat and mass transfer model, the moisture profile (Figure 4.3) discussed in 4.2.3 causes some difficulty for the finite difference method. At and near the drying front, there are sharp changes in gas pressure and moisture content. In order to obtain accurate numerical solutions, a very fine mesh is required in this region. This means for a

uniform mesh, very many mesh points are required for the distance between the boundaries. As a result, a large Jacobian matrix is generated, which takes a lot of computer storage space, and tremendously increases the computation time. Therefore, the finite difference method is not efficient for this heat and mass transfer problem.

The problem of accuracy does not only happen at the drying front for the wood drying process, it could happen for fixed boundary conditions too, where the boundary values are sharply different from the values at the mesh points next to the boundary points. The physical problems we try to simulate using the one dimensional mathematical model are quite complicated. This is because of the interactions of the heat and mass transfer. When the temperature is above the boiling temperature, the phase change becomes more significant. This causes difficulty for numerical solutions. Under such extreme physical conditions, the numerical solutions may become unstable and unreliable, even with a fine mesh.

The second disadvantage of the finite difference approach is that, because the method requires fixed specified mesh points, if we want to know the solution at certain points, we must either include the points as mesh points, or apply interpolation or extrapolation to find the solution. The accuracy depends on the method chosen for interpolation. This is not convenient.

In addition, for this problem the boundary values are solved explicitly prior to the next time step. This procedure requires root finding iteration, takes up some computation time; and the initial guess for the solution is very important in order to get convergenc to the boundary value solutions.

Table 4.1 Input for Simulation Model

Thickness of specimen	0.0508	m
Dry wood density	480	kg/m^3
Moisture content (dry base)	45	%
Initial temperature	20	°C
Permeability of dry wood, K^g_d	$5x10^{-15}$	m^2
Permeability of saturate wood, K^f_s	$5x10^{-16}$	m^2
Bound water diffusivity, D^b	$3x10^{-13}$	$kg/s/m^2$
Irreducible saturation, S_{ir}	0.1	
Attenuation factor, α	0.05	
External mass transfer coefficient k	0.03	$mol/m^2/s$
Heat transfer coefficient, h	50	$J/m^2/s/K$
Saturate vapor pressure, p_v^{sat}	47324	Pa
Environment temperature, T	80	°C
Relative humidity, RH	2	%

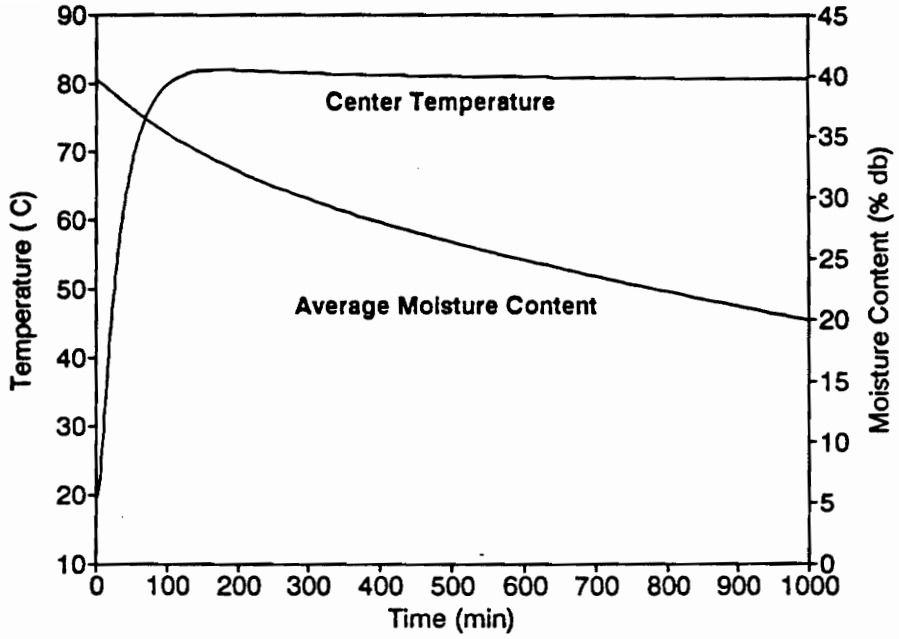

Figure 4.1. Model simulation results for conditions given in Table 4.1.

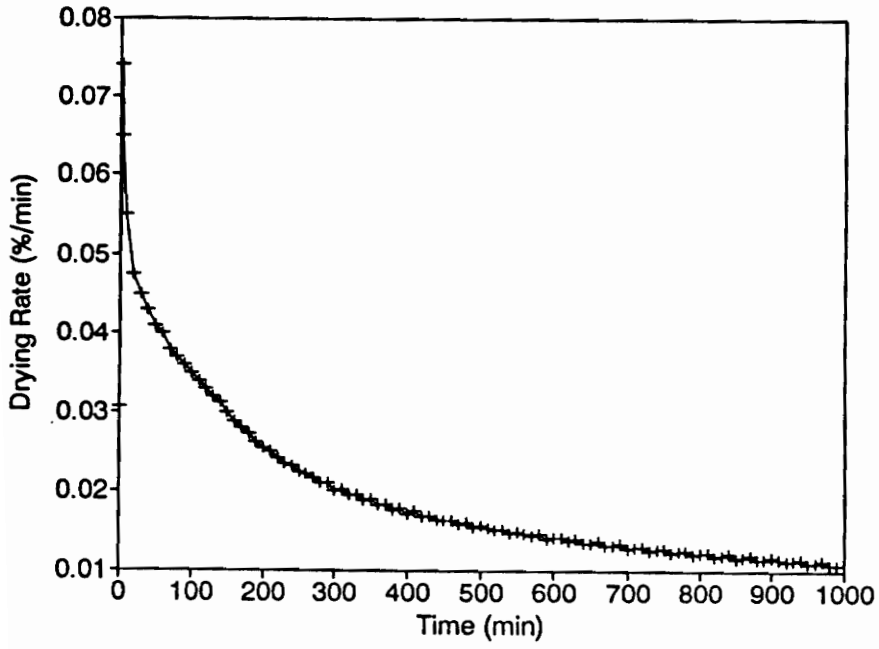

Figure 4.2. Moisture drying rate for conditions given in Table 4.1.

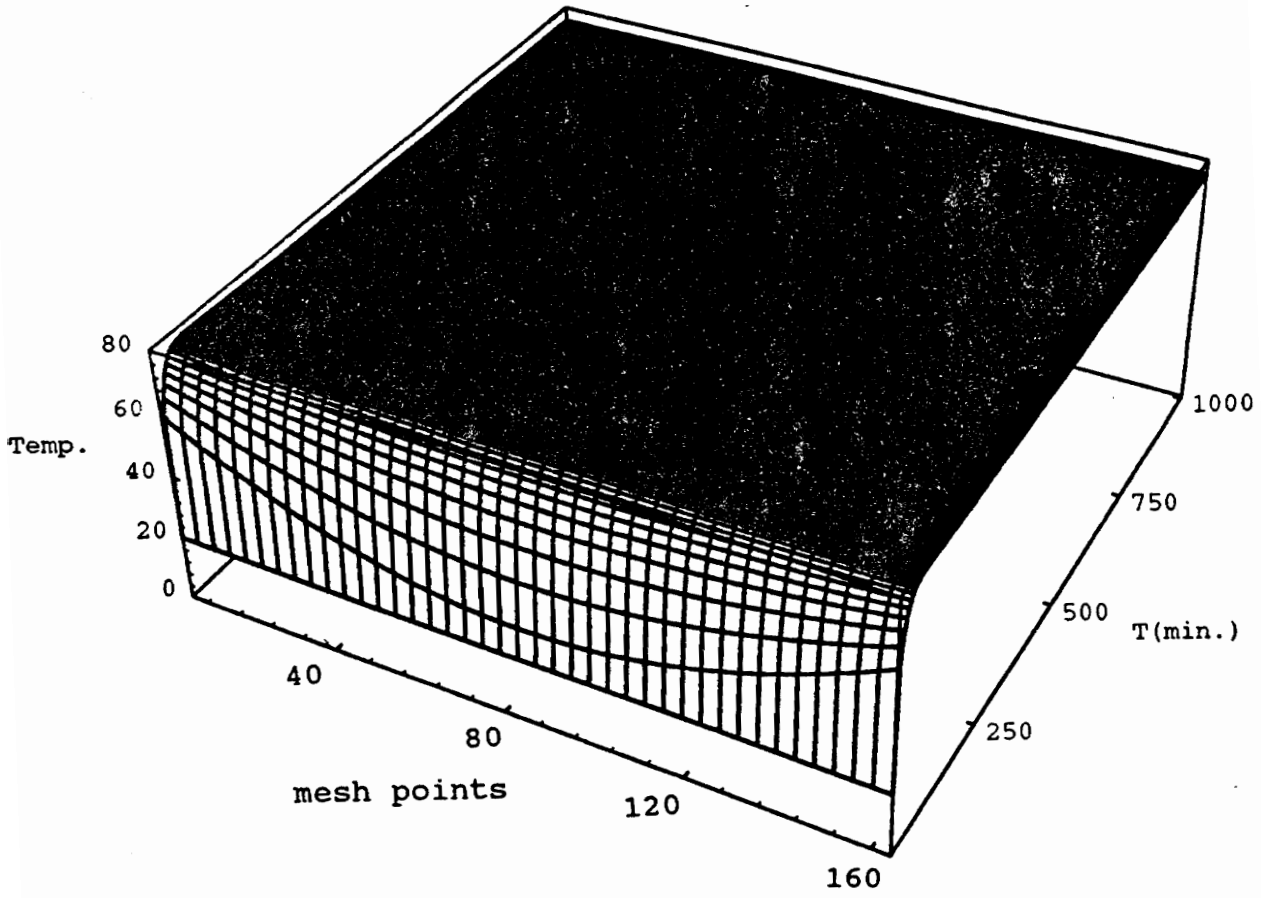

Figure 4.3. Temperature profile for conditions given in Table 4.1.

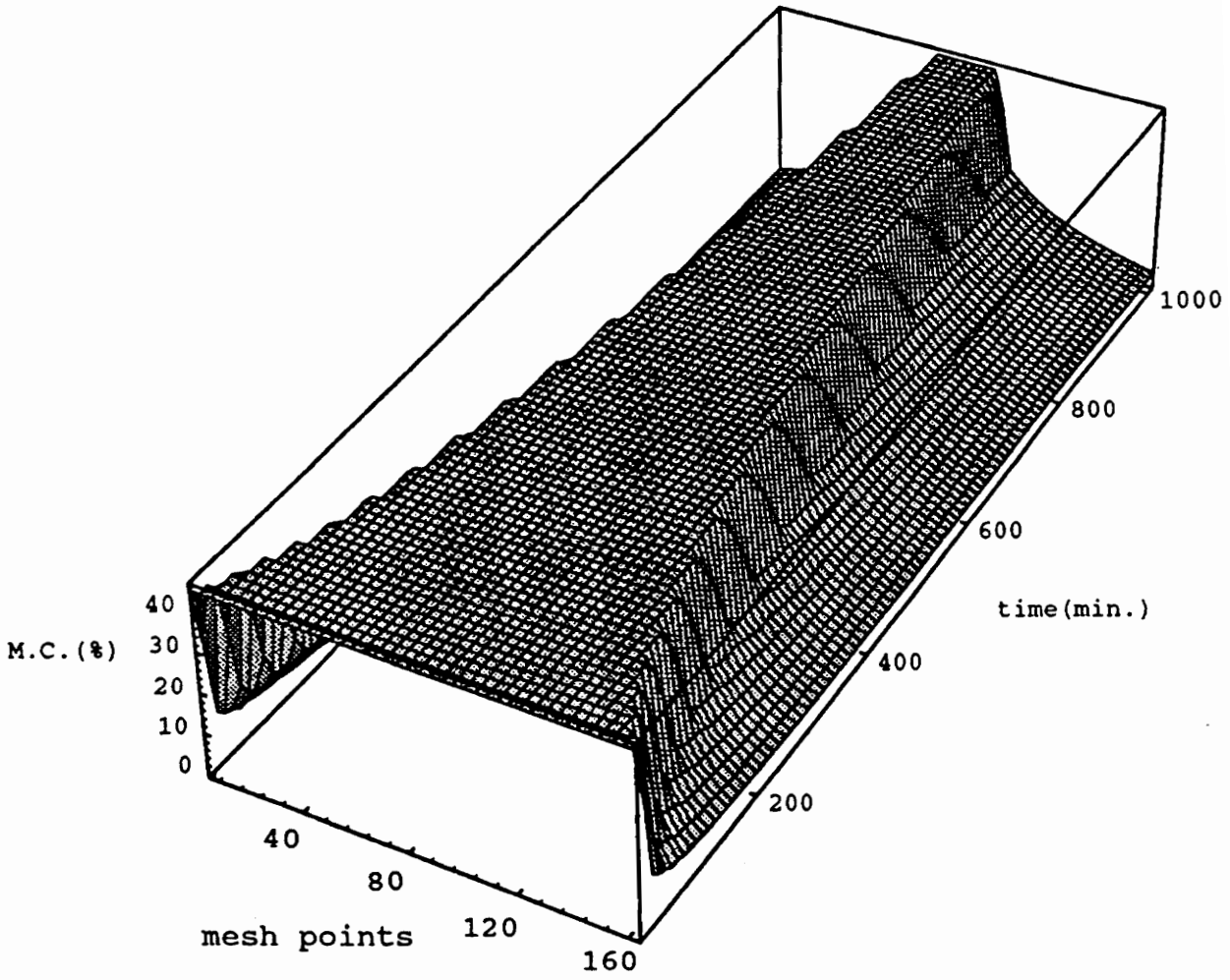

Figure 4.4. Moisture profile for conditions given in Table 4.1.

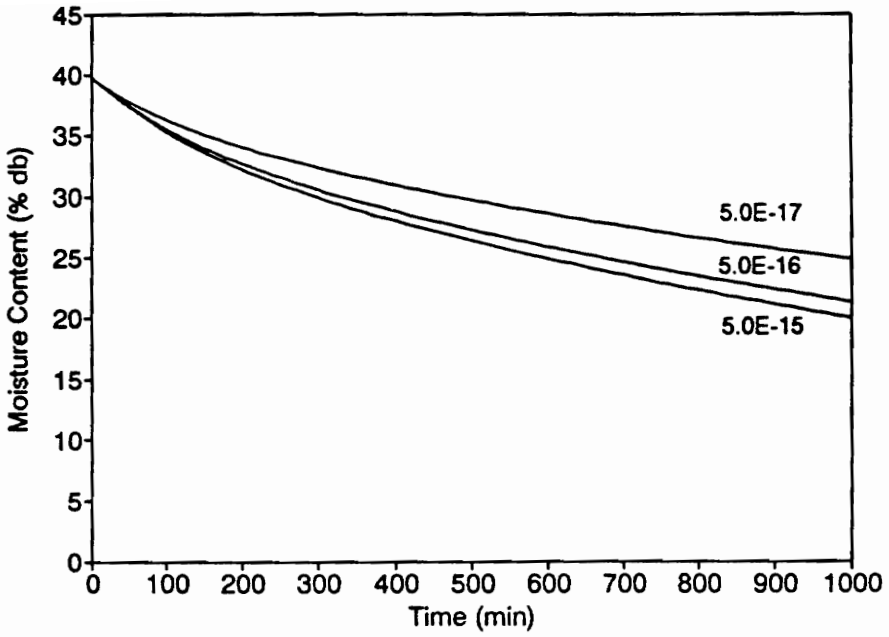

Figure 4.5. Effects of dry wood gas permeability, K_g^d (m^2), on moisture transfer.

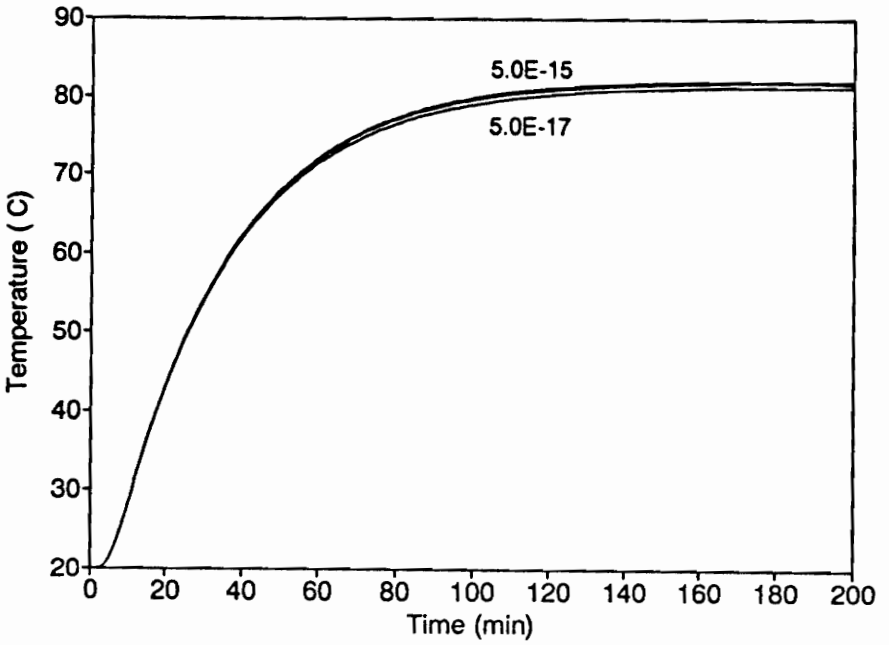

Figure 4.6. Effects of dry wood gas permeability, K_g^d (m^2), on temperature (top to bottom: 5.0E-15, 5.0E-16 and 5.0E-17).

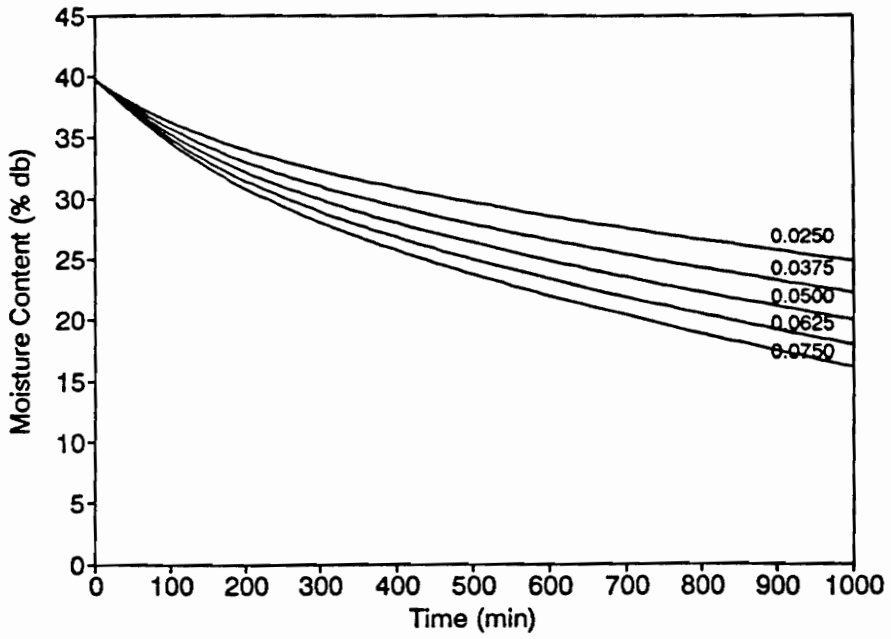

Figure 4.7. Effects of attenuation factor, α, on moisture transfer.

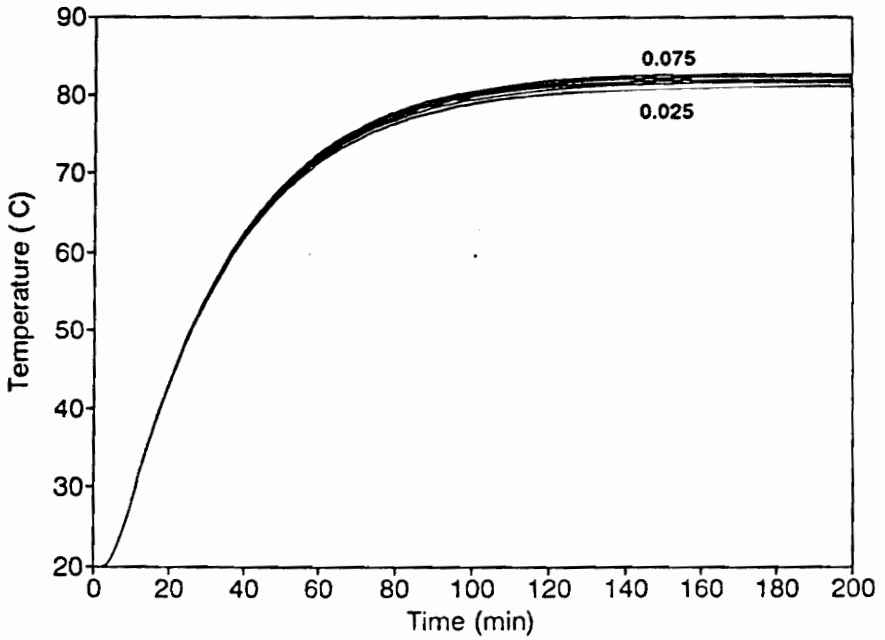

Figure 4.8. Effects of attenuation factor, α, on temperature (top to bottom: .075, .0625, .05, .0375 and .025).

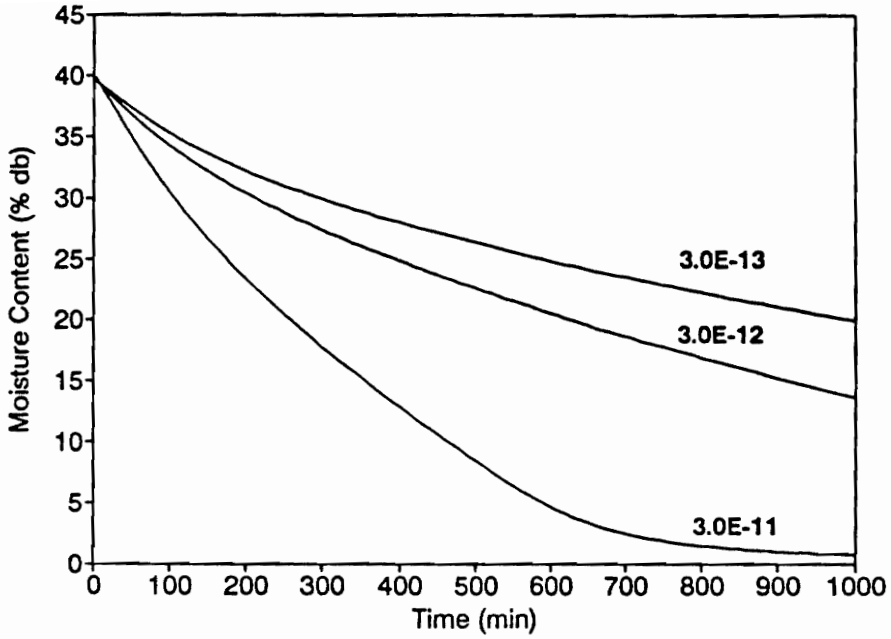

Figure 4.9. Effects of bound water diffusivity, D_b (kg.s/m^3), on moisture transfer.

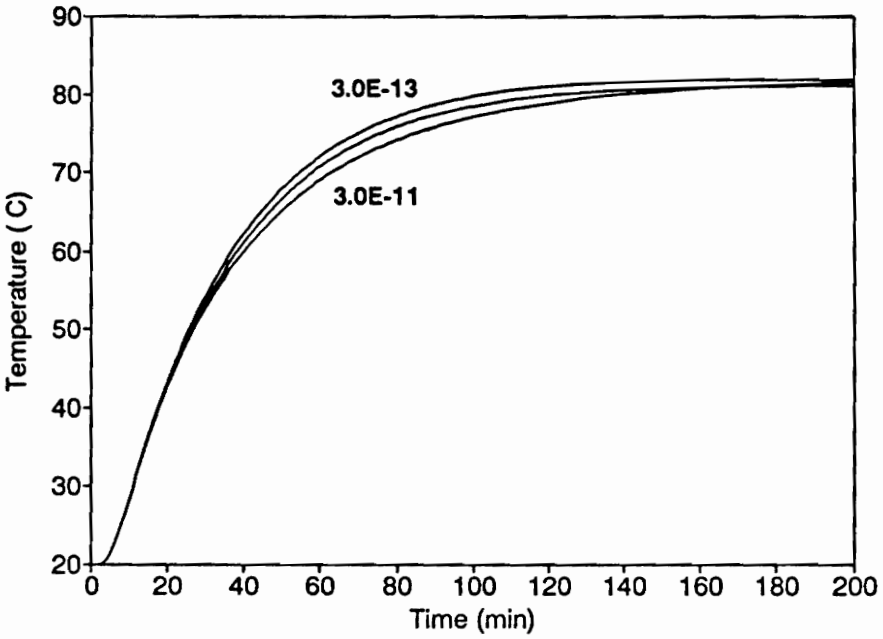

Figure 4.10. Effects of bound water diffusivity, D_b (kg.s/m^3), on temperature (top to bottom: 3.0E-13, 3.0E-12 and 3.0E-11).

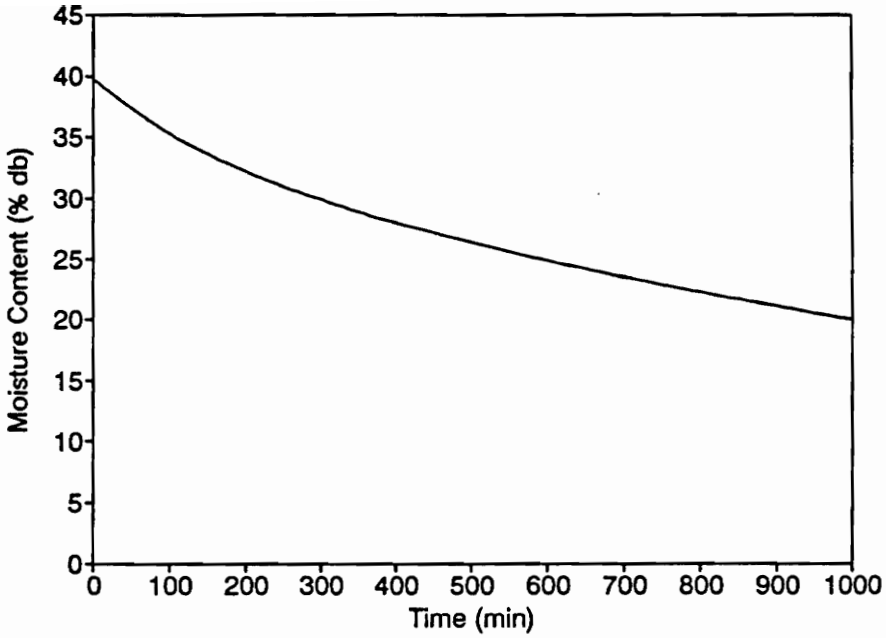

Figure 4.11. Effects of saturated water permeability, K_f' (m^2), on moisture transfer (5.0E-17, 5.0E-16 and 5.0E-15).

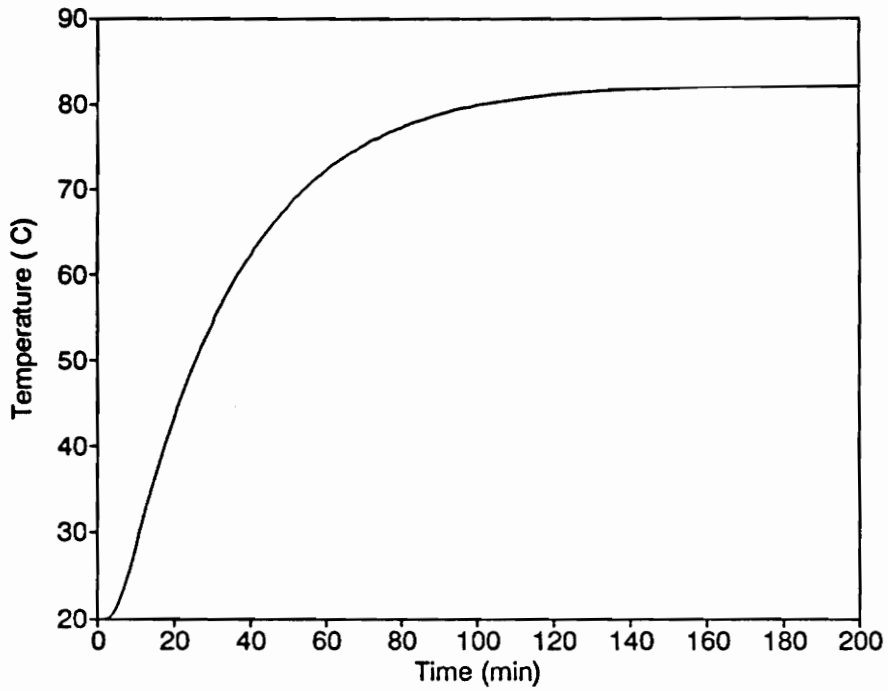

Figure 4.12. Effects of saturated water permeability, K_f' (m^2), on temperature (5.0E-17, 5.0E-16 and 5.0E-15).

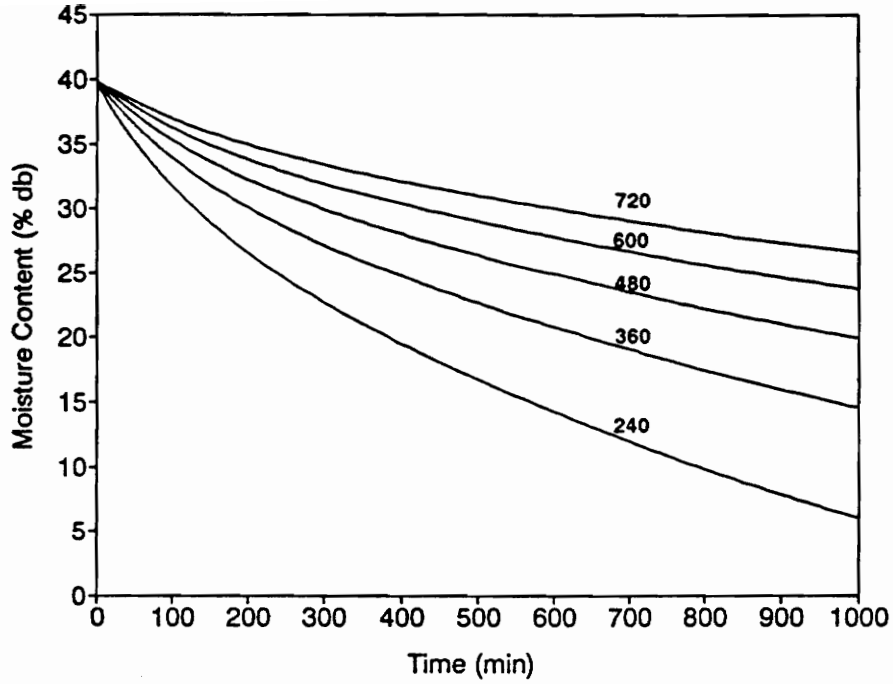

Figure 4.13. Effects of dry wood density, ρ_d (kg/m^3), on moisture transfer.

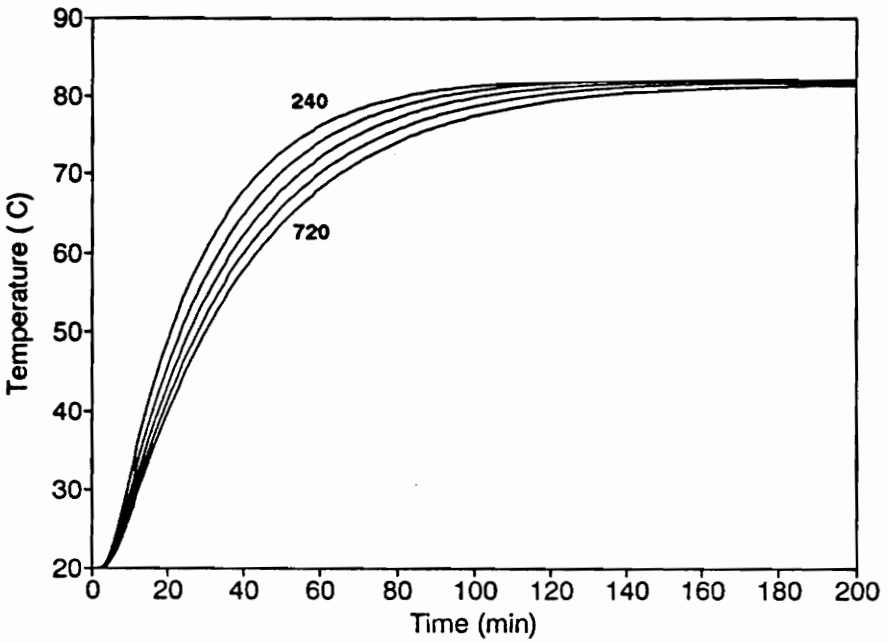

Figure 4.14. Effects of dry wood density, ρ_d (kg/m^3), on temperature (top to bottom: 240, 360, 480, 600, and 720).

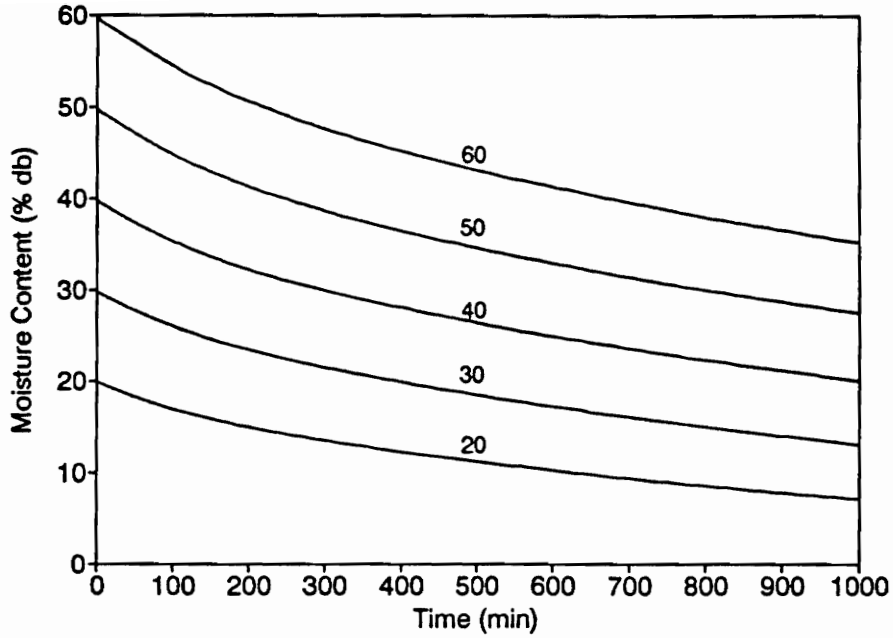

Figure 4.15. Effects of initail moisture content, MC (%), on moisture transfer.

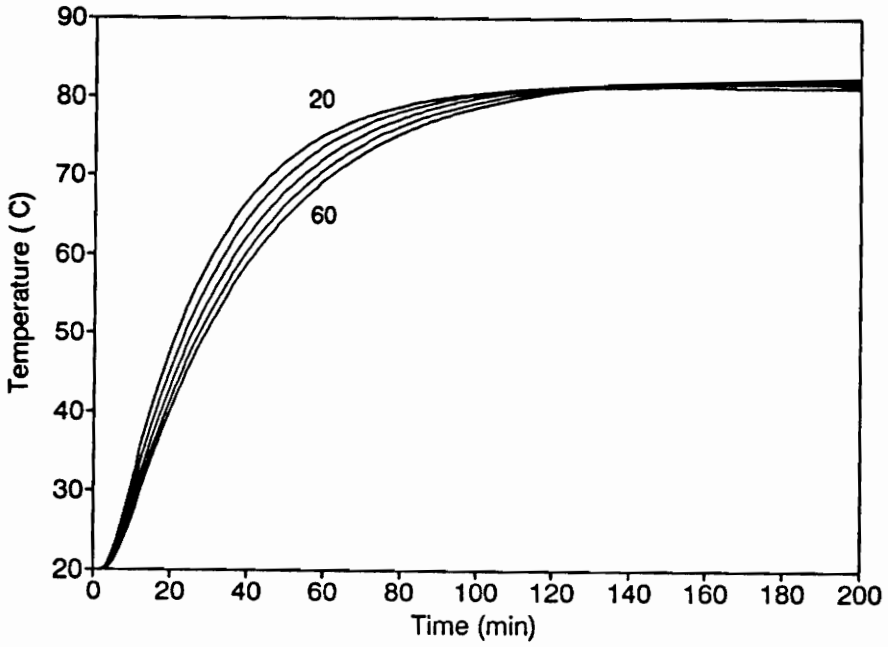

Figure 4.16. Effects of initail moisture content, MC (%), on temperature (top to bottom: 20, 30, 40, 50 and 60).

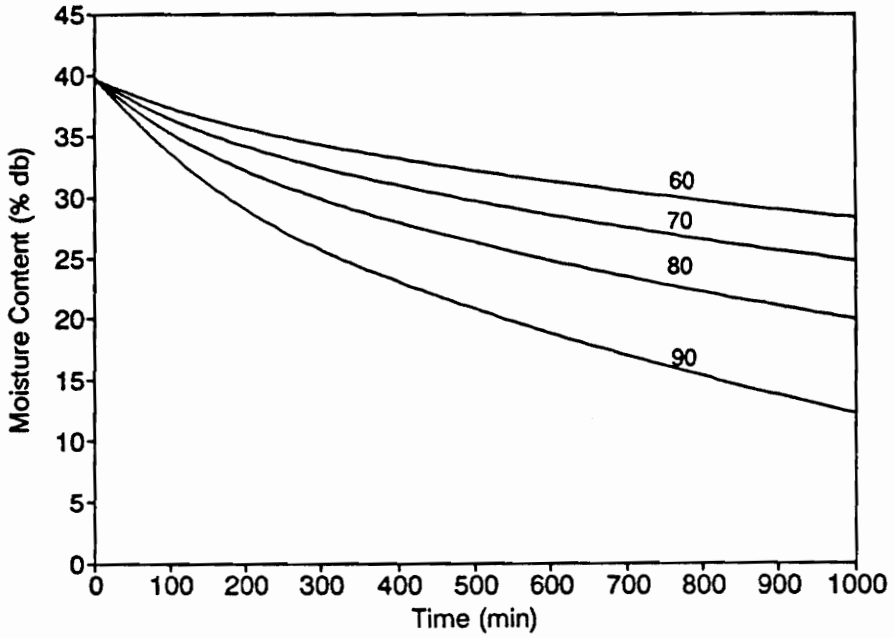

Figure 4.17. Effects of drying temperature, T (°C), on moisture transfer.

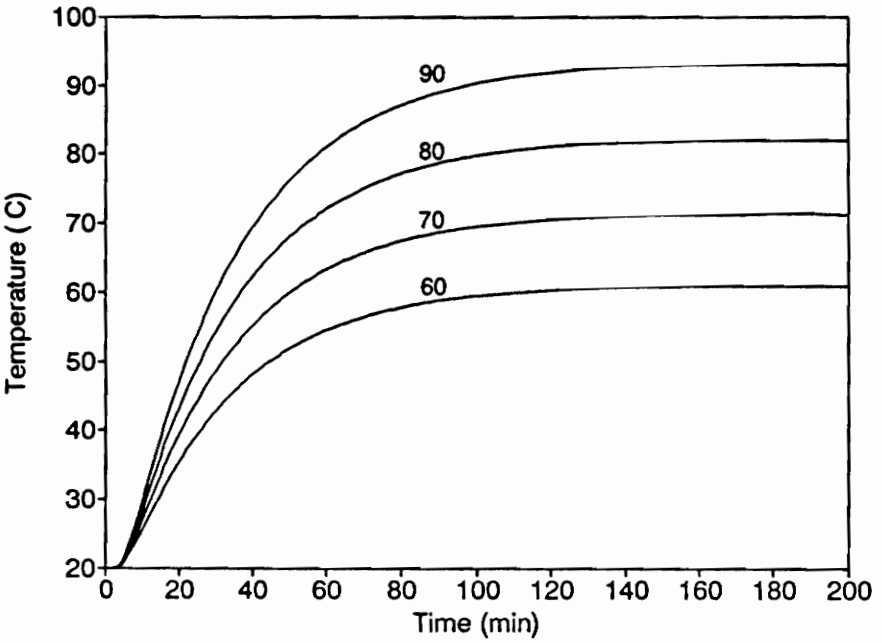

Figure 4.18. Effects of drying temperature, T (°C), on temperature.

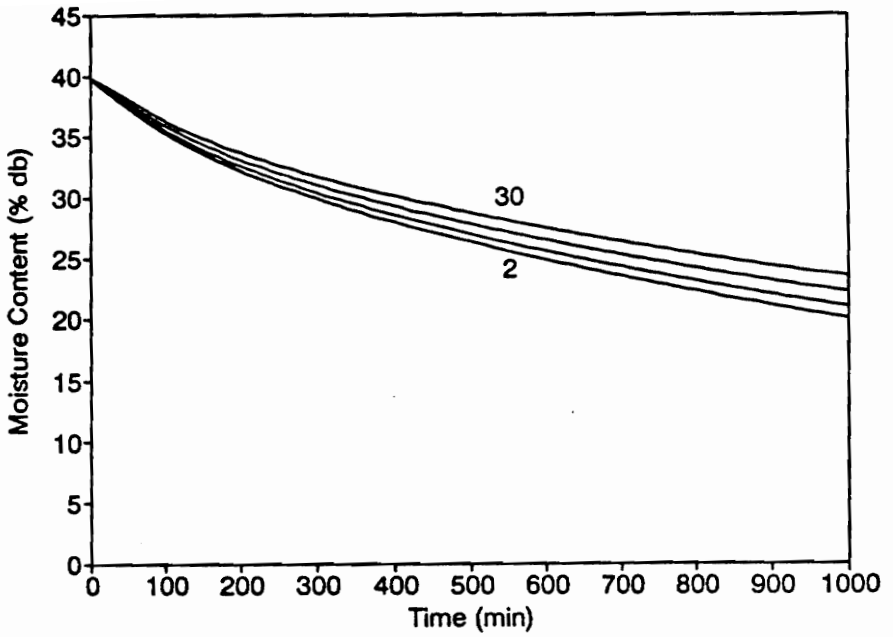

Figure 4.19. Effects of relative humidity, RH (%) on moisture transfer (top to bottom: 30, 20, 10, and 2).

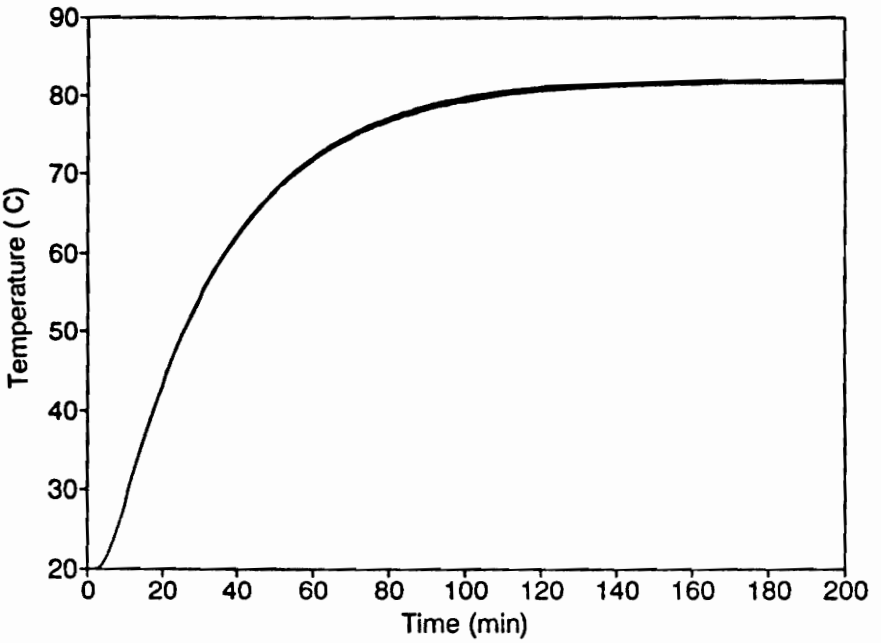

Figure 4.20. Effects of relative humidity, RH (%), on temperature.

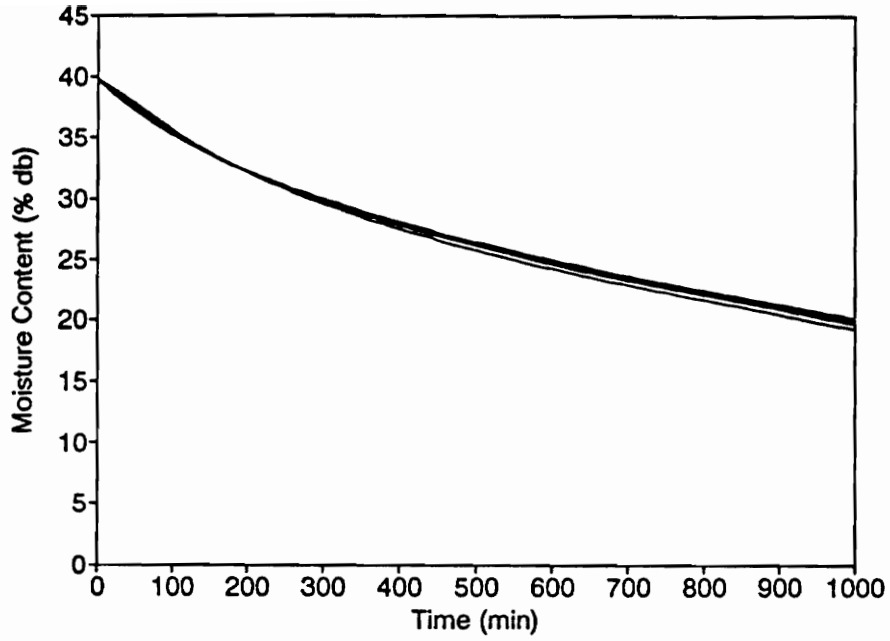

Figure 4.21. Effects of heat transfer coefficient, k_h (J/s/K/m^2), on moisture transfer.

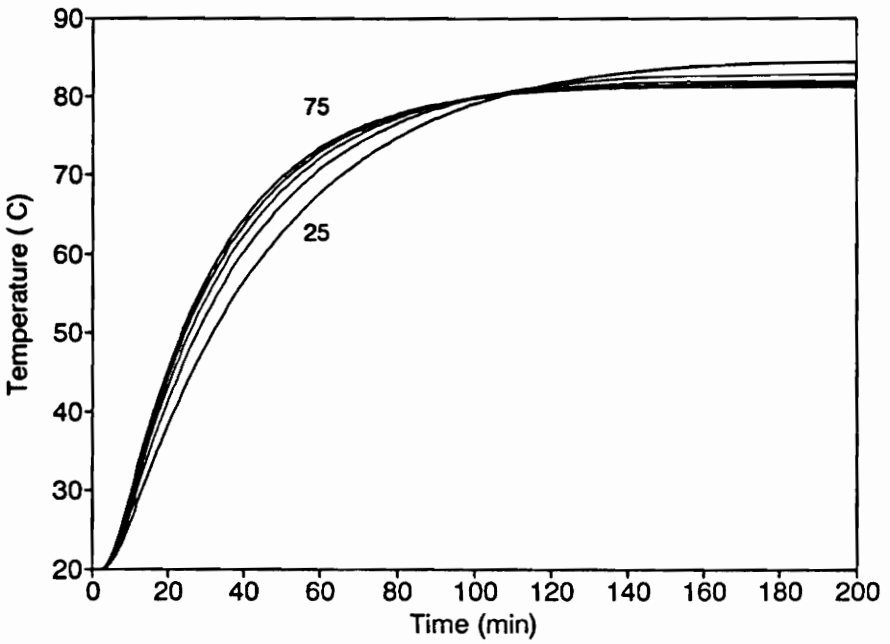

Figure 4.22. Effects of heat transfer coefficient, k_h (J/s/K/m^2), on temperature.

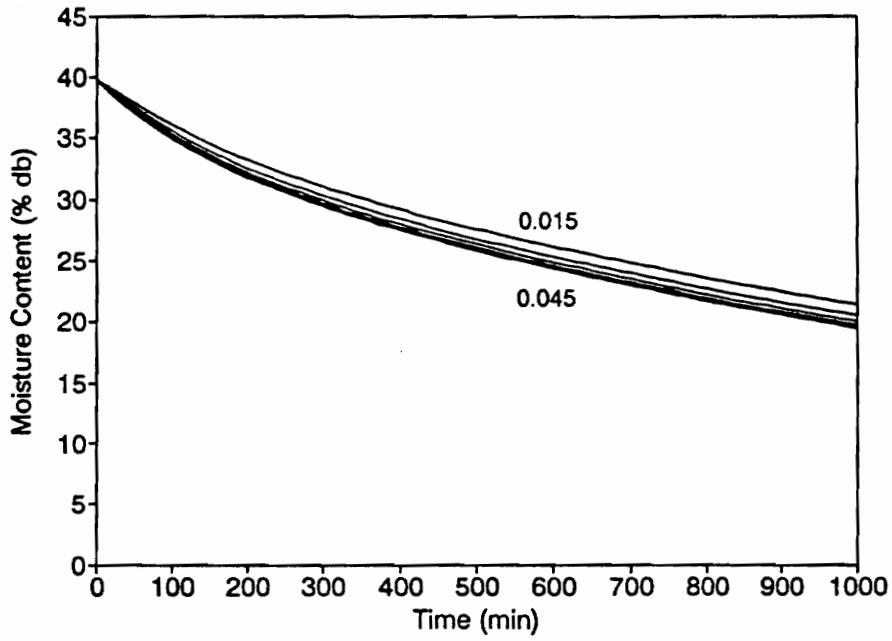

Figure 4.23. Effects of mass transfer coefficient, k_m (mol/s/m^2), on moisture transfer.

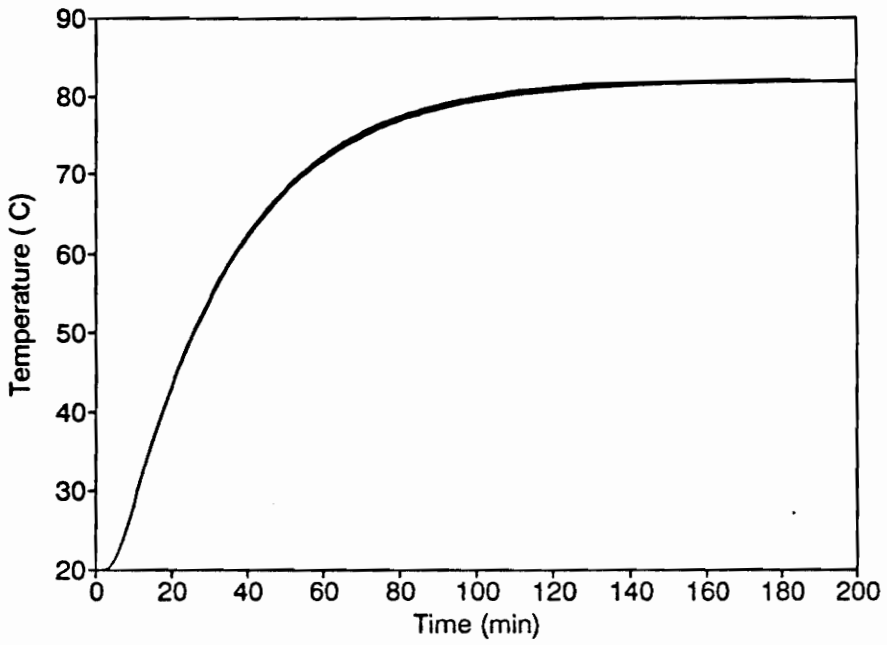

Figure 4.24. Effects of mass transfer coefficient, k_m (mol/s/m^2), on temperature.

CHAPTER V

CONCLUSIONS AND FUTURE WORK

The fundamental and quantitative study of heat and mass transfer in wood will give us a better understanding of many important production processes, such as wood drying and hot-pressing, help us improve the existing products and production techniques, and develop new manufacturing technology. Based on such important expectations, this fundamental research has been conducted. A successful effort has been made to incorporate an existing mathematical model into a computer-based numerical model to simulate simultaneous heat and mass transfer in wood.

In previous chapters, the fundamental principles of heat and mass transfer, and research on mathematical and numerical modeling of drying and hot pressing, have been reviewed. The basics of the existing mathematical model, as well as the development of a computer-based finite difference model, have been introduced. The modeling results and the sensitivity studies have been discussed. The research work has resulted in the following conclusions:

1) Heat and mass transfer in wood is complicated and difficult to study, because of the interactions of those two physical processes. Numerical methods can serve as a very powerful tool to help solve complicated mathematical models, such as the coupled, second order partial differential equations used here. The numerical approach used simulates the process of heat and mass transfer, observes the

development of temperature and moisture profiles, and predicts the final results of heat and mass transfer. This can give us a better understanding of the complicated physical process and help us optimize the production process.

2) Extensive characterization of those physical processes using a strictly experimental approach is extremely difficult because of the excessively large number of variables that must be considered. However, using the numerical model we can perform sensitivity studies to determine the effects of the wood properties and environmental conditions on the process of heat and mass transfer. Based on the drying conditions we have simulated, some comments can be made.

a) The heat transfer process happens much faster than the mass transfer process during wood drying.

b) Temperature and initial moisture contents are the most sensitive and determining parameters to the process of heat and mass transfer.

c) The coefficients of effective gas permeability, effective gas diffusivity, and bound water diffusivity have significant effects on the mass transport process. These values are greatly affected by the wood structure.

d) The drying boundary condition, especially the convective heat and mass transfer coefficients and the humidity, can affect the rate of wood drying. However, the thick specimen that was used in the simulation was more influenced by internal mechanisms of mass transfer.

3) The most serious disadvantage of the finite difference method appears at the very steep drying front resulting from water evaporation, which moves inward during

the drying process. In order to obtain accurate solutions, a dense mesh was required, which requires a large Jacobian matrix and considerable computation time.

The future work could include:

1) Sensitivity study of the finite difference model for drying temperature above 100°C. The physical phenomena under high temperature drying conditions have not been fully discussed in the literature. Other mechanisms of heat and mass transfer may become significant.

2) Working on the collocation model to simulate drying boundary conditions. To deal with the numerical difficulty at steep fronts, the collocation method has great advantages. 1) The collocation method allows us to select nonuniformly distributed mesh points, and no extra programming is required. 2) Because the output of the collocation method is a smooth function, we can follow the drying fronts closely. Also the PDECOL solver estimates the approximation error for each piecewise polynomial between each two collocation points, which gives an indication how to redistribute the collocation points, so that we can accurately follow the drying front. We can design the collocation points based on the experience on the differential equations. 3) The collocation method approximates the solution using a piecewise polynomial. The solutions are more accurate by using the collocation approach than by using the finite difference approach. Therefore, the collocation method is much more accurate and efficient.

3) Develop a model that includes stress and strain. This will reflect the effects of shrinking and swelling, and externally applied forces, on heat and mass transfer. Stress and strain behavior is an integral part of wood drying and wood-based composites manufacture.

BIBLIOGRAPHY

Bazant, Z.P. 1985. Constitutive Equation of Wood at Variable Humidity and Temperature. Wood Sci. Technol. 19:159-177

Berger, D. and D. C. T. Pei. 1973. Drying of Hygroscopic Capillary Porous Solids - A Theoretical Approach. Int. J. of Heat and Mass Transfer. 16, 293-302.

Bolton, A.J. and P.E. Humphrey. 1994. The Permeability of Wood-Based Composite Materials. Hotzforschung 48(1994):95-100

Bowen, M.E. 1970. Heat Transfer in Particleboard During Pressing. Ph.D. Dissertation, Colorado State Univ., U.S.A.

Bramhall, G. 1976. Semi-Empirical Method to Calculate Kiln-Schedule Modifications From Some Lumber Species, Wood Sci. 8(4):213-222.

Bramhall, G. 1979. Mathematical Model for Lumber Drying. Wood Sci. 12(1):14-31.

Choong, E.T. 1963. Movement of Moisture Through a Softwood In the Hygroscopic Range. Forest products Journal. (13):489-498.

Comstock, G.L. 1968. Physical and Structural Aspects of the Longitudinal Permeability of Wood. Ph.D. Dissertation, SUNY, college of Forestry, Syracuse.

Comstock, G.L. 1970. Directional Permeability of Softwoods. Wood Fiber. (1):283-289.

Dushman, S. and J.M. Lafferty. 1962. Scientific Foundations of Vacuum Technique. Wiley, New York.

Frank, P.I. and D.P. Dewitt. 1990. Fundamentals of Heat and Mass Transfer. John Wiley & Sons, New York.

Gammon, B.W. 1987. Reliability Analysis of Wood-Frame Wall Assemblies Exposed to Fire. Ph.D Dissertation, Univ. of California, Berkeley.

Gilbo, C. F. 1951. Experiments with a guarded hot plate Thermal Conductivity Set. In Pro. Symp. on Thermal Insulating Materials. ASTM Special Tech. Pub. 119:45-55.

Hindmarsh, A.C., 1980. LSODE and LSODI, Two New Initial Value ordinary Differential Equation Solvers, ACM-SIGNUM Newsletter, 15(4):10-11

Humphrey, P.E. 1982. Fundamental Aspects of Wood Particleboard Manufacture. Ph.D. Dissertation, Univ. of Wales, U.K.

Humphrey, P.E., and A.J. Bolton. 1989. The Hot Pressing of Dry-Formed Wood-Based Composites. Part ll. A Simulation Model for Heat and Moisture Transfer, and Typical Results. Holzforschung 43(3):190-206.

Harless, T.E.G., F.G. Wagner, and P.H. Short. et al. 1987. A Model to Predict the Density Profile of Particleboard. Wood and Fiber Sci. 19(1)8-92.

Kamke, F.A. 1989. Thermal Conductivity of Wood-Based Panels. Thermal Conductivity, 20.

Kamke, F.A., and L.J. Casey. 1988a. Gas pressure and Temperature in the Mat During Flakeboard Manufacture. For. Prod. J. 38(3):41-43.

Kamke, F.A., and L.J. Casey. 1988b. Fundamentals of Flakeboard Manufacture: Internal-Mat Conditions. For. Prod. J. 38(6):38-44.

Kamke, F.A.,and M.P. Wolcott, 1991. Fundamentals of flakeboard manufacture: Wood-moisture relationships. Wood Sci. & Tech. 25(1): 57-71.

Kamke, F.A., and L.T. Watson. 1992. Modelling Simultaneous Heat, Mass, and Stress Transfer in Wood. USDA proposal. Dept. Wood Sci. and For. Prod., Virginia Poly. Inst. and State Univ., Blacksburg, Virginia.

Kayihan, F., and J.A. Johnson. 1983. Heat and Moisture Movement in Wood Composite Materials During the Prossing Operation - A Simplified Model. Numerical Methods in Heat Transfer Vol.(2)511-531.

Kininmonth, J.A, 1971. Permeability and Fine Structure of Certain Hardwoods and Effects on Drying. Holzforschung. (25):127-133

Kollmann, F. and L. Malmquist. 1956. The Coefficient of Thermal Conductivity of Wood and Wood Based Material. Holz als Rouhund Werkstoff. 14(6):201-204.

Kollmann, F.F.P. and Cote, Jr., W.A. 1975. Principles of Wood Science and Technology l. Spring-Verlag, Inc. New York.

Kollmann, F.F.P., E.W. Kuenzi, and A.J. Stamm. 1975. Principles of wood science and Technology II. Springer-Verlang New York Heidelberg Berlin.

Kollmann, F.F.P. 1951. Technology of Wood and Wood Based Materials, Vol. 1, and Ed., Springer-Verlag, Berlin, 1951.

Lehmann, W.F. 1972. Moisture Stability Relationships in Wood-Based Composition Boards. For.Prod.J. 22(7):53-59.

Lewis, W. C. 1967. Termal Conductivity of Wood-Based Fiber and Particle Panel Materials. USDA Forest Serv. Research Paper, FRL-77. Forest Prod. Lab. Madison, WI.

Lowery, D.P. 1972. Vapor Pressures Generated in Wood During Drying. Wood Sc. 5(1)73-80.

Luikov, A.V. 1966. Heat and Mass Transfer in Capillary-Porous Bodies, Pergamon press, New York, 1966.

Luikov, A.V. 1975. Systems of Differential Equations of Heat and Mass Transfer in Capillary-Porous Bodies. Int. J. of Heat and Mass Transfer. 18, 1-14.

Maclean, J.D. 1941. Thermal Conductivity of Wood. Heating, Piping and Air Conditioning. 13:380-391.

Madsen N.K and R.F. Sincovec, 1979. ALGORITHM 540 PDECOL, General Collocation Software for Partial Differential Equations [D3], ACM Transactions on Mathematical Software. 5(3):326-351.

Maku, T. 1954. Studies on the Heat Conductivity in Wood. Bulletin of the Wood Research Institute. No.13, Kyoto University.

Nanassy, A. J. and T. Szabo. 1978. Thermal properties of Waferboards as Determined by a Transient Method. Wood Science. 11(1): 17-22.

Rosen, H.N. 1980. Empirical Model for Characterizing Wood Drying Curves. Wood Sci. 12(4):201-206.

Rosen, H.N. 1982. Functional Relations and Approximation Techniques for Characterizing Wood Drying Curves. Wood Sci. 15(1):49-55.

Rowley, F.B. 1933. The Heat Conductivity of Wood at Climatic Temperature Differences. Heating, Piping and Air Conditioning. 5:313-323.

Schajer G.S., M.A. Stanish and F. Kayihan, 1984. A Computationally Efficient Fundamental Approach to Drying of Hygroscopic and Non-Hygroscopic Porous Materials. Proceeding: ASME Winter Annual Meeting in New Orleans. 1-8.

Siau, J.F. 1980. Nonisothermal Moisture Movement in Wood. Wood Sci. (13):11-13.

Siau, J.F. 1984. Transport Processes in Wood. Springer-Verlag. Berlin, Heidelberg, New York. Simpson, W.T. 1971. Equilibrium Moisture Content Prediction for Wood. For Prod. J. 21(5):48-52.

Simpson, W.T. 1971. Equilibrium Moisture Content Prediction for Wood. For Prod. J. 21(5):48-52.

Skaar, C. 1988. Wood-Water Relations. Springer-Verlag. Berlin, Heidelberg, New York.

Smith, D.N and E. Lee. 1958. The Longitudinal Permeability of Some Hardwoods and Softwoods. Dep. Sci. Ind. Res. For Prod Res. Special Rep. 13, London.

Spolek, G.A., and O.A. Plumb. 1980. A Numerical Model of Heat and Mass Transport in Wood During Drying. Drying'80, Proceedings of the Second International Drying Symposium, Montreal, Canada. Hemisphere Publishing Co., New York. pp. 84-92.

Stamm, A.J. 1959. Bound-Water Diffusion Into Wood in the Fiber Direction. Forest Product Journal. (9):27-32.

Stamm, A.J. 1964. Wood and Cellulose Science. Ronald, New York, 549pp.

Stanish, M.A., G.S. Schajer, and F.Kayihan. 1986. A Mathematical Model of Drying for Hygroscopic Porous Media. AIChE Journal, Vol.32, No.8, August 1986, pp. 1301-1311.

Stanish, M.A. 1986. The Role of Bound Water Chemical Potential and Gas Phase Diffusion in Moisture Transport Through Wood. Wood Sci. Technol.19:53-70.

Stanish M.A., G.S. Schajer and F. Kayihan, 1985. Mathematical Modeling of Wood Drying From Heat and Mass Transfer Fundamentals. Drying '85, Toei and Mujumdar (eds.), Hemisphere R.K, NY

Thomas, H.R, R.W. Lewis and K. Morgan. 1980. An Application of the Finite Element Method to the Drying of Timber. Wood and Fiber. 11(4),237-243.

Wang, J.H and F.C. Beall. 1975. Laboratory Press-Drying of Red Oak. Wood Sci. 8(2):131-140.

Ward, R.J. 1960. A Dynamic Method Fir Determining Specific Heat and Thermal Conductivity of Wood Based Materials as a Function of Temperature. Master's Thesis, State University College of Forestry at Syracuse University.

Ward, R.J. and C. Skaar. 1963. Specific Heat and Conductivity of Particleboard as Function of Temperature. Forest Products Journal. 13(1):31-38.

Wangaard, F.F. 1969. Heat Transmissivity of Southern Pine Wood, Plywood, Fiberboard, and Particleboard. Wood Science. 2(1):54-60.

APPENDIX A

Main Program (Fortran)

```
C     ******************************************************************
C     PROGRAM SHMDRY.F  5/11/1994
C     ******************************************************************

      EXTERNAL FEX,FCN
      INTEGER M,IT,IWORK,MXSTEP,NUMBER
      INTEGER I,NEQ,ITOL,IOUT,ITASK,ISTATE,IOPT,LRW,LIW,MF,ML,MU
      DOUBLE PRECISION Y,T,TOUT,RTOL,ATOL,RWORK,YOUT
      DOUBLE PRECISION LENGTH,ROA0,ROM0,TEMP0,SUM,TERM,MC
      DOUBLE PRECISION BCVVSAT,RH,M1,M2,M3,M4,ROV0,ROB0,ROF0,TSTOP
      PARAMETER (NEQ=501)
      DIMENSION Y(NEQ),RWORK(22+25*NEQ),ATOL(NEQ),IWORK(NEQ+20),
     $ YOUT(NEQ)
      DOUBLE PRECISION GUESS1,GUESS2,GUESS3,GUESS4,GUESS5,GUESS6,
     $              GUESS7,GUESS8
C
      DOUBLE PRECISION RHOD,EMZLOD,MA,MV,R,KGD,KFS,ALFA,DB,SIR,H
      DOUBLE PRECISION KMASS,KHEAT,ENTEMP,T2,T3,T122,T123,BCVA,BCVV
      COMMON /TRY1/RHOD,EMZLOD,MA,MV,R,KGD,KFS,ALFA,DB,SIR,H
      COMMON /TRY2/KMASS,KHEAT,ENTEMP,T2,T3,T122,T123,BCVA,BCVV
      COMMON /TRY3/GUESS1,GUESS2,GUESS3,GUESS4,GUESS5,GUESS6,
     $ GUESS7,GUESS8
      CHARACTER*10 TMESH
      CHARACTER*10 MCMESH
      CHARACTER*10 AVMOIST
      CHARACTER*10 CENTEMP
      CHARACTER*10 RECORD
      CHARACTER*10 BCMOIST
C
      DOUBLE PRECISION DATA,GUESS
      CHARACTER CONTENT*55,JUGE*1
      DIMENSION DATA(15),CONTENT(15),GUESS(8)
C
C     ***********************************************************
C     PARAMETERS RELATED TO THERMAL CONSTANT
C     MA      -- MOLECULAR WEIGHT OF AIR (KG/KMOL)
C     MV      -- MOLECULAR WEIGHT OF VAPOR (KG/KMOL)
C     R       -- GAS CONSTANT (J/KMOL/K)
C
      MA=28.968D0/1000.D0
      MV=18.016D0/1000.D0
      R=8316.96D0/1000.D0
C
C     +++++++++++++++++++++++++++++++++++++++++++++++++++++
C     INPUT SECTION !!!!!!
C     +++++++++++++++++++++++++++++++++++++++++++++++++++++
C
C     LENGTH  -- SPECIMEN THICKNESS (M)
C     RHOD    -- DENSITY OF WOOD (KG/M3)
C     ROM0    -- INITIAL MOISTURE CONTENT (%)
C     TEMP0   -- INITIAL TEMPERATURE (C)
C     KGD     -- PERMEABILITY OF DRY WOOD (M2)
C     KFS     -- PERMEABILITY OF SATURATED WOOD (M2)
C     DB      -- BOUND WATER DIFFUSIVITY (KG/S/M2)
```

```
C     SIR     - IRREDUCIBLE SATURATION
C     ALFA    - ATTENUATION FACTOR FOR VAPOR DIFFUSIVITY IN WOOD
C     KMASS   - EXTERNAL MASS TRANSFER COEFFICIENT (MOL/M2/S)
C     KHEAT   - HEAT TRANSFER COEFFICIENT (J/M2/S/K)
C     ENTEMP  - ENVIROMENT TEMPERATURE (C)
C     BCVVSAT - SATURATE VAPOR PRESSURE (Pa)
C     RH      - RELATIVE HUMIDITY (%)
C     TSTOP   - RUN TIME (MIN)
C     ++++++++++++++++++++++++++++++++++++++++++++++++++++++++++++++++++++
C     PARAMETER RELATED TO WOOD PROPERTIES (DEFAULT VALUE)
      LENGTH=0.0508D0
      RHOD=480.D0
      ROM0=40.D0
      TEMP0=20.D0
      KGD=5.D-15
      KFS=5.D-16
      DB=3.D-13
      SIR=.1D0
      ALFA=.05D0
C     PARAMETERS RELATED TO BOUNDARY CONDITION (DEFAULT VALUE)
      KMASS=.03D0
      KHEAT=50.D0
      ENTEMP=80.D0
      BCVVSAT=47324.2D0
      RH=2.0
      TSTOP=1000.D0
C
      DATA(1)=LENGTH
      DATA(2)=RHOD
      DATA(3)=ROM0
      DATA(4)=TEMP0
      DATA(5)=KGD
      DATA(6)=KFS
      DATA(7)=DB
      DATA(8)=SIR
      DATA(9)=ALFA
      DATA(10)=KMASS
      DATA(11)=KHEAT
      DATA(12)=ENTEMP
      DATA(13)=BCVVSAT
      DATA(14)=RH
      DATA(15)=TSTOP
C
      CONTENT(1)=' 1. SPECIMEN THICKNESS, M'
      CONTENT(2)=' 2. DRY WOOD DENSITY, KG/M3'
      CONTENT(3)=' 3. INITIAL MOISTURE CONTENT, %'
      CONTENT(4)=' 4. INITIAL TEMPERATURE, C'
      CONTENT(5)=' 5. PERMEABILITY OF DRY WOOD, M2'
      CONTENT(6)=' 6. PERMEABILITY OF SATURATED WOOD, M2'
      CONTENT(7)=' 7. BOUND WATER DIFFUSIVITY, KG.S/M3'
      CONTENT(8)=' 8. IRREDUCIBLE SATURATION'
      CONTENT(9)=' 9. ATTENUATION FACTOR OF VAPOR DIFFUSIVITY IN WOOD'
      CONTENT(10)=' 10. EXTERNAL MASS TRANSFER COEFFICIENT, MOL/M2/S'
      CONTENT(11)=' 11. HEAT TRANSFER COEFFICIENT, J/M2/S/K'
      CONTENT(12)=' 12. ENVIROMENT TEMPERATURE, C'
      CONTENT(13)=' 13. SATURATE VAPOR PRESSURE, Pa'
      CONTENT(14)=' 14. RELATIVE HUMIDITY, %'
      CONTENT(15)=' 15. RUN TIME, MIN'
C     WRITE CURRENT INPUT DATA
99    CONTINUE
```

```
C     WRITE OUT INPUT DATA
      DO 11 I=1,15
       WRITE(*,'(A55,5X,E12.6)')CONTENT(I),DATA(I)
11    CONTINUE
C
C
C     ++++++++++++++++++++++++++++++++++++++++++++++++++++++++++++++
C     ALLOW SOME MODIFICATION
C     ++++++++++++++++++++++++++++++++++++++++++++++++++++++++++++++
      WRITE(*,*)'DO YOU WANT TO MAKE SOME CHANGE?  y/n'
      READ(*,'(A)')JUGE
C
      IF(JUGE.EQ.'y')THEN
       WRITE(*,*)'TYPE THE NUMBER FOR CHANGE (1/2/3....)'
       READ(*,*)I
       WRITE(*,*)CONTENT(I), '= ?'
       READ(*,*)DATA(I)
       GOTO 99
      ENDIF
C
C     OPEN FILE FOR RECORD INPUT DATA
C
      WRITE(*,*)'DOCUMENT FILE NAME (RECORD=?)'
      READ(*,'(A)')RECORD
      OPEN(UNIT=8,STATUS='NEW',FILE=RECORD)
      DO 12 I=1,15
       WRITE(8,'(A55,5X,E12.6)')CONTENT(I),DATA(I)
12    CONTINUE
C
C
C     ++++++++++++++++++++++++++++++++++++++++++++++++++++++++++++++
C     M -- NUMBER OF MESH POINTS
C     NEQ -- 3*M
C     H -- INTERVAL SPACE
C     BCVA   -- BOUNDARY AIR PRESSURE (Pa)
C     BCVV   -- BOUNDARY WATER VAPOR PRESSURE (Pa)
C
      M=NEQ/3
      H=LENGTH/(M+1)
      BCVV=BCVVSAT*RH/100.D0
      BCVA=101325.D0-BCVV
C
C     ++++++++++++++++++++++++++++++++++++++++++++++++++++++++++++++
C     UNIT CONVERSION
C     THE PROGRAM USING ABSOLUTE TEMPERATURE (K)
C     THE MOISTURE CONTENT IS THE WATER WEIGHT PER CUBIC METER OF WOOD
C     INITIAL CONDITIONS
C     ROA0   -- INITIAL AIR DENSITY (KG/M3)
C     ROB0   -- SATURATE BOUND WATER
C     ROV0   -- SATURATE VAPOR PRESSURE
C     ROM0   -- INITIAL MOISTURE CONTENT (DRY BASE) (%)
C     TEMP0  -- INITIAL TEMPERATURE (K)
C     EMZLOD -- DRY WOOD VOID FRACTION
C     ++++++++++++++++++++++++++++++++++++++++++++++++++++++++++++++
C
C
      TEMP0=TEMP0+273.D0
      ROM0=RHOD*ROM0/100.D0
      EMZLOD=1.D0-RHOD/1500.D0
      ENTEMP=ENTEMP+273.D0
C
```

```
C     CALCULATE ROA0
C     ++++++++++++++++++++++++++++++++++++++++++++++++++++++++++++++++
C     SEE (Schajer et. al., 1984):
C     EQUATION (6) WHEN MC IS HIGHER THAN FIBER SATURATION
C     POINT, RELATIVE HUMIDITY=100%
C     ++++++++++++++++++++++++++++++++++++++++++++++++++++++++++++++++
C     CALCULATE ROA0
      M1=-45.7D0+.3216D0*TEMP0-5.012D-4*TEMP0**2
      M2=-.1722D0+4.732D-3*TEMP0-5.553D-6*TEMP0**2
      M3=1417.D0-9.43D0*TEMP0+1.853D-2*TEMP0**2
      M4=(1.D0-18.D0*RHOD/M3/ROM0)/2.D0/M2-
     $   (1.D0+18.D0*RHOD/M3/ROM0)/2.D0/M1/M2

      ROB0=18.D0*M2/M3*(1.D0/(1.D0-M2)+M1/(1.D0+M1*M2))*RHOD
C
C     ++++++++++++++++++++++++++++++++++++++++++++++++++++++++++++++++
C     SEE (Stanish et. al., 1986): EQ.(4)
C     ++++++++++++++++++++++++++++++++++++++++++++++++++++++++++++++++
      ROV0=DEXP(-46.490D0+.26179D0*TEMP0-5.0104D-4*TEMP0*TEMP0
     $   +   3.4712D-7*TEMP0*TEMP0*TEMP0)
C     SEE "A MATHEMATICAL MODEL OF DRYING" : PG1303 TOP AND EQ.(45)
C     EMZLO=EMZLOD-ROVF/ROW
C     ROW=157.8-.5361*TEMP
C     ALSO P=R*T*ROA/EMZLO/MA+R*T*ROV/EMZLO/MV
C     SO: ROA0=(EMZLOD-ROVF/(1157.8D0-.5361D0*TEMP0))*MA/R/TEMP0
C     *(101325.D0-R*TEMP0/MV*ROV0)
C
      ROF0=ROM0-ROB0-ROV0
      IF(ROF0.LE.0)THEN
        ROF0=0.D0
        ROV0=ROV0*(M4+(M4**2+1.D0/M1/M2**2)**0.5)
        ROA0=MA*(101325*EMZLOD/R/TEMP0-ROV0/MV)
      ELSE
        ROA0=(EMZLOD-ROF0/(1157.8D0-.5361D0*TEMP0))/R/TEMP0
     $ *101325.D0*MA-ROV0/MV*MA
      ENDIF
C
C     ++++++++++++++++++++++++++++++++++++++++++++++++++++++++++++++++
C     INITIAL GUESS OF FOUR ROOTS FOR SOLVE BOUNDARY CONDITION.
C     THE GUESSES ARE OBTAINED BY TRYING OUT
C     ++++++++++++++++++++++++++++++++++++++++++++++++++++++++++++++++
      GUESS1=.7D0
      GUESS2=300.D0
      GUESS3=-0.00005D0
      GUESS4=1.0D0
      GUESS5=GUESS1
      GUESS6=GUESS2
      GUESS7=-GUESS3
      GUESS8=GUESS4
C
      GUESS(1)=GUESS1
      GUESS(2)=GUESS2
      GUESS(3)=GUESS3
      GUESS(4)=GUESS4
      GUESS(5)=GUESS5
      GUESS(6)=GUESS6
      GUESS(7)=GUESS7
      GUESS(8)=GUESS8
C
999   CONTINUE
```

```
      DO 13 I=1,8
       WRITE(*,'(2X,A5,2X,I3,2X,A3,2X,E12.6)')'GUESS',I,'=',GUESS(I)
13    CONTINUE
C
C     ++++++++++++++++++++++++++++++++++++++++++++++++++++++++++++++
C     ALLOW SOME CHANGE
C     ++++++++++++++++++++++++++++++++++++++++++++++++++++++++++++++
      WRITE(*,*)'DO YOU WANT TO MAKE SOME CHANGE?  y/n'
      READ(*,'(A)')JUGE
C
      IF(JUGE.EQ.'y')THEN
       WRITE(*,*)'TYPE THE NUMBER FOR CHANGE (1/2/3....)'
       READ(*,*)I
       WRITE(*,*)'GUESS',I, '= ?'
       READ(*,*)GUESS(I)
       GOTO 999
      ENDIF
C
      GUESS1=GUESS(1)
      GUESS2=GUESS(2)
      GUESS3=GUESS(3)
      GUESS4=GUESS(4)
      GUESS5=GUESS(5)
      GUESS6=GUESS(6)
      GUESS7=GUESS(7)
      GUESS8=GUESS(8)
C
C     ++++++++++++++++++++++++++++++++++++++++++++++++++++++++++++++
C     CALL LSODE SECTION !!!!!
C     PARAMETERS REQUIRED BY LSODE
C     SEE "LSODE" PROGRAM DOCUMENT (Hindmash, 1980)
C     ++++++++++++++++++++++++++++++++++++++++++++++++++++++++++++++
      DO 10 I=1,M
       Y(3*I-2)=ROA0
       Y(3*I-1)=ROM0
       Y(3*I)=TEMP0
10    CONTINUE
      T=0.D0
      TOUT=0.D0
      ITOL=2
      RTOL=1.D-6
      DO 20 I=1,M
       ATOL(3*I-2)=1.D-8
       ATOL(3*I-1)=1.D-8
       ATOL(3*I)=1.D-8
20    CONTINUE
      ITASK=1
      ISTATE=1
      IOPT=1
      LRW=22+25*NEQ
      LIW=NEQ+20
      MF=25
      DO 30 I=5,10
       RWORK(I)=0.D0
       IWORK(I)=0
30    CONTINUE
C
C
      MXSTEP=100000
      IWORK(6)=MXSTEP
C
```

```
      ML=5
      MU=5
      IWORK(1)=ML
      IWORK(2)=MU
C
C     OPEN FILES TO RECORD OUT PUTS
      WRITE(*,*)'FILE OF TEMPERATURE AT DESIRED POINTS (TMESH=?)'
      READ(*,'(A)')TMESH
      WRITE(*,*)'FILE OF MC AT DESIRED POINTS (MCMESH=?)'
      READ(*,'(A)')MCMESH
      WRITE(*,*)'FILE OF AVERAGE MC (AVMOIST=?)'
      READ(*,'(A)')AVMOIST
      WRITE(*,*)'FILE OF CENTER TEMP (CENTEMP=?)'
      READ(*,'(A)')CENTEMP
      OPEN(UNIT=10,STATUS='NEW',FILE=TMESH)
      OPEN(UNIT=11,STATUS='NEW',FILE=MCMESH)
      OPEN(UNIT=12,STATUS='NEW',FILE=AVMOIST)
      OPEN(UNIT=13,STATUS='NEW',FILE=CENTEMP)
C
C     WRITE(*,*)'FILE OF BOUNDARY MOISTURE (BCMOIST=?)'
C     READ(*,*)BCMOIST
C     OPEN(UNIT=14,STATUS='NEW',FILE=BCMOIST)
C
      IT=101+INT((TSTOP-101)/10.D0)+1
      DO 40 IOUT=1,IT
50     CONTINUE
       CALL LSODE(FEX,NEQ,Y,T,TOUT,ITOL,RTOL,ATOL,ITASK,ISTATE,IOPT,
     $         RWORK,LRW,IWORK,LIW,FEX,MF)
       WRITE(*,*)ISTATE,GUESS4
       IF(ISTATE.LT.0)THEN
            ISTATE=2
            GOTO 50
       ENDIF
C
       WRITE(11,'(167F10.4)')(Y(3*I-1)/RHOD*100.d0,I=1,M)
       WRITE(10,'(167F10.4)')(Y(3*I)-273.D0,I=1,M)
       WRITE(13,'(F7.1,F10.4)')T/60,Y(3*(M+1)/2)-273.15D0
C
       SUM=0.D0
       DO 5 I=1,M
        TERM=Y(3*I-1)
            SUM=SUM+TERM
5      CONTINUE
       SUM=SUM+GUESS4+GUESS8
       MC=SUM/(M+1)/RHOD*100.D0
       WRITE(12,'(F7.1,F10.4)')T/60,MC
C
       IF(ISTATE.LT.0)GOTO 50
       IF(IOUT.LT.101)TOUT=60.D0*IOUT
       IF(IOUT.GE.101)TOUT=TOUT+600.D0
40    CONTINUE
100   CONTINUE
      WRITE(*,*)ISTATE,TOUT,IOUT
      CLOSE(UNIT=9)
      CLOSE(UNIT=10)
      CLOSE(UNIT=11)
      CLOSE(UNIT=12)
      CLOSE(UNIT=13)
      STOP
      END
```

APPENDIX B

Subroutine for LSODE

```
C     ***************************************************************
      SUBROUTINE FEX(NEQ,T,Y,YOUT)
C     ***************************************************************
C     SUBROUTINE FEX IS REQUIRED BY THE LSODE. FEX BASICALLY
C     PROVIDE THE VALUES F(X,Y) AT RIGHT HAND SIDE OF ODE EQUATIONS:
C     DY/DX=F(X,Y).
C     SEE "LSODE" PROGRAM DOCUMENT (Hindmash, 1980)
C     ***************************************************************
C
      EXTERNAL FCN
C
C     GLOBAL VARIBLES
C     +++++++++++++++++++++++++++++++++++++++++++++++++++++++++++++++++
      INTEGER NEQ
      DOUBLE PRECISION Y,T,YOUT
      DIMENSION Y(NEQ),YOUT(NEQ)
C
C     VARIABLES RELATED TO ROOT FINDING SUBROUTINE "HYBRD1"
C     +++++++++++++++++++++++++++++++++++++++++++++++++++++++++++++++++
      INTEGER N,IFLAG
      INTEGER INFO,LWA
      PARAMETER(N=4)
      DOUBLE PRECISION X,FVEC,TOL,WA
      DIMENSION X(4),FVEC(4),WA(50)
C
C     LOCAL VARIABLES
C     +++++++++++++++++++++++++++++++++++++++++++++++++++++++++++++++++
      DOUBLE PRECISION EPS,PI
      PARAMETER(EPS=.1D-8,PI=3.141592654)
      DOUBLE PRECISION RHOW
      DOUBLE PRECISION A1,A2,A3,A4
      DOUBLE PRECISION Z1,Z2,Z3,Z4,U1,U2,U3,U4
C
      DOUBLE PRECISION KG,KF,DEFF,EITAG,EITAW,PC,CEXP,
     $ MRHOA,MRHOV,MRHOVSAT,MRHOB,MRHOBFSP,MRHOF,MPA,MPV,MPVSAT,
     $ MANA,MBNA,MCNA,MDNA,MANV,MBNV,MCNV,MDNV,MANB,MBNB,MCNB,
     $ MANF,MBNF,MANBFSP,MBNBFSP,MCNBFSP,MTHK,MEMZLO,
     $ RRHOA,RRHOV,RRHOVSAT,RRHOB,RRHOBFSP,RRHOF,
     $ RPA,RPV,RPVSAT,RRHOM,
     $ RANA,RBNA,RCNA,RDNA,RANV,RBNV,RCNV,RDNV,RANB,RBNB,RCNB,
     $ RANF,RBNF,RANBFSP,RBNBFSP,RCNBFSP,RTHK,RTEMP,REMZLO,
     $ LRHOA,LRHOV,LRHOVSAT,LRHOB,LRHOBFSP,LRHOF,LPA,LPV,LPVSAT,
     $ LANA,LBNA,LCNA,LDNA,LANV,LBNV,LCNV,LDNV,LANB,LBNB,LCNB,
     $ LANF,LBNF,LANBFSP,LBNBFSP,LCNBFSP,LTHK,LEMZLO,LTEMP,LRHOM,
     $ DNA,DNV,DNB,DNF,LAMDA,TDP,DTDPPV,DHVDP,DLAMDA,MCONST,
     $ CNA,CNV,CNB,CNF, DNBFSP,CK,CT,CNVSAT,CPV,SV,SVSAT
C
      COMMON MANA,MCNA,RBNA,RDNA,LBNA,LDNA,MANV,MCNV,RBNV,RDNV,
     $ LBNV,LDNV,MANF,RBNF,LBNF,
     $ MANB,MBNB,RCNB,LCNB,MPV,RPV,LPV,MRHOB,MRHOBFSP
C
      INTEGER I,M
      DOUBLE PRECISION RHOD,EMZLOD,MA,MV,R,KGD,KFS,ALFA,DB,SIR,H
```

```
      DOUBLE PRECISION KMASS,KHEAT,ENTEMP,T2,T3,T122,T123,BCVA,BCVV
      DOUBLE PRECISION GUESS1,GUESS2,GUESS3,GUESS4,GUESS5,GUESS6,
     $                 GUESS7,GUESS8
C
      COMMON I,M
      COMMON /TRY1/RHOD,EMZLOD,MA,MV,R,KGD,KFS,ALFA,DB,SIR,H
      COMMON /TRY2/KMASS,KHEAT,ENTEMP,T2,T3,T122,T123,BCVA,BCVV
      COMMON /TRY3/GUESS1,GUESS2,GUESS3,GUESS4,GUESS5,GUESS6,
     $  GUESS7,GUESS8
C
C     ++++++++++++++++++++++++++++++++++++++++++++++++++++++++++++++++++++
      M=NEQ/3

C     ++++++++++++++++++++++++++++++++++++++++++++++++++++++++++++++++++++
C     N,LWA,TOL,T2,T3,T122,T123 is required by HYBRD1
C     ++++++++++++++++++++++++++++++++++++++++++++++++++++++++++++++++++++
      T2=Y(2)
      T3=Y(3)
      T122=Y(NEQ-1)
      T123=Y(NEQ)
C
      LWA=50
      TOL=1.D-8
C
C     ++++++++++++++++++++++++++++++++++++++++++++++++++++++++++++++++++++
C     ASSIGN THE DUMMY VARIBELS
C     ++++++++++++++++++++++++++++++++++++++++++++++++++++++++++++++++++++
      MPA=0.D0
      MPV=0.D0
      MPVSAT=0.D0
      MRHOA=0.D0
      MRHOV=0.D0
      MRHOVSAT=0.D0
      MRHOB=0.D0
      MRHOBFSP=0.D0
      MRHOF=0.D0
      MANA=0.D0
      MBNA=0.D0
      MCNA=0.D0
      MDNA=0.D0
      MANB=0.D0
      MBNB=0.D0
      MCNB=0.D0
      MANV=0.D0
      MBNV=0.D0
      MCNV=0.D0
      MDNV=0.D0
      MANBFSP=0.D0
      MBNBFSP=0.D0
      MCNBFSP=0.D0
      MANF=0.D0
      MBNF=0.D0
      MTHK=0.D0
      MEMZLO=0.D0
C     ************************************************************
C     CALCULATE FIRST POINT BELOW THE FIRST BOUNDARY
C     ************************************************************
C
C     ++++++++++++++++++++++++++++++++++++++++++++++++++++++++++++++++++++
C     VARIABLE SEPERATION
C     ++++++++++++++++++++++++++++++++++++++++++++++++++++++++++++++++++++
C
```

```
C     RHOW - (Stanish et. al., 1986) EQ.(45): DENSITY OF LIQUID WATER
C     CEXP - (Stanish et. al., 1986) EQ.(4):
C     A1,A2,A3,A4 - (Stanish et. al., 1986) EQ.(6),(7),(8),(9)
C     RRHOBFSP - (Schajer et.al., 1984) EQ. (6):
C     REMZLO - (Stanish et. al., 1986) PG1303
C     RRHOV - (Stanish et. al., 1986) EQ.(4)
C
      RHOW=1157.8D0-.5631D0*Y(3)
      CEXP=DEXP(-46.49D0+.26179*Y(3)-5.0104D-4*Y(3)**2+
     $     3.4712D-7*Y(3)**3)
      A1=-45.7D0+.3216D0*Y(3)-5.012D-4*Y(3)**2
      A2=-.1722D0+4.732D-3*Y(3)-5.553D-6*Y(3)**2
      A3=1417.D0-9.43D0*Y(3)+1.853D-2*Y(3)**2
      A4=(1.D0-18.D0*RHOD/A3/Y(2))/2.D0/A2-
     $   (1.D0+18.D0*RHOD/A3/Y(2))/2.D0/A1/A2
C     ASSUME RHOF.NEQ.0 THEN H=1
      RRHOBFSP=18.D0*A2/A3*(1.D0/(1.D0-A2)+A1/(1.D0+A1*A2))*RHOD
      RRHOF=(Y(2)-RRHOBFSP-EMZLOD*CEXP)/(1.D0-CEXP/RHOW)
      IF(RRHOF.GT.EPS)THEN
        REMZLO=EMZLOD-RRHOF/RHOW
        RRHOV=REMZLO*CEXP
        RRHOVSAT=RRHOV
        RRHOB=RRHOBFSP
        IF(RRHOF.LT.EMZLOD*RHOW*SIR)THEN
          KF=0.D0
        ELSE
          KF=KFS*(1.D0-DCOS(PI/2.D0*((RRHOF/EMZLOD/RHOW-SIR)/
     $       (1.D0-SIR))))
        ENDIF
      ELSE
        REMZLO=EMZLOD
        RRHOF=0.D0
        RRHOVSAT=REMZLO*CEXP
        RRHOV=RRHOVSAT*(A4+(A4**2+1.D0/A1/A2**2)**.5)
        RRHOB=Y(2)-RRHOV
      ENDIF
      RRHOA=Y(1)
C
C     END OF VARIABLE SEPERATIOM
C     ++++++++++++++++++++++++++++++++++++++++++++++++++++++++++++++
C
C
C     ++++++++++++++++++++++++++++++++++++++++++++++++++++++++++++++
C     PARAMETERS RELATED TO NA
C     SEE (Stanish et. al., 1986) EQ.(25)
C     ++++++++++++++++++++++++++++++++++++++++++++++++++++++++++++++
C     RPA,RPV,RPVSAT - (Stanish et. al., 1986) PG1303
C     KG - (Stanish et. al., 1986) EQ.(29)
C     EITAG - (Stanish et. al., 1986) EQ.(46)
C     DEFF - (Stanish et. al., 1986) EQ.(28)
      RPA=R/MA*Y(3)*Y(1)/REMZLO
      RPV=R/MV*Y(3)*RRHOV/REMZLO
      RPVSAT=R/MV*Y(3)*RRHOVSAT/REMZLO
      KG=KGD*(1.D0-RRHOF/EMZLOD/RHOW)
      EITAG=((4.06D-8*Y(3)+6.36D-6)*RPA+
     $     (3.8D-8*Y(3)-1.57D-6)*RPV)/(RPA+RPV)
      RANA=Y(1)/REMZLO*KG/EITAG
      RBNA=RPA+RPV
      DEFF=1.22D-4*Y(3)**.75D0*REMZLO**3*ALFA/R/(Y(1)/MA+RRHOV/MV)
      RCNA=MA/REMZLO*(Y(1)/MA+RRHOV/MV)*DEFF
```

```
      RDNA=RPA/(RPA+RPV)
C     PARAMETERS RELATED TO NV
      RANV=RRHOV/REMZLO*KG/EITAG
      RBNV=RPA+RPV
      RCNV=MV/REMZLO*(Y(1)/MA+RRHOV/MV)*DEFF
      RDNV=RPV/(RPA+RPV)
C
C     ++++++++++++++++++++++++++++++++++++++++++++++++++++++++++++++
C     PARAMETERS RELATED TO NB
C     SEE (Stanish et. al., 1986) EQ.(33)
C     ++++++++++++++++++++++++++++++++++++++++++++++++++++++++++++++
C
C     SV - (Stanish et. al., 1986) EQ.(35)
      SV=187.D0+35.1D0*DLOG(Y(3)/298.15D0)-8.314D0*
     $ DLOG(RPV/101325.D0)
      RANB=SV/MV
      RBNB=REMZLO/RRHOV
      RCNB=Y(3)
C
C     PARAMETERS RELATED TO NBFSP
      SVSAT=187.D0+35.1D0*DLOG(Y(3)/298.15D0)-
     $      8.314*DLOG(RPVSAT/101325.D0)
      RANBFSP=SVSAT/MV
      RBNBFSP=REMZLO/RRHOVSAT
      RCNBFSP=Y(3)
C
C     ++++++++++++++++++++++++++++++++++++++++++++++++++++++++++++++
C     PARAMETERS RELATED TO NF
C     SEE (Stanish et. al., 1986) EQ.(21)
C     ++++++++++++++++++++++++++++++++++++++++++++++++++++++++++++++
C
C     EITAW - (Stanish et. al., 1986) EQ.(47)
C     PC - (Stanish et. al., 1986) EQ.(22)
C
      IF(RRHOF.GT.0.D0)THEN
        EITAW=10.D0**(-13.73D0+1828.D0/Y(3)+1.966D-2*Y(3)-
     $       1.466D-5*Y(3)**2)
        RANF=KF/RHOW/EITAW
        PC=10000.D0*EMZLOD**.61D0*(RRHOF/RHOW)**(-.61D0)
        RBNF=RPA+RPV-PC
      ELSE
        RANF=0.D0
        RBNF=0.D0
      ENDIF
C
C     ++++++++++++++++++++++++++++++++++++++++++++++++++++++++++++++
C     PARAMETERS RELATED TO THERMAL CONDUCTIVITY
C     SEE (Stanish et. al., 1986) EQ.(48)
C     ++++++++++++++++++++++++++++++++++++++++++++++++++++++++++++++
C
      RTHK=RHOD/1000.D0*(.4D0+.5D0*Y(2)/RHOD)+.024D0
C
C
C     ***************************************************************
C     BEGIN MAIN LOOP
C     ***************************************************************
      DO 10 I=1,M
C     CHANGE POSITION
        LPA=MPA
        LPV=MPV
```

```
      LPVSAT=MPVSAT
      LRHOA=MRHOA
      LRHOV=MRHOV
      LRHOVSAT=MRHOVSAT
      LRHOB=MRHOB
      LRHOBFSP=MRHOBFSP
      LRHOF=MRHOF
      LANA=MANA
      LBNA=MBNA
      LCNA=MCNA
      LDNA=MDNA
      LANV=MANV
      LBNV=MBNV
      LCNV=MCNV
      LDNV=MDNV
      LANB=MANB
      LBNB=MBNB
      LCNB=MCNB
      LANBFSP=MANBFSP
      LBNBFSP=MBNBFSP
      LCNBFSP=MCNBFSP
      LANF=MANF
      LBNF=MBNF
      LTHK=MTHK
      LEMZLO=MEMZLO
C
      MPA=RPA
      MPV=RPV
      MPVSAT=RPVSAT
      MRHOA=RRHOA
      MRHOV=RRHOV
      MRHOVSAT=RRHOVSAT
      MRHOB=RRHOB
      MRHOBFSP=RRHOBFSP
      MRHOF=RRHOF
      MANA=RANA
      MBNA=RBNA
      MCNA=RCNA
      MDNA=RDNA
      MANB=RANB
      MBNB=RBNB
      MCNB=RCNB
      MANV=RANV
      MBNV=RBNV
      MCNV=RCNV
      MDNV=RDNV
      MANBFSP=RANBFSP
      MBNBFSP=RBNBFSP
      MCNBFSP=RCNBFSP
      MANF=RANF
      MBNF=RBNF
      MTHK=RTHK
      MEMZLO=REMZLO

C     ************************************************************
C     CALCULATE THE SECOND POINT BELOW THE FIRST BOUNDARY
C     ************************************************************
C
      IF(I.LT.M)THEN
C
```

```
      RHOW=1157.8D0-.5631D0*Y(3+3*I)
       CEXP=DEXP(-46.49D0+.26179*Y(3+3*I)-5.0104D-4*Y(3+3*I)**2+
     $       3.4712D-7*Y(3+3*I)**3)
       A1=-45.7D0+.3216D0*Y(3+3*I)-5.012D-4*Y(3+3*I)**2
       A2=-.1722D0+4.732D-3*Y(3+3*I)-5.553D-6*Y(3+3*I)**2
       A3=1417.D0-9.43D0*Y(3+3*I)+1.853D-2*Y(3+3*I)**2
       A4=(1.D0-18.D0*RHOD/A3/Y(2+3*I))/2.D0/A2-
     $     (1.D0+18.D0*RHOD/A3/Y(2+3*I))/2.D0/A1/A2
C     ASSUME RHOF.NEQ.0 THEN H=1
       RRHOBFSP=18.D0*A2/A3*(1.D0/(1.D0-A2)+
     $       A1/(1.D0+A1*A2))*RHOD
       RRHOF=(Y(2+3*I)-RRHOBFSP-EMZLOD*CEXP)/(1.D0-CEXP/RHOW)
       IF(RRHOF.GT.EPS)THEN
        REMZLO=EMZLOD-RRHOF/RHOW
        RRHOV=REMZLO*CEXP
            RRHOVSAT=RRHOV
        RRHOB=RRHOBFSP
            IF(RRHOF.LT.EMZLOD*RHOW*SIR)THEN
             KF=0.D0
        ELSE
         KF=KFS*(1.D0-DCOS(PI/2.D0*((RRHOF/EMZLOD/RHOW-SIR)
     $             /(1.D0-SIR))))
        ENDIF
       ELSE
        REMZLO=EMZLOD
        RRHOF=0.D0
        RRHOVSAT=REMZLO*CEXP
              RRHOV=RRHOVSAT*(A4+(A4**2+1.D0/A1/A2**2)**.5)
              RRHOB=Y(2+3*I)-RRHOV
       ENDIF
       RRHOA=Y(1+3*I)
C
C     PARAMETERS RELATED TO NA
       RPA=R/MA*Y(3+3*I)*Y(1+3*I)/REMZLO
       RPV=R/MV*Y(3+3*I)*RRHOV/REMZLO
       RPVSAT=R/MV*Y(3+3*I)*RRHOVSAT/REMZLO
       KG=KGD*(1.D0-RRHOF/EMZLOD/RHOW)
       EITAG=((4.06D-8*Y(3+3*I)+6.36D-6)*RPA+
     $       (3.8D-8*Y(3+3*I)-1.57D-6)*RPV)/(RPA+RPV)
       RANA=Y(1+3*I)/REMZLO*KG/EITAG
       RBNA=RPA+RPV
       DEFF=1.22D-4*Y(3+3*I)**.75D0*REMZLO**3*ALFA/R/
     $     (Y(1+3*I)/MA+RRHOV/MV)
            RCNA=MA/REMZLO*(Y(1+3*I)/MA+RRHOV/MV)*DEFF
            RDNA=RPA/(RPA+RPV)
C     PARAMETERS RELATED TO NV
       RANV=RRHOV/REMZLO*KG/EITAG
       RBNV=RPA+RPV
       RCNV=MV/REMZLO*(Y(1+3*I)/MA+RRHOV/MV)*DEFF
       RDNV=RPV/(RPA+RPV)
C
C     PARAMETERS RELATED TO NB
       SV=187.D0+35.1D0*DLOG(Y(3+3*I)/298.15D0)-8.314D0*
     $       DLOG(RPV/101325.D0)
       RANB=SV/MV
       RBNB=REMZLO/RRHOV
       RCNB=Y(3+3*I)
C
C
C     PARAMETERS RELATED TO NBFSP
```

```
      SVSAT=187.D0+35.1D0*DLOG(Y(3+3*I)/298.15D0)-
     $       8.314*DLOG(RPVSAT/101325.D0)
        RANBFSP=SVSAT/MV
          RBNBFSP=REMZLO/RRHOVSAT
        RCNBFSP=Y(3+3*I)
C
C     PARAMETER RELATED TO NF
        IF(RRHOF.GT.0.D0)THEN
         EITAW=10.D0**(-13.73D0+1828.D0/Y(3+3*I)+
     $      1.966D-2*Y(3+3*I)-1.466D-5*Y(3+3*I)**2)
         RANF=KF/RHOW/EITAW
         PC=10000.D0*EMZLOD**.61D0*(RRHOF/RHOW)**-.61D0
         RBNF=RPA+RPV-PC
        ELSE
         RANF=0.D0
         RBNF=0.D0
        ENDIF
C     PARAMETERS RELATED TO THERMAL CONDUCTIVITY
        RTHK=RHOD/1000.D0*(.4D0+.5D0*Y(2+3*I)/RHOD)+.024D0
C
C     ++++++++++++++++++++++++++++++++++++++++++++++++++++++++++++++
C     WHEN I=1, BOUNDARY VALUES ARE CALCULATED BY 'HBRD1'
C     ++++++++++++++++++++++++++++++++++++++++++++++++++++++++++++++
C     X(1)-X(4) - ARRAY TO STORE THE MULTIPLE ROOTS
C     HYBRD1 - NONLINEAR MULTIPLE ROOTS SOLVE SUBROUTINE
C
        IF(I.EQ.1)THEN
         X(1)=GUESS1
         X(2)=GUESS2
         X(3)=GUESS3
         X(4)=GUESS4
         CALL HYBRD1(FCN,N,X,FVEC,TOL,INFO,WA,LWA)
C
         IF(INFO.EQ.4)THEN
          GUESS1=GUESS1
          GUESS2=GUESS2
          GUESS3=GUESS3
          GUESS4=GUESS4
         ELSE
          GUESS1=X(1)
          GUESS2=X(2)
          GUESS3=X(3)
          GUESS4=X(4)
         ENDIF
C
C     CALCULATE BOUNDARY POINT
         LRHOA=X(1)
         LRHOF=0.D0
         LTEMP=X(2)
         LRHOM=X(4)
C
         CEXP=DEXP(-46.49D0+.26179*LTEMP-5.0104D-4*LTEMP**2+
     $       3.4712D-7*LTEMP**3)
         A1=-45.7D0+.3216D0*LTEMP-5.012D-4*LTEMP**2
         A2=-.1722D0+4.732D-3*LTEMP-5.553D-6*LTEMP**2
         A3=1417.D0-9.43D0*LTEMP+1.853D-2*LTEMP**2
         A4=(1.D0-18.D0*RHOD/A3/LRHOM)/2.D0/A2-
     $      (1.D0+18.D0*RHOD/A3/LRHOM)/2.D0/A1/A2
C
C     RHOF.EQ.0 AND H=1
```

```
      LRHOBFSP=18.D0*A2/A3*(1.D0/(1.D0-A2)+A1/
     $     (1.D0+A1*A2))*RHOD
      LEMZLO=EMZLOD
      LRHOVSAT=LEMZLO*CEXP
      LRHOV=LRHOVSAT*(A4+(A4*A4+1.D0/A1/A2/A2)**.5D0)
        LRHOB=X(4)-LRHOV
C
      LPA=R/MA*LTEMP*LRHOA/LEMZLO
      LPV=R/MV*LTEMP*LRHOV/LEMZLO
      LPVSAT=R/MV*LTEMP*LRHOVSAT/LEMZLO
C   PARAMETERS RELATED TO NA
      KG=KGD*(1.D0-LRHOF/EMZLOD/RHOW)
      EITAG=((4.06D-8*LTEMP+6.36D-6)*LPA+
     $     (3.8D-8*LTEMP-1.57D-6)*LPV)/(LPA+LPV)
      LANA=LRHOA/LEMZLO*KG/EITAG
      LBNA=LPA+LPV
      DEFF=1.22D-4*LTEMP**.75D0*LEMZLO**3*ALFA/R/
     $        (LRHOA/MA+LRHOV/MV)
      LCNA=MA/LEMZLO*(LRHOA/MA+LRHOV/MV)*DEFF
      LDNA=LPA/(LPA+LPV)
C   PARAMETERS RELATED TO NV
      LANV=LRHOV/LEMZLO*KG/EITAG
      LBNV=LPA+LPV
      LCNV=MV/LEMZLO*(LRHOA/MA+LRHOV/MV)*DEFF
      LDNV=LPV/(LPA+LPV)
C
C   PARAMETERS RELATED TO NB
      SV=187.D0+35.1D0*DLOG(LTEMP/298.15D0)-8.314D0*
     $   DLOG(LPV/101325.D0)
      LANB=SV/MV
      LBNB=LEMZLO/LRHOV
      LCNB=LTEMP
C
C   PARAMETERS RELATED TO NBFSP
      SVSAT=187.D0+35.1D0*DLOG(LTEMP/298.15D0)-
     $     8.314*DLOG(LPVSAT/101325.D0)
      LANBFSP=SVSAT/MV
      LBNBFSP=LEMZLO/LRHOVSAT
      LCNBFSP=LTEMP
C
C   PARAMETER RELATED TO NF
      IF(LRHOF.GT.0.D0)THEN
          EITAW=10.D0**(-13.73D0+1828.D0/LTEMP+1.966D-2*LTEMP-
     $      1.466D-5*LTEMP**2)
          LANF=KF/RHOW/EITAW
          PC=10000.D0*EMZLOD**.61D0*(LRHOF/RHOW)**(-.61D0)
          LBNF=LPA+LPV-PC
      ELSE
          LANF=0.D0
          LBNF=0.D0
      ENDIF
C
C   PARAMETERS RELATED TO THERMAL CONDUCTIVITY
      LTHK=RHOD/1000.D0*(.4D0+.5D0*LRHOM/RHOD)+.024D0
C
     ENDIF
C   ++++++++++++++++++++++++++++++++++++++++++++++++++++++++
C   END OF BOUNDARY VALUES CALCULATION
C   ++++++++++++++++++++++++++++++++++++++++++++++++++++++++
     ELSE
```

```
C     ********************************************************
C     SECOND BOUNDARY
C     ********************************************************
C
C     WHEN I=M, THE SECOND BOUNDARY VALUES ARE REQUIRED

        X(1)=GUESS5
            X(2)=GUESS6
            X(3)=GUESS7
            X(4)=GUESS8
C
        CALL HYBRD1(FCN,N,X,FVEC,TOL,INFO,WA,LWA)
        IF(INFO.EQ.4)THEN
          GUESS5=GUESS5
          GUESS6=GUESS6
              GUESS7=GUESS7
              GUESS8=GUESS8
        ELSE
          GUESS5=X(1)
          GUESS6=X(2)
              GUESS7=X(3)
              GUESS8=X(4)
        ENDIF
C
        RRHOA=X(1)
        RRHOF=0.D0
            RTEMP=X(2)
        RRHOM=X(4)
C
        CEXP=DEXP(-46.49D0+.26179*RTEMP-5.0104D-4*RTEMP**2+
     $      3.4712D-7*RTEMP**3)
        A1=-45.7D0+.3216D0*RTEMP-5.012D-4*RTEMP**2
        A2=-.1722D0+4.732D-3*RTEMP-5.553D-6*RTEMP**2
        A3=1417.D0-9.43D0*RTEMP+1.853D-2*RTEMP**2
        A4=(1.D0-18.D0*RHOD/A3/RRHOM)/2.D0/A2-
     $     (1.D0+18.D0*RHOD/A3/RRHOM)/2.D0/A1/A2
C
C     RHOF.EQ.0 AND H=1
        RRHOBFSP=18.D0*A2/A3*(1.D0/(1.D0-A2)+
     $      A1/(1.D0+A1*A2))*RHOD
        REMZLO=EMZLOD
        RRHOVSAT=REMZLO*CEXP
        RRHOV=RRHOVSAT*(A4+(A4*A4+1.D0/A1/A2/A2)**.5D0)
            RRHOB=X(4)-RRHOV
C
        RPA=R/MA*RTEMP*RRHOA/REMZLO
        RPV=R/MV*RTEMP*RRHOV/REMZLO
        RPVSAT=R/MV*RTEMP*RRHOVSAT/REMZLO
C     PARAMETERS RELATED TO NA
        KG=KGD*(1.D0-RRHOF/EMZLOD/RHOW)
        EITAG=((4.06D-8*RTEMP+6.36D-6)*RPA+
     $      (3.8D-8*RTEMP-1.57D-6)*RPV)/(RPA+RPV)
        RANA=RRHOA/REMZLO*KG/EITAG
        RBNA=RPA+RPV
        DEFF=1.22D-4*RTEMP**.75D0*REMZLO**3*ALFA/R/
     $    (RRHOA/MA+RRHOV/MV)
        RCNA=MA/REMZLO*(RRHOA/MA+RRHOV/MV)*DEFF
        RDNA=RPA/(RPA+RPV)
C
C     PARAMETERS RELATED TO NV
```

```
      RANV=RRHOV/REMZLO*KG/EITAG
      RBNV=RPA+RPV
      RCNV=MV/REMZLO*(RRHOA/MA+RRHOV/MV)*DEFF
      RDNV=RPV/(RPA+RPV)
C
C   PARAMETERS RELATED TO NB
      SV=187.D0+35.1D0*DLOG(RTEMP/298.15D0)-8.314D0*
     $          DLOG(RPV/101325.D0)
      RANB=SV/MV
      RBNB=REMZLO/RRHOV
      RCNB=RTEMP
C
C   PARAMETERS RELATED TO NBFSP
      SVSAT=187.D0+35.1D0*DLOG(RTEMP/298.15D0)-
     $       8.314*DLOG(RPVSAT/101325.D0)
            RANBFSP=SVSAT/MV
            RBNBFSP=REMZLO/RRHOVSAT
      RCNBFSP=RTEMP
C
C   PARAMETER RELATED TO NF
      IF(RRHOF.GT.0.D0)THEN
            EITAW=10.D0**(-13.73D0+1828.D0/RTEMP+1.966D-2*RTEMP-
     $       1.466D-5*RTEMP**2)
            RANF=KF/RHOW/EITAW
            PC=10000.D0*EMZLOD**.61D0*(RRHOF/RHOW)**-.61D0
            RBNF=RPA+RPV-PC
      ELSE
            RANF=0.D0
            RBNF=0.D0
      ENDIF
C
C   PARAMETERS RELATED TO THERMAL CONDUCTIVITY
      RTHK=RHOD/1000.D0*(.4D0+.5D0*RRHOM/RHOD)+.024D0
C
    ENDIF
C
C
C   ++++++++++++++++++++++++++++++++++++++++++++++++++++++++++++
C   CONSTRUCT RIGHT HAND SIDE
C   ++++++++++++++++++++++++++++++++++++++++++++++++++++++++++++
C
C   ---------------------------------
C   EQ(1): (Stanish et. al., 1986) EQ.(1)
C   ---------------------------------
    DNA=(RANA-LANA)*(RBNA-LBNA)/(4.D0*H*H)+
   $  MANA*(RBNA-2.D0*MBNA+LBNA)/(H*H)+
   $  (RCNA-LCNA)*(RDNA-LDNA)/(4.D0*H*H)+
   $  MCNA*(RDNA-2.D0*MDNA+LDNA)/(H*H)
    YOUT(3*I-2)=DNA
C   ---------------------------------
C   EQ(2): (Stanish et. al., 1986) EQ.(2)
C   ---------------------------------
    DNV=(RANV-LANV)*(RBNV-LBNV)/(4.D0*H*H)+
   $  MANV*(RBNV-2.D0*MBNV+LBNV)/(H*H)+
   $  (RCNV-LCNV)*(RDNV-LDNV)/(4.D0*H*H)+
   $  MCNV*(RDNV-2.D0*MDNV+LDNV)/(H*H)
C
    DNB=DB*(1.D0-EMZLOD)*(-(RANB-LANB)*(RCNB-LCNB)/(4.D0*H*H)
   $  -MANB*(RCNB-2.D0*MCNB+LCNB)/(H*H)+(RBNB-LBNB)*(RPV-LPV)
   $  /(4.D0*H*H)+MBNB*(RPV-2.D0*MPV+LPV)/(H*H))
```

```
      DNF=(RANF-LANF)*(RBNF-LBNF)/(4.D0*H*H)+
     $    MANF*(RBNF-2.D0*MBNF+LBNF)/(H*H)
C
      YOUT(3*I-1)=DNV+DNB+DNF
C
C
C     ------------------------------
C     EQ(3) (Stanish et. al., 1986) EQ.(3)
C     ------------------------------
C     PARAMETER BEFORE DTEMP/DT
C     LAMDA - (Stanish et. al., 1986) EQ.(40)
C     TDP - (Stanish et. al., 1986) EQ.(42)
C
      LAMDA=2.792D6-160.D0*Y(3*I)-3.43D0*Y(3*I)**2
      TDP=230.9D0+2.1D-4*MPV-.639D0*MPV**.5D0+
     $     6.95*MPV**(1.D0/3.D0)
      DTDPPV=2.1D-4-.5D0*.639D0*MPV**-.5D0+1.D0/3.D0*6.95D0*MPV**
     $    (-2.D0/3.D0)
      DHVDP=2070.D0-2.D0*3.43D0*TDP
      DLAMDA=-160.D0-2.D0*3.43D0*Y(3*I)
      MCONST=1000.D0*Y(3*I-2)+1950.D0*MRHOV
     $   +DTDPPV*DHVDP*R/MV/MEMZLO*MRHOV**2
     $   +4180.D0*MRHOB-.4*(1.D0-MRHOB/MRHOBFSP)**2*DLAMDA*MRHOB
     $   +4180.D0*MRHOF+1360.D0*RHOD
      CNA=MANA*(RBNA-LBNA)/(2.D0*H)+MCNA*(RDNA-LDNA)/(2.D0*H)
      CNV=MANV*(RBNV-LBNV)/(2.D0*H)+MCNV*(RDNV-LDNV)/(2.D0*H)
      CNB=DB*(1.D0-EMZLOD)*(-(MANB*(RCNB-LCNB))/(2.D0*H)+
     $    MBNB*(RPV-LPV)/(2.D0*H))
      CNF=MANF*(RBNF-LBNF)/(2.D0*H)
C
      Z1=-(RANBFSP-LANBFSP)*(RCNB-LCNB)/(4.D0*H*H)
      Z2=-MANBFSP*(RCNB-2.D0*MCNB+LCNB)/(H*H)
      Z3=(RBNBFSP-LBNBFSP)*(RPVSAT-LPVSAT)/(4.D0*H*H)
      Z4=MBNBFSP*(RPVSAT-2.D0*MPVSAT+LPVSAT)/(H*H)
      DNBFSP=DB*(1.D0-EMZLOD)*(Z1+Z2+Z3+Z4)
C
C
      IF(I.EQ.1)THEN
       CK=(RTHK-LTHK)*(Y(3*I+3)-LTEMP)/(4.D0*H*H)+
     $    MTHK*(Y(3*I+3)-2.0*Y(3*I)+LTEMP)/(H*H)
C
       CT=1000.D0*CNA+4180.D0*CNF+4180.D0*CNB-0.4D0*(1.D0-MRHOB
     $    /MRHOBFSP)**2*DLAMDA*CNB+1950.D0*CNV+
     $    DTDPPV*DHVDP*R/MV/MEMZLO*MRHOV*CNV
C
       YOUT(3*I)=(CK+CT*(Y(3*I+3)-LTEMP)/(2.D0*H))/MCONST
       GOTO 1001
      ENDIF
C
      IF(I.EQ.M)THEN
C
       CK=(RTHK-LTHK)*(RTEMP-Y(3*I-3))/(4.D0*H*H)+
     $    MTHK*(RTEMP-2.0*Y(3*I)+Y(3*I-3))/(H*H)
       CT=1000.D0*CNA+4180.D0*CNF+4180.D0*CNB-0.4D0*(1.D0-MRHOB
     $    /MRHOBFSP)**2*DLAMDA*CNB+1950.D0*CNV+
     $    DTDPPV*DHVDP*R/MV/MEMZLO*MRHOV*CNV
       YOUT(3*I)=(CK+CT*(RTEMP-Y(3*I-3))/(2.D0*H))/MCONST
      ELSE
```

```
      CK=(RTHK-LTHK)*(Y(3*I+3)-Y(3*I-3))/(4.D0*H*H)+
     $    MTHK*(Y(3*I+3)-2.0*Y(3*I)+Y(3*I-3))/(H*H)
      CT=1000.D0*CNA+4180.D0*CNF+4180.D0*CNB-0.4D0*(1.D0-MRHOB
     $    /MRHOBFSP)**2*DLAMDA*CNB+1950.D0*CNV+
     $    DTDPPV*DHVDP*R/MV/MEMZLO*MRHOV*CNV
      YOUT(3*I)=(CK+CT*(Y(3*I+3)-Y(3*I-3))/(2.D0*H))/MCONST
C
      ENDIF
C
1001  CONTINUE
C
10    CONTINUE
      RETURN
      END
C
C
C
C     ******************************************************
      SUBROUTINE FCN(N,X,FVEC,IFLAG)
C     ******************************************************
C
C     THE SUBROUTINE FCN IS REQUIRED SUBROUTINE BY HYBRD1:
C     FCN PROVIDES THE VALUES OF NONLINEAR EQUATIONS F(U).
C     ++++++++++++++++++++++++++++++++++++++++++++++++++++++++++++++
C
      EXTERNAL VAPOR
      INTEGER I,M,N,IFLAG
      DOUBLE PRECISION X,FVEC,VAPOR
      DIMENSION X(N),FVEC(N)
C
      DOUBLE PRECISION MANA,MCNA,RBNA,RDNA,LBNA,LDNA,MANV,MCNV,
     $ RBNV,RDNV,LBNV,LDNV,MANF,RBNF,LBNF,MANB,MBNB,RCNB,LCNB,
     $ MPV,RPV,LPV,MRHOB,MRHOBFSP
      DOUBLE PRECISION TDP,LAMDA,TDPP
      DOUBLE PRECISION A1,A2,A3,B1,B2,B3,B4,B5,C1,C2,C3,C4,C5,C6
      COMMON MANA,MCNA,RBNA,RDNA,LBNA,LDNA,MANV,MCNV,RBNV,RDNV,
     $ LBNV,LDNV,MANF,RBNF,LBNF,
     $ MANB,MBNB,RCNB,LCNB,MPV,RPV,LPV,MRHOB,MRHOBFSP
      COMMON I,M
C
      DOUBLE PRECISION RHOD,EMZLOD,MA,MV,R,KGD,KFS,ALFA,DB,SIR,H
      DOUBLE PRECISION KMASS,KHEAT,ENTEMP,T2,T3,T122,T123,BCVA,BCVV
C
      COMMON /TRY1/RHOD,EMZLOD,MA,MV,R,KGD,KFS,ALFA,DB,SIR,H
      COMMON /TRY2/KMASS,KHEAT,ENTEMP,T2,T3,T122,T123,BCVA,BCVV
C
      IF(I.EQ.1)THEN
C     ++++++++++++++++++++++++++++++++++++++++++++++++++++++++++++++++
C     THIS IS THE EQ (12A) OF DR. KAMKE'S NOTES ON BOUNDARY
C     VALUE DISCUSSION:
C     APPENDEX C.
C     ++++++++++++++++++++++++++++++++++++++++++++++++++++++++++++++++
      FVEC(1)=X(2)*R/EMZLOD*(X(1)/MA+VAPOR(X)/MV)-101325.D0
C     ++++++++++++++++++++++++++++++++++++++++++++++++++++++++++++++++
C     THE EQ (13I) OF DR. KAMKE'S NOTES ON BOUNDARY
C     VALUE DISCUSSION: APPENDEX C
C     A1,A2 IS TO CALCULATE NA USING THE VALUES AT 2 MESH
C     POINTS RIGHT NEXT TO THE BOUNDARY SURFACE.
C     A3 IS THE RIGHT HAND SIDE  VALUE IN EQ (13I)
C     ++++++++++++++++++++++++++++++++++++++++++++++++++++++++++++++++
```

```
      A1=MANA*(R/EMZLOD*X(2)*(X(1)/MA+VAPOR(X)/MV)-RBNA)/2.D0/H
      A2=MCNA*(X(1)/(X(1)+VAPOR(X)*MA/MV)-RDNA)/2.D0/H
      A3=(X(1)*MV/VAPOR(X)/MA*X(3)+KMASS*(BCVA/101325.D0-
     $    X(1)/(X(1)+VAPOR(X)*MA/MV)))*MA
      FVEC(2)=A1+A2-A3
C
C     ++++++++++++++++++++++++++++++++++++++++++++++++++++++++++++
C     THE EQ (13H) OF DR. KAMKE'S NOTES ON BOUNDARY
C     VALUE DISCUSSION: APPENDEX C
C     B1,B2 IS TO CALCULATE NV USING THE
C     VALUES AT 2 MESH POINTS RIGHT NEXT TO THE BOUNDARY
C     SURFACE. B3 IS TO CALCULATE NF USING THE VALUE
C     AT 2 MASH POINTS RIGHT NEXT TO THE BOUNDARY SURFACE.
C     B4 IS TO CALCULATE NB USING THE VALUE AT 2 MESH POINTS
C     RIGHT NEXT TO THE BOUNDARY SURFACE. B5 IS THE VALUE AT
C     RIGHT SIDE OF EQ (13H)
C     ++++++++++++++++++++++++++++++++++++++++++++++++++++++++++++
      B1=MANV*(R/EMZLOD*X(2)*(X(1)/MA+VAPOR(X)/MV)-RBNV)/2.D0/H
      B2=MCNV*(VAPOR(X)/(X(1)*MV/MA+VAPOR(X))-RDNV)/2.D0/H
      B3=MANF*(R/EMZLOD*X(2)*(X(1)/MA+VAPOR(X)/MV)-RBNF)/2.D0/H
      B4=DB*(1.D0-EMZLOD)*(-MANB*(X(2)-RCNB)+
     $          MBNB*(R/EMZLOD/MV*VAPOR(X)*X(2)-RPV))/2.D0/H
      B5=(X(3)+KMASS*(BCVV/101325.D0-
     $          VAPOR(X)/(X(1)/MA*MV+VAPOR(X))))*MV
      FVEC(3)=B1+B2+B3+B4-B5
C
C     ++++++++++++++++++++++++++++++++++++++++++++++++++++++++++++
C     THE EQ (13H) OF DR. KAMKE'S NOTES ON BOUNDARY
C     VALUE DISCUSSION: APPENDEX C
C     C1 IS TO CALCULATE NA*HA USING THE VALUES AT 2 MESH POINTS
C     RIGHT NEXT TO THE BOUNDARY SURFACE. C2 IS TO CALCULATE NV*HV
C     USING THE VALUES AT 2 MESH POINTS RIGHT NEXT TO THE BOUNDARY
C     SURFACE. C3 IS TO CALCULATE NF USING THE VALUE AT 2 MESH
C     POINTS RIGHT NEXT TO THE BOUNDARY SURFACE. C4 IS TO CALCULATE
C     NB*HB USING THE VALUE AT 2 MESH POINTS RIGHT NEXT TO THE
C     BOUNDARY SURFACE. C5 IS TO CALCULATE HEAT ENERGY, C6 IS THE
C     VALUE AT RIGHT HAND SIDE OF EQ (13J)
C     ++++++++++++++++++++++++++++++++++++++++++++++++++++++++++++
      C1=(A1+A2)*1000.D0*(T3-273.15D0)
      TDP=230.9D0+2.10D-4*MPV-.639D0*MPV**(1.D0/2.D0)+
     $     6.95D0*MPV**(1.D0/3.D0)
      C2=(B1+B2)*(1950.D0*T3+1.65D6+2070.D0*TDP-3.43*TDP*TDP)
      LAMDA=2.792D6-160.D0*T3-3.43D0*T3*T3
      C3=B4*(4180.D0*(T3-273.15D0)-.4D0*LAMDA*
     $    (1.D0-MRHOB/MRHOBFSP)**2)
      C4=B3*4180.D0*(T3-273.15D0)
      C5=(RHOD/1000.D0*(.4D0+.05D0*T2/RHOD)+.024D0)*(X(2)-RCNB)
     $    /2.D0/H
      TDPP=230.9D0+2.10D-4*R/EMZLOD/MV*VAPOR(X)*X(2)-
     $     .639D0*(R/EMZLOD/MV*VAPOR(X)*X(2))**(1.D0/2.D0)+
     $     6.95*(R/EMZLOD/MV*VAPOR(X)*X(2))**(1.D0/3.D0)
      C6=X(3)*(MV*(1950.D0*X(2)+1.65D6+2070.D0*TDPP-
     $     3.43D0*TDPP**2)+MA*1000.D0*(X(2)-273.15D0)*X(1)/
     $     VAPOR(X)*MV/MA)+KHEAT*(ENTEMP-X(2))
      FVEC(4)=C1+C2+C3+C4+C5-C6
    ENDIF
C
    IF(I.EQ.M)THEN
      FVEC(1)=X(2)*R/EMZLOD*(X(1)/MA+VAPOR(X)/MV)-101325.D0
C
      A1=MANA*(LBNA-R/EMZLOD*X(2)*(X(1)/MA+VAPOR(X)/MV))/2.D0/H
```

```
      A2=MCNA*(LDNA-X(1)/(X(1)+VAPOR(X)*MA/MV))/2.D0/H
      A3=(X(1)*MV/VAPOR(X)/MA*X(3)+KMASS*(-BCVA/101325.D0+
     $    X(1)/(X(1)+VAPOR(X)*MA/MV)))*MA
      FVEC(2)=A1+A2-A3
C
      B1=MANV*(LBNV-R/EMZLOD*X(2)*(X(1)/MA+VAPOR(X)/MV))/2.D0/H
      B2=MCNV*(LDNV-VAPOR(X)/(X(1)*MV/MA+VAPOR(X)))/2.D0/H
      B3=MANF*(LBNF-R/EMZLOD*X(2)*(X(1)/MA+VAPOR(X)/MV))/2.D0/H
      B4=DB*(1.D0-EMZLOD)*(-MANB*(LCNB-X(2))+
     $          MBNB*(LPV-R/EMZLOD/MV*X(2)*VAPOR(X)))/2.D0/H
      B5=(X(3)+KMASS*(-BCVV/101325.D0+
     $          VAPOR(X)/(X(1)/MA*MV+VAPOR(X))))*MV
      FVEC(3)=B1+B2+B3+B4-B5
C
      C1=(A1+A2)*1000.D0*(T123-273.15D0)
      TDP=230.9D0+2.10D-4*MPV-.639D0*MPV**(1.D0/2.D0)+
     $     6.95D0*MPV**(1.D0/3.D0)
      C2=(B1+B2)*(1950.D0*T123+1.65D6+2070.D0*TDP-3.43*TDP*TDP)
      LAMDA=2.792D6-160.D0*T123-3.43D0*T123*T123
      C3=B4*(4180.D0*(T123-273.15D0)-.4D0*LAMDA*
     $    (1.D0-MRHOB/MRHOBFSP)**2)
      C4=B3*4180.D0*(T123-273.15D0)
      C5=(RHOD/1000.D0*(.4D0+.05D0*T122/RHOD)+.024D0)*(LCNB-X(2))
     $    /2.D0/H
           TDPP=230.9D0+2.10D-4*R/EMZLOD/MV*VAPOR(X)*X(2)-
     $          .639D0*(R/EMZLOD/MV*VAPOR(X)*X(2))**(1.D0/2.D0)+
     $      6.95*(R/EMZLOD/MV*VAPOR(X)*X(2))**(1.D0/3.D0)
      C6=X(3)*(MV*(1950.D0*X(2)+1.65D6+2070.D0*TDPP-
     $    3.43D0*TDPP**2)+MA*1000.D0*(X(2)-273.15D0)*X(1)/
     $    VAPOR(X)*MV/MA)+KHEAT*(X(2)-ENTEMP)
      FVEC(4)=C1+C2+C3+C4+C5-C6
C
      ENDIF
C
      RETURN
      END


C     ************************************************************
      DOUBLE PRECISION FUNCTION VAPOR(X)
C     ************************************************************
C     VAPOR CALCULATE THE VALUES OF RHOV
      DOUBLE PRECISION X(4)
      DOUBLE PRECISION U,V1,V2,V3,V4,BCRHOVSAT
      DOUBLE PRECISION RHOD,EMZLOD,MA,MV,R,KGD,KFS,ALFA,DB,SIR,H
      COMMON /TRY1/RHOD,EMZLOD,MA,MV,R,KGD,KFS,ALFA,DB,SIR,H
C
      U=DEXP(-46.490+.26179*X(2)-5.0104D-4*X(2)*X(2)+
     $ 3.4712D-7*X(2)*X(2)*X(2))
      V1=-45.70+.3216*X(2)-5.012D-4*X(2)*X(2)
      V2=-.1722+4.732D-3*X(2)-5.553D-6*X(2)*X(2)
      V3=1417.D0-9.43D0*X(2)+1.853D-2*X(2)*X(2)
      V4=(1.D0-18.D0*RHOD/V3/X(4))/2.D0/V2-
     $  (1.D0+18.D0*RHOD/V3/X(4))/2.D0/V1/V2
C
      BCRHOVSAT=EMZLOD*U
      VAPOR=BCRHOVSAT*(V4+(V4*V4+1.D0/V1/V2/V2)**.5D0)
C
      RETURN
      END
```

APPENDIX C

Boundary Conditions

DRYSIM (Refer to Stanish et. al, Drying '85, pp 360)

Doundary conditions at z=0 and z=L:

$$p_a\ (z,t)\ +\ p_v\ (z,t)\ =\ p_a^{\infty}\ (t)\ +\ p_v\infty(t) \qquad (12)$$

$$\rho_a\ \frac{RT}{\epsilon M_a}\ (z,t)\ +\ \rho_v \frac{RT}{\epsilon M_v}\ (z,t)\ =\ p_a^{\infty}\ +\ p_v^{\infty} \qquad (12a)$$

$$n_v+n_b+n_f\ =\ [x_v(N_v+N_a)+k_x(t)\ (\frac{p_v^{\infty}}{p_a^{\infty}(t)+p_v^{\infty}\ (t)+p_v^{\infty}(t)}-x_v)\ ]M_v \qquad (13)$$

$$x_v\ =\ \frac{\rho_v\ /\ M_v}{\rho_a\ /M_a\ +\ \rho_v\ /\ M_v} \qquad (13a)$$

$$\begin{aligned} & n_a h_a\ +\ n_v h_v\ +\ n_b h_b^*\ +\ n_f h_f\ -\ k\frac{\partial T}{\partial z} \\ &= M_v N_v h_v + M_a N_a h_a\ +\ h(t)\ \ [T^{\infty}(t)\ -\ T(z,t)\ ] \end{aligned} \qquad (14)$$

$$**\quad n_a\ =\ [x_a(N_v+N_a)+k_x(t)\ (\frac{p_a^{\infty}(t)}{p_a^{\infty}(t)+p_v^{\infty}(t)}-x_a)\ ]M_a \qquad (13b)$$

** not previously defined in Stanish. This is analogous to (13).

$$x_a\ =\ 1\ -\ x_v\ =\ \frac{\rho_a\ /\ M_a}{\rho_a\ /\ M_a\ +\ \rho_v\ /\ M_v} \qquad (13c)$$

$$n_a\ +\ n_b\ +\ n_f\ =\ N_v\ M_v \qquad (13d)$$

$$n_a\ =\ N_a\ M_a \qquad (13e)$$

$$N_v\ =\ x_v\ (N_v\ +\ N_a) \qquad (13f)$$

This assumes that the mole fraction of water vapor leaving the surface is equal to the mole fraction of water vapor at the surface.

Solve (13f) for N_a:

$$N_a = N_v \frac{(1 - x_v)}{x_v} = N_v \frac{x_a}{x_v} \qquad (13g)$$

Substitute (13g) into (13):

$$n_v+n_b+n_f = [N_v+k_x(t)\,(\frac{p_v^{\infty}(t)}{p_v^{\infty}(t)+p_a^{\infty}(t)}-x_v)]\,M_v \qquad (13h)$$

substitute (13g) into (13b):

$$n_a = [\ \frac{x_a}{x_v}\ N_v + k_x(t)\ (\frac{p_a^{\infty}\ (t)}{p_v^{\infty}\ (t)\ +\ p_a^{\infty}\ (t)}\ -\ x_a)\ ]\ M_a \qquad (13i)$$

Substitute (13g) into (14):

$$n_a h_a + n_v h_v + n_b h_b^* + n_f h_f - k \frac{\partial T}{\partial z}$$
$$= N_v\ (M_v h_v + M_a h_a \frac{x_a}{x_v}) + h(t)\ [\ T^{\infty}\ (t)\ -\ T(z,t)\ ] \qquad (13j)$$

Equations (12a), (13h), (13i) and (13j) define the boundary conditions at z=0 and z=L. The unknown variables in these four equations are ρ_a, ρ_v, N_v and T.

VITA

The author was born in Beijing, People's Republic of China on November 21, 1957. She received her Bachelor of Science degree in Mechanical Engineering from Xian-Jiaotong University in January 1982, and her Master of Science degree in Forest Products from Oregon State University in January of 1990. Prior to study in USA, she served five years as a lecturer of mechanical engineering in Beijing Forestry University.

The author enrolled in Virginia Polytechnic Institute and State University in January of 1992, and completed a Master of Science degree in Wood Science in May of 1994.

Ming Shao